

Musculoskeletal Loading and Pre-clinical Analysis of Primary Stability after Cementless Total Hip Arthroplasty *in vitro*

Vorgelegt von
Diplom Ingenieur Jean-Pierre Kassi
Kamerun

Von der Fakultät V – Verkehrs- und Maschinensysteme
der Technischen Universität Berlin
zur Erlangung des akademischen Grades
Doktor der Ingenieurwissenschaften
– Dr.-Ing. –

genehmigte Dissertation

Promotionsausschuss:

Vorsitzender: Prof. Dr. med Wolfgang Friesdorf
Berichter: Prof. Dr.-Ing. Georg N. Duda
Berichter: Prof. Dr.-Ing. Lucienne Blessing

Tag der wissenschaftlichen Aussprache: 25. Oktober 2004

Berlin 2004
D83

To my beloved and devoted parents, Françoise Ngo Nkaga and Jean-Pierre Kassi

Preface

The present thesis arose from my activities as research assistant at the Musculoskeletal Research Centre Berlin – Centre for Musculoskeletal Surgery (Director: Prof. Dr. med. N. P. Haas), Charité - University Medicine Berlin, a joint institution of the Free University and the Humboldt-University of Berlin. This work would not have been possible without the support of numerous people. Accordingly I would like to express my sincere gratitude to all of you for your valuable assistance.

I would first like to thank Prof. Georg Duda for introducing me to the field of orthopaedic and trauma biomechanical research and for giving me the opportunity to work on this specific topic and guiding my steps throughout the course of my research activities. His invaluable advice and his perpetual drive for perfection have considerably added to the quality of this thesis and to my perception of scientific work.

I would also like to extend my warmest thanks to the second referee, Prof. Lucienne Blessing for accepting to co-review and co-assess this thesis. Her commitment and helpfulness has made it possible for me to graduate from the Technical University of Berlin.

Many thanks also to Prof. Wolfgang Friesdorf for taking the chair of the examination board.

I am grateful to Dr. Markus Heller for his continuous assistance and invaluable input. His tutelage of fundamental aspects of musculoskeletal loading and modelling were indispensable in completing my thesis. Moreover, many parts of this work had the opportunity to go through his critical review and were subjected to intensive and constructive discussions.

I certainly would like to thank all the other colleagues of the Research Laboratory for the very pleasant atmosphere, the recreational activities and the

support throughout the years I have been working there. It has been an exciting and rewarding experience working with you. Many thanks also to Mr. Klaus Dannenberg from the Medical Technical Facilities of the Charité who untiringly manufactured the experimental set-up.

Furthermore, I gratefully acknowledge the contributions of Dr. William R. Taylor, MS Devakara Epari and MS Andrew Speirs. They invested so much time proofreading the manuscript to detect numerous misspellings as well as grammatical errors and thus making the text more comprehensible.

Both to the State of Cameroon, who gave me the opportunity to study in Germany by awarding me a scholarship, and to the German Federal Institute for Drugs and Medical Devices (Bundesinstitut für Arzneimittel und Medizinprodukte, BfArM), for financially supporting this research project, I would also like to express my profound gratitude.

I am most grateful and deeply indebted to my entire family at home. They believed in me at all times and gave me the freedom to find my own way and always encouraged me to pursue it. In spite of the huge distance separating us, my family inspires and helps me to give a sense to my life by always striving to place the Human Being in the middle of my activities.

All my friends, particularly Dipl.-Ing. Patrick Ndjiki-Nya Mbanya, also deserve special and cordial thanks for their permanent and tactful backing. Without them, the distance to the homeland would have appeared endless.

Last but definitely not least, I would like to turn the spotlight on the kindest and most lovely person I share my life with: Thank you so much, Elianne, for always and boundlessly giving me the support and the balance I needed during this demanding time and for being so sacrificially present despite the many challenges you simultaneously have to deal with.

Contents

Preface.....	i
Contents	iii
Zusammenfassung.....	vi
Abstract.....	viii
Nomenclature.....	x
1 Introduction	1
1.1 Anatomy and pathology of the hip joint	1
1.2 Hip joint replacement.....	4
1.3 Loading of the hip joint	7
1.3.1 <i>Soft tissues and femoral loading</i>	7
1.3.2 <i>Assessment of the loads at the hip joint</i>	8
1.4 Stability of hip prostheses	12
1.4.1 <i>Significance of prosthesis stability</i>	12
1.4.2 <i>Assessment of prosthesis stability</i>	15
1.5 Summary and Goal	20
2 Methods	22
2.1 Loading conditions for pre-clinical testing of hip implants <i>in vitro</i>	22
2.1.1 <i>Simplified musculoskeletal model</i>	22
2.1.2 <i>Load profiles for primary stability assessment in vitro</i>	25
2.2 Mechanical loading set-up.....	27
2.2.1 <i>Requirements and design specification</i>	29
2.2.2 <i>Design and realisation of the set-up</i>	32

2.3	<i>In vitro</i> assessment of primary stability.....	39
2.3.1	<i>Implants and bones</i>	39
2.3.2	<i>Mechanical testing</i>	46
3	Results	53
3.1	Simplified loading conditions	53
3.1.1	<i>Model simplification and validation</i>	53
3.1.2	<i>Load profiles for in vitro testing</i>	56
3.2	Mechanical loading set-up.....	61
3.2.1	<i>Evaluation of the set-up</i>	61
3.2.2	<i>Accuracy of load simulation</i>	62
3.3	Primary stability	65
3.3.1	<i>Implantation procedure</i>	65
3.3.2	<i>Muscle force simulation and interface movements</i>	66
3.3.3	<i>Patient activity and interface movements</i>	74
3.3.4	<i>Anchorage principle and interface movements</i>	80
4	Discussion	84
4.1	Primary stability of cementless prostheses	85
4.1.1	<i>Influence of active simulation of muscle forces</i>	85
4.1.2	<i>Influence of patient activity</i>	90
4.1.3	<i>Influence of anchorage principle</i>	92
4.2	Discussion of the methods	95
4.2.1	<i>Muscle model and load profiles</i>	95
4.2.2	<i>Mechanical loading set-up</i>	98
4.2.3	<i>Testing protocol for prosthesis stability</i>	101
4.3	Conclusion	105

5	Consequences.....	107
5.1	Pre-clinical analysis of primary stability <i>in vitro</i>	107
5.2	Clinical use	108
	Literature	109
	Appendix	132
	A-I Hip and thigh muscles of the complex model	132
	A-II Hip and thigh muscles of the simplified model.....	134
	Curriculum Vitae.....	136

Zusammenfassung

“Muskuloskeletale Belastung und prä-klinische Analyse der Primärstabilität nach zementfreier Totalhüftarthroplastik *in vitro*”

Die langfristige biologische Integration und damit der klinische Erfolg zementfreier Prothesen werden von ihrer Primärstabilität bestimmt. Prä-klinische Analysen der Primärstabilität setzen *in vivo* ähnliche Lastbedingungen voraus. Aus Mangel an adäquaten Daten zur Muskelbelastung und an einem allgemein anerkannten, validierten Lastprofil werden oft sehr vereinfachte Lastprofile implementiert. Ungeeignete *in vitro* Belastungen können jedoch zu kleineren Mikrobewegungen als bei Patienten und folglich zu einer unrealistischen Evaluation der Primärstabilität führen. Das Ziel dieser Studie war es daher a) vereinfachte, aber repräsentative Lastprofile einzuführen, b) einen entsprechenden mechanischen, physiologisch-ähnlichen Prüfstand zu realisieren und c) den Einfluss eines solchen Prüfstands auf die Primärstabilität zementfreier Prothesen zu ermitteln.

Die Bestimmung der Lastprofile basierte auf ein Computermodell der unteren Extremitäten, das durch Gruppieren von Hüftmuskeln mit ähnlicher Funktion vereinfacht wurde. Muskuloskeletale Belastungen wurden für das Gehen und das Treppensteigen ermittelt. Die berechneten Hüftkontaktkräfte wurden mit *in vivo* Daten validiert. Die vereinfachten Lastprofile beinhalteten Kräfte von maximal vier Muskeln. Es wurde ein Prüfstand verwendet, um die Hüftkontaktkraft durch Aufbringung der Muskelkräfte am Femur, mittels vier unabhängiger Aktuatoren mit Seilzügen und Kraftsensoren, zu erzeugen. Zum Vergleich wurde eine Lastkonfiguration, welche nur die beim Treppensteigen auftretende Hüftkontaktkraft am Prothesenkopf applizierte, simuliert. Metaphysär und meta-diaphysär verankernde Prothesen wurden in Kunstfemora implantiert und mit Wegaufnehmern bestückt. Während der anschließenden zyklischen Belastung wurden elastische und plastische Mikrobewegungen gemessen.

Die mit dem vereinfachten Computermodell ermittelten Muskel- und Hüftkontaktkräfte waren mit den *in vivo* Daten vergleichbar. Die berechneten

Hüftkontaktkräfte waren um weniger als 10% größer als die *in vivo* Werte und um bis zu 12% größer als die *in vitro* erzeugten Hüftkontaktkräfte. Treppensteigen mit der Hüftkontaktkraft alleine bewirkte eine charakteristische Valgus-Kippung der Prothese mit signifikant kleineren Mikrobewegungen als nach aktiver Simulation von Muskelkräften. Im Vergleich zu Gehen führte Treppensteigen zu größeren Mikrobewegungen mit ausgeprägten Axial- und Rotationskomponenten. Metaphysär und meta-diaphysär verankernde Prothesen zeigten ähnliche Bewegungsmuster mit vorwiegend Distalbewegungen und Drehung nach dorsal. Die metaphysäre Prothese wies jedoch höhere Mikrobewegungen auf.

Basierend auf *in vivo* Daten von THA Patienten war es möglich, vereinfachte Lastprofile des Femur abzuleiten und zu validieren. Der entwickelte Prüfstand konnte die Belastung im proximalen Femur beim Gehen und Treppensteigen nachahmen. Die Analysen legen nahe, dass die aktive Simulation von Muskelkräften die Primärstabilität zementfreier Prothesen wesentlich beeinflusst. Treppensteigen verursacht die höchste mechanische Instabilität am Knochen-Prothesen-Interface in einem Ausmaß, welches den notwendigen Osseointegrationsprozess beeinträchtigen könnte. Die Analysen betonen ebenfalls die Rolle des metaphysären Knochens bei proximaler Verankerung und die Notwendigkeit einer präzisen Aufbereitung des Femurkanals, um einer exzessiven Initialmigration vorzubeugen. Der neue, physiologisch-ähnliche Prüfstand erlaubt eine realistischere prä-klinische Evaluierung der Primärstabilität zementfreier Hüftprothesen *in vitro* und kann als Basis zur Standardisierung dienen. Ein solches Belastungsmodell mit aktiver Simulation von Muskelkräften sollte daher bei Analyse der Primärstabilität vor dem klinischen Einsatz berücksichtigt werden. Andernfalls könnten Mikrobewegungen unterschätzt und die Primärstabilität überschätzt werden, mit der Folge einer höheren Rate an Prothesenlockerungen und Re-Operationen.

Schlagwörter: *Zementfreie Hüftprothesen, Muskelkräfte, mechanischer Prüfstand, in vivo ähnliche Belastung, Primärstabilität in vitro, prä-klinische Analyse*

Abstract

The long-term biological integration and thus the clinical success of cementless prostheses are influenced by their primary stability. Pre-clinical analyses of the primary stability require loading conditions similar to those found *in vivo*. Due to a lack of appropriate muscle force data and of a consensual, validated loading scenario, oversimplified loading conditions are often implemented. Inappropriate loading *in vitro* may, however, lead to lower micro-movements than those occurring in patients and thus to an unrealistic assessment of primary stability. The goal of this thesis was therefore a) to introduce simplified, but representative load profiles of the femur, b) to implement a corresponding mechanical, physiological-like loading model and c) to determine the influence of such a model on the primary stability of cementless hip prostheses.

The development of the load profile was based on a computer model of the lower extremities. The model was simplified by grouping functionally similar hip muscles. Musculoskeletal loads were computed throughout walking and stair climbing. The calculated joint contact forces were validated against *in vivo* data and the simplified load profiles include the forces of up to four muscles. A set-up consisting of a testing machine and four independent actuators was used to generate the hip contact force by transmitting muscle forces through the femur using fibre ropes with force sensors. For comparison, a loading configuration which only generated the hip contact force occurring during stair climbing at the prosthesis head was simulated. Metaphyseal and meta-diaphyseal anchoring cementless prostheses were implanted in composite femora which were instrumented with displacement transducers to measure elastic and plastic interface micro-movements during cyclical loading.

The joint and muscle forces determined with the simplified computer model were comparable to the *in vivo* data. The computed hip contact forces overestimated the *in vivo* values by less than 10%, while the *in vitro* applied hip contact forces were up to 12% lower than the computed values. Stair climbing with the femur loaded by

the resultant hip contact force only exhibited a characteristic valgus tilt of the stem with significantly lower interface micro-movements than under active simulation of muscle forces. Compared to walking, stair climbing generated higher micro-movements, with pronounced axial and rotational components. Metaphyseal and meta-diaphyseal anchoring stems showed similar movement patterns and principally moved distally with a backwards twist. However, the metaphyseal stem exhibited higher interface movements than the meta-diaphyseal stem.

Based on data recorded in THA patients *in vivo*, it has been possible to derive and validate simplified load profiles of the femur. The implemented set-up mimics the loading of the proximal femur that occurs during walking and stair climbing. The analyses suggest that active simulation of muscle forces considerably affects the primary stability of cementless hip endoprotheses. Stair climbing induced the highest mechanical instability at the bone-prosthesis interface, a level which may compromise the necessary osseointegration process. The analyses also emphasize the importance of metaphyseal bone in proximal anchorage and the necessity of an accurate canal preparation to prevent excessive initial migration. The new, physiological-like loading set-up allows a more realistic pre-clinical evaluation of the primary stability of cementless hip prostheses *in vitro* and may form the basis for further standardisation. Such a loading procedure that includes the active simulation of muscles should therefore be taken into consideration in primary stability analyses of hip prostheses prior to clinical release. Otherwise micro-movements may be underestimated and the primary stability overestimated, leading to a higher rate of prosthesis loosening and re-operations.

Keywords: *Cementless hip prostheses, Muscle forces, mechanical test set-up, physiological-like loading, primary stability in vitro, pre-clinical analysis*

Nomenclature

Anterior	Toward the front, in front of
Distal	Farther from any point of reference
Dorsal	Pertaining to the back
Endoprosthesis	Prosthesis within the body
Frontal	Pertaining to the forehead
<i>In vitro</i>	In an artificial environment
<i>In vivo</i>	Within the living body
Lateral	Denoting a position farther from the median plane or midline of the body or of a structure. Pertaining to a side
Lig.	Ligamentum
M.	Musculus
Medial	The side of the body or body part that is nearer to the middle or centre of the body
Posterior	Situated in back of or in the back part of
Prosthesis	An artificial substitute for a missing body part
Proximal	Nearest, closer to any point of reference, e.g. the joint centre
Sagittal	Relating to, situated in the median plane of the body or any plane parallel thereto
THA	Total Hip Arthroplasty
Transversal	Acting or being across the body

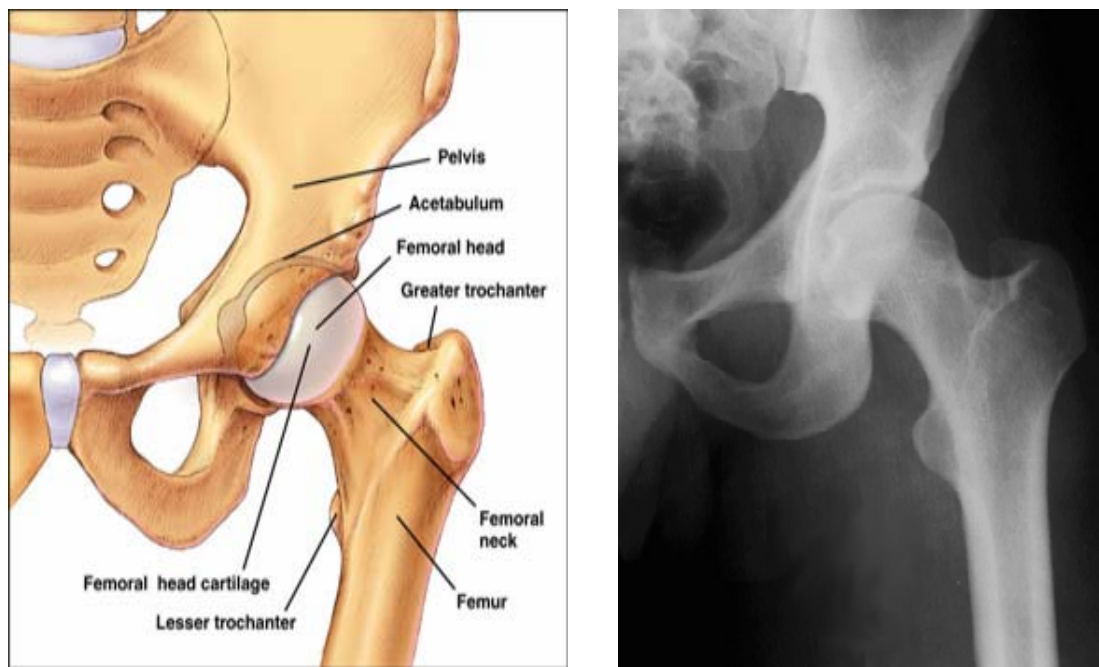
1 Introduction

The increasing socio-economic impact of bone and joint disorders led in 1998 to a Consensus Meeting in Sweden and an agreement to launch a global, multidisciplinary initiative, the “Bone and Joint Decade 2000-2010”, endorsed by the World Health Organisation (WHO) (Bjorklund 1998).

In the United States of America (USA) alone, direct and indirect costs of musculoskeletal conditions have been evaluated at \$254 billion per year in 2000 compared to \$215 billion in 1995 (Rice 2000). By 2010, for the first time in Europe, there will be more people over 60 years of age than people less than 20 years of age and by the year 2020, the number of individuals over 50 is expected to double (Murray and Lopez 1997). Musculoskeletal disorders are predicted to grow in the next years as they are most prevalent in the elderly. Furthermore, due to changes in lifestyle, the risk to sustain a musculoskeletal impairment is still growing. Efforts are therefore being undertaken to prevent and improve the treatment of musculoskeletal disorders such as joint diseases.

1.1 Anatomy and pathology of the hip joint

The hip joint connects the trunk to the lower limbs and is located at the intersection of the pelvic bone and the thigh bone (femur). It is a so-called ball-and-socket joint formed by the reception of the round-shaped head of the femur into a cup-shaped cavity in the pelvic bone (acetabulum) (Figure 1). In a healthy joint, both the head of the femur and the acetabulum are covered with a layer of smooth cartilage which cushions the joint. The space between the articulating surfaces of the joint is filled with a synovial fluid that allows the bones to move easily with almost no friction.



© Centerpulse Orthopedics Inc.

Figure 1 ▲

Graphical representation (left) and X-ray (right) of a healthy hip joint with pelvic and thigh bones (Source: www.centerpulseorthopedics.com).

The head of the femur is held in the acetabulum by very dense and powerful ligaments which contribute to balance and stabilise the joint and, therefore, to prevent hip dysfunctions such as impingement and joint dislocations. In addition to the ligaments, the joint capsule is surrounded and spanned by a complex network of muscles with attachment points on the pelvis, the femur and in certain cases the tibia (Figure 2, Appendix A-I). These soft tissues (muscles, ligaments, tendons) have the ability to generate and transmit forces to bony structures and thus to help perform different tasks of daily life such as level walking and stair climbing. According to the type of movement to which they mainly contribute, hip muscles can be divided into four groups: the adductors on the medial, the abductors on the lateral, the flexors on the anterior and the extensors on the posterior side of the joint. Due to the length of the neck of the femur and its inclinations to the body of the bone, angular movements of flexion, extension, adduction and abduction are partially converted into internal or external rotational movements of the femur.

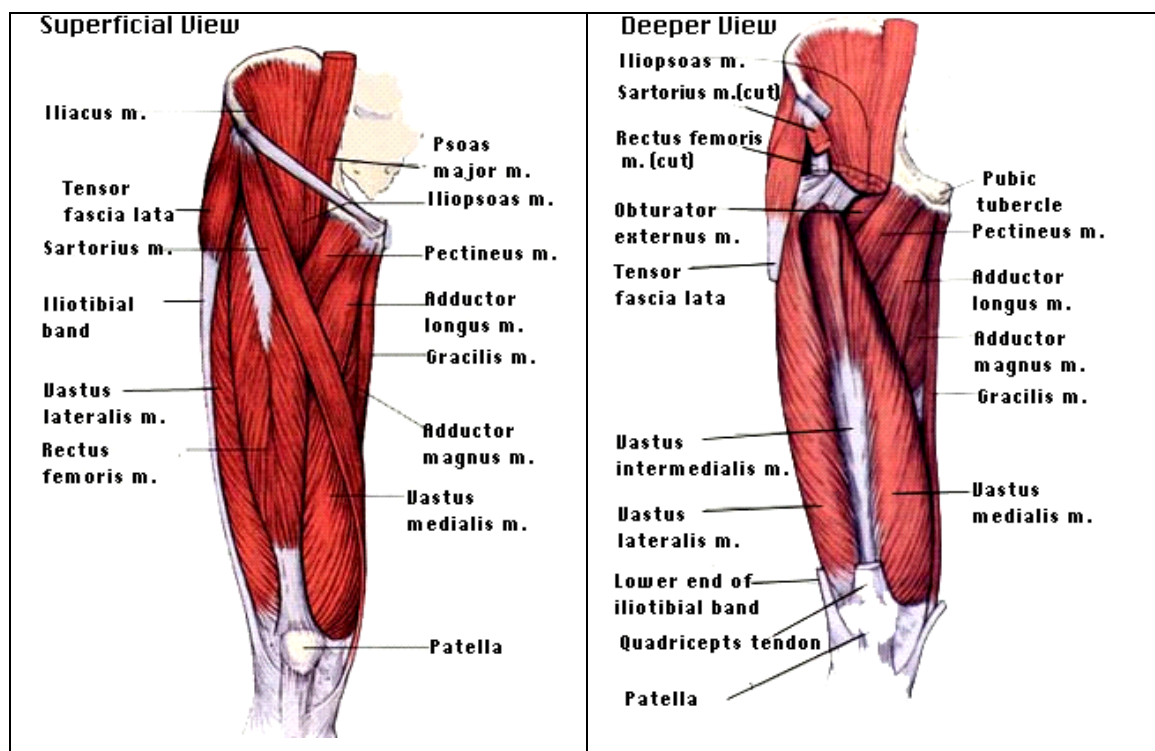


Figure 2 ▲

Schematic representation of the multi-layered muscles of the hip joint and of the thigh
(Source: <http://summit.stanford.edu>).

The ability of the hip joint to generate movement and transfer loads from the trunk to the lower extremities can be altered by a trauma or pathological diseases (Figure 3). Fractures of the neck of the femur following a trauma are often associated with an interruption of the blood supply to the femoral head, which may lead to necrosis of the head. In the case of patients suffering from degenerative joint diseases (e.g. osteoarthritis), the joint cartilage often undergoes structural damage which is caused by an inflammation of the synovial fluid. Both the acute and the progressive alterations are commonly associated with reduced range of motion and painful movements of the hip joint. In the long-term, a total failure of the hip joint occurs which makes a total joint replacement operation indispensable (Malchau *et al.* 2002).

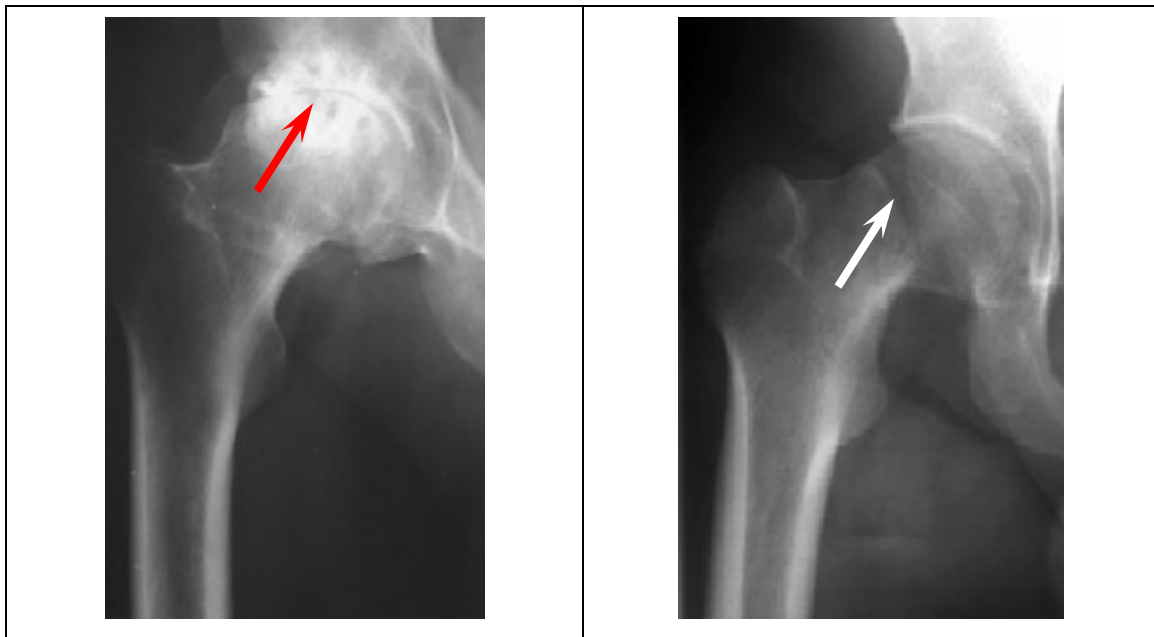


Figure 3 ▲

X-ray of a patient suffering from a hip joint degeneration (left) and a patient with a fracture of the femoral neck (right).

1.2 Hip joint replacement

Total Hip Arthroplasty (THA) is a treatment technique in orthopaedic and trauma surgery, in which a failed hip joint is replaced by an artificial one. The reconstructed hip joint consists of two components: a socket which is fixed into the acetabulum and a stem inserted into the cavity of the femur. The objective of the surgical procedure is to enhance the quality of life of THA patients by restoring the joint mobility and ensuring a total relief of pain (Laupacis *et al.* 1993). Two methods are currently used to fix the components of the artificial joint in the surrounding healthy bone: the cement fixation technique by means of polymethylmethacrylate (PMMA) developed by Charnley and the cementless fixation technique based on the press-fit principle, which is characterised by a forced stem insertion into a femoral cavity prepared with slightly smaller dimensions (Figure 4) (Charnley *et al.* 1968; Amstutz 1985; Herren *et al.* 1987; Callaghan 1992; Willert 1993; Willert and Buchhorn 1999; Rosenberg 2002). Nowadays, both fixation techniques are practiced and the benefit of the one over the other technique remains a controversially debated issue (Van Rietbergen *et*

al. 1993; Huiskes 1997; Bourne and Rorabeck 1998; Breusch *et al.* 2000; Rosenberg 2002).

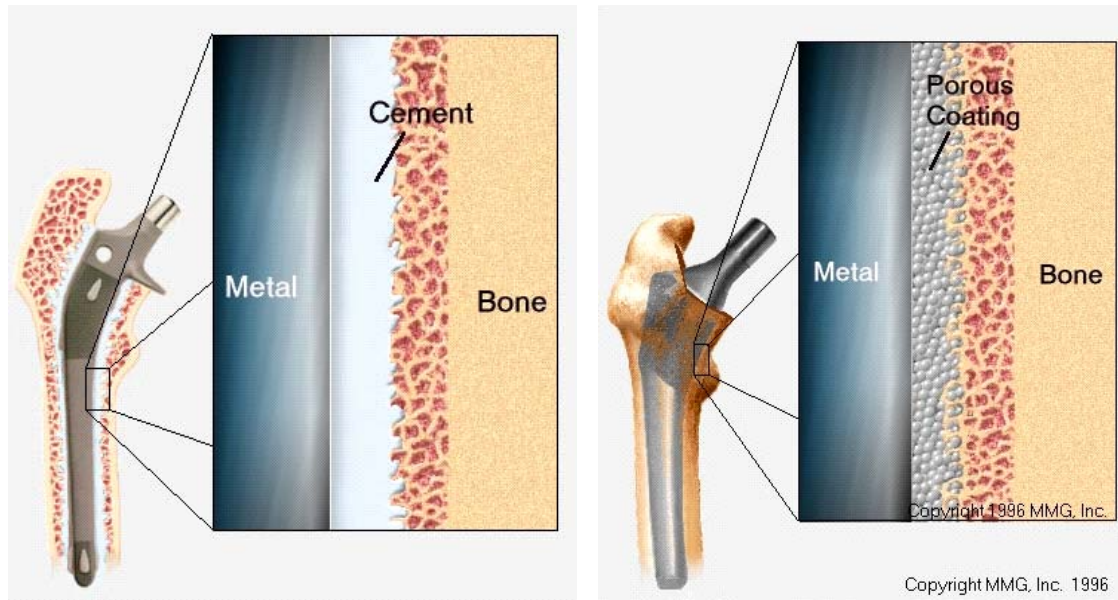


Figure 4 ▲

Graphic representation of a cemented (left) and a cementless (right) fixation of a hip endoprosthesis in total joint replacement (Source: www.castleortho.com).

The large number of operations performed each year shows that total hip arthroplasty is a very effective and well-established procedure with an average of 135,000 operations in Germany, 138,000 in the USA and approximately 1,000,000 world-wide (Graves and Kozak 1998). The success of this procedure is also reflected in the low rate of post-operative complications, as reported in a nation-wide, multi-centre study conducted in Sweden (The Swedish National Hip Arthroplasty Register): at nine years after surgery, only 6.4% of THA patients above 65 years needed a revision operation (Malchau *et al.* 1993).

Even though Total hip arthroplasty has become a method of choice in the surgical treatment of failed hip joints, there are still some points of concern. The functional lifetime of a reconstructed hip joint, which is usually referred to as its survival and is typically represented by a survivorship curve or a revision rate, rarely

exceeds 20 years (Sutherland CJ *et al.* 1982). A follow-on (revision) operation is, therefore, often inevitable, particularly in patients with high life expectancy. Furthermore, the average revision rate in younger and more active patients is superior to the overall revision rate (Torchia *et al.* 1996).

Clinical failure of a reconstructed hip joint can be caused by different factors such as septic (due to an infection) or aseptic (without infection) loosening of the components. In a multi-centre study analysing the outcome of different hip replacement systems, Malchau and co-workers (2002) also documented the causes that have led to the failure of at least one component of the artificial joint and subsequently to a revision operation. The authors reported an incidence of 75.4% for hip revisions due to aseptic loosening, followed by primary deep infections with only 7.4%. Aseptic loosening of hip prostheses therefore remains the most common complication and one of the most frequent failure modes of primary hip arthroplasties (Havelin *et al.* 1993; Malchau *et al.* 1993; Malchau *et al.* 2002).

Besides prosthesis loosening with or without infections, failure of a reconstructed hip joint is partially attributed to the reliability of the prosthesis components (Letournel 1987). The introduction of a new prosthesis design into clinical use should be preceded by tests concerning the biocompatibility of the materials (Davidson *et al.* 1994; Rhalmi *et al.* 1999; Schmidt *et al.* 2001) and the fatigue strength of the components (Viceconti *et al.* 1995; Baleani *et al.* 1999). In the last decades, the development of new biomaterials like titanium alloys has contributed to considerably reduce the risk of allergic tissue reactions. At the same time, the evaluation of fatigue properties according to the ISO 7206 standard has led to a significant reduction of the percentage of THA failures due to prosthesis breakage (Dall *et al.* 1993; Wroblewski and Siney 1993).

Another determinant parameter for the clinical success of a total hip arthroplasty is the mechanical stability of the bone-prosthesis complex in the early post-operative period, also known as the initial or primary stability (Mjoberg 1991; Kim and Kim 1993; Freeman and Plante-Bordeneuve 1994; Kobayashi A *et al.* 1997). The more

stable the implant is in the first few months following the procedure, the greater will be the chance for a long-lasting fixation. Primary stability is influenced *in vivo* by the surgical technique and patient- and implant-specific factors (Gustilo *et al.* 1989; Gebauer *et al.* 1990; Callaghan *et al.* 1992; Berzins *et al.* 1993; Kobayashi *et al.* 2000). In addition, the loads acting on a reconstructed hip joint influence the stability of hip prostheses (Bergmann *et al.* 1995; Lu *et al.* 1997; Lu *et al.* 1998).

1.3 Loading of the hip joint

1.3.1 Soft tissues and femoral loading

The loading conditions at the hip are determined by the joint contact force and the forces of the muscles spanning the joint (Pedersen *et al.* 1997; Krebs *et al.* 1998). The forces exerted by muscle structures have been shown to considerably influence the load and stress distribution within the bones: using analytical and experimental models of the hip joint, Pauwels (1951; 1973) demonstrated that the resultant contact force at the hip joint is affected more by muscles such as the abductor and the ilio-tibial band than by the loading due to body weight. Moreover, the author reported a decrease in bending stress along the femur as a result of the inclusion of muscle forces and, in consequence, a predominantly compressive stressing of the bone. These findings have been confirmed by other investigators (Rybicki *et al.* 1972; Ghista *et al.* 1976; Rohlmann *et al.* 1982, 1983b; Cristofolini *et al.* 1995). The latter analyses were, however, restricted to a small number of muscles and conducted with a two dimensional model of the hip. As a result, the internal loads in the femur may have been underestimated by up to 60% (Glitsch and Baumann 1997).

In a further attempt to investigate the effect of muscular activity on the stress behaviour of the femur, experimental and finite element analyses have been conducted in which the stress and strain within the femur were determined under the effect of different loading regimes, including a loading configuration comparable to that occurring during human gait (Taylor *et al.* 1996; Duda *et al.* 1997; Duda *et al.*

1998b; Latour and Brattain 2000; Fetto *et al.* 2002). The loads that were applied to the femur were often a compilation of muscle and joint forces taken from different studies for which no direct validation against *in vivo* measured forces had been conducted. The results of these investigations indicated that muscle forces considerably affected the femoral straining. Moreover, a reduction of the femur loads to a few major muscles led to a significant strain reduction within the femur compared to the load configuration with all thigh muscles. Similar conclusions were drawn from experimental *in vivo* measurements (Lu *et al.* 1997).

In the light of these findings, a thorough knowledge of the musculoskeletal loads acting at the hip joint as well as the inter-action between the different load components appears mandatory for a better understanding of the loading mechanisms at the hip joint and for the definition of consistent load cases to be used in biomechanical analyses involving the hip joint and the femur. Furthermore, a direct validation of computed joint loads against *in vivo* data is indispensable.

1.3.2 Assessment of the loads at the hip joint

In vivo measurements

The most common *in vivo* technique used to determine the loading conditions at the hip consists of measuring the contact forces which are transmitted between the pelvic bone and the femur by means of instrumented devices (English and Kilvington 1979; Brand *et al.* 1982; Bergmann *et al.* 1993). Patients requiring a total hip replacement operation are implanted with an instrumented femoral prosthesis. Hip contact force measurements are then conducted post-operatively and the recorded force values are transmitted telemetrically to an external data logger.

To date, the most complete and comprehensive description of hip contact forces measured *in vivo* has been provided by Bergmann and co-workers (2001a). In their study, six patients received instrumented hip prostheses and individual anthropometric parameters were determined for each patient. Post-operative gait

analysis was then performed under different activities of daily life, including level walking and stair climbing, whilst simultaneously measuring the contact forces at the hip joint. Thanks to the synchronous measurement method employed in their study, the authors were able to generate a consistent set of joint contact force and gait analysis data. Although the patterns of the hip contact forces were specific to each patient, the average peak forces were similar and ranged from 211 to 285% of the bodyweight during normal level walking and from 265 to 314% of the bodyweight during stair climbing activities. Comparable force magnitudes have been found by other investigators (Rydell 1966; English and Kilvington 1979; Davy *et al.* 1988; Kotzar *et al.* 1991). In peculiar situations such as disturbed gait due to muscular dysfunction or such as stumbling, much higher joint contact forces of up to 870% of the bodyweight were recorded (Bergmann *et al.* 1993, 2004).

Based on the measurement data of four of the six investigated subjects, average hip joint loads were computed using an averaging procedure derived from Fourier analysis (Bergmann *et al.* 2001b). The objective of this step was to create a representative data set of a “typical THA patient” that could be used for *in vitro* analyses. The peak joint contact force for this fictional “typical patient” added up to 238% of the bodyweight during normal level walking and 251% during stair climbing. Among all regular patient activities reported in their study, stair climbing generated the highest axial and torsional loads at the hip joint, followed by walking. Furthermore, analyses of the loading history and the activity levels of THA patients have shown that walking occurred in approximately 10% of the time and therefore represented the most frequent activity after sitting (44%) and standing (24%) (Morlock *et al.* 2001). These two activities have therefore been considered representative for the loading of the hip joint.

In addition to the contact forces transmitted at the hip joint, *in vivo* studies have been conducted to indirectly determine the forces exerted by muscles that span the hip joint (Neumann and Cook 1985; Neumann and Hase 1994; Lu *et al.* 1997; Krebs *et al.* 1998; De Visser *et al.* 2000; Mitoma *et al.* 2000). Although there is strong evidence that muscles considerably contribute to femoral loading, the muscle forces

acting *in vivo* are hardly accessible. The most widespread method of assessing muscle activity is electromyography (EMG) and consists in recording the electrical signals sent out by stimulated muscle structures by means of special electrodes. Due to the multilayered disposition of the hip joint musculature, a determination of the activity of each single muscle is not feasible in humans, since the use of invasive methods is constrained by ethical considerations. Consequently, the measurements are often limited to a small number of muscles (adductor, gluteus, biceps femoris, gastrocnemius, vastus lateralis) and subjects (Lu *et al.* 1998; Sutherland DH 2001). Moreover, electromyographic measurement data can not be transferred to muscle force values. EMG signals are instead used to compare the activation patterns of muscles in patients and in normal subjects (De Visser *et al.* 2000; Mitoma *et al.* 2000). Even though muscle force measurements are restricted to a small number of subjects and to qualitative descriptions, they provide valuable information for the validation of the results of mathematical analyses using models of patient anatomy.

Computer analyses

Musculoskeletal loading conditions at the hip joint can be predicted by computer models of the lower extremity (Seireg and Arvikar 1975; Brand *et al.* 1986; Glitsch and Baumann 1997; Pedersen *et al.* 1997). Using the inverse dynamic approach (Chao and Rim 1973; Andrews and Mish 1996), the forces and moments occurring at the different joints of the model can be predicted. A basic requirement is, however, knowledge of the external forces acting on the model (ground reaction forces) as well as knowledge of the kinematics (positions, velocities, and accelerations) of the limb segments. The forces exerted by muscular structures can then be determined out of the resultant joint loads and the kinematics data using optimisation algorithms (Seireg and Arvikar 1973; Seireg and Arvikar 1975; Brand *et al.* 1986; Brand *et al.* 1994; Glitsch and Baumann 1997). However, the validation of the results of these mathematical analyses against *in vivo* data remained a difficult issue and was, for example, conducted with data measured on different subjects or at different time points.

The first direct comparison of musculoskeletal loading conditions computed from gait data with simultaneously measured hip contact forces has been conducted by Heller and co-workers (2001). They generated a computer model of the bones and muscles of the human lower extremities which was subsequently scaled to match the anatomies of four THA patients with telemeterised femoral components (Bergmann *et al.* 2001a). The gait data and the individual musculoskeletal models were then used to calculate the inter-segmental resultant joint forces at the ankle, hip and knee joint, as well as the muscle and joint contact forces throughout the gait cycle. In addition, the musculoskeletal loads of the “typical THA patient” as defined by Bergmann and co-workers were computed. The calculated hip joint contact forces were finally validated against the contact forces measured *in vivo* during walking and stair climbing. The computer model predicted *in vivo* joint contact forces with an average error of only 12% to 14%. Similar findings have been reported by Stansfield and co-workers (2002; 2003) using the same mathematical approach, but with a different criterion for the optimisation algorithm to compute muscle forces. According to the authors, the prediction errors could be attributed to non-volumetric modelling of the muscle structures and to the method of force calculation (inverse dynamic).

Based on the model proposed by Heller and co-workers (2001), it seems possible to determine physiological-like musculoskeletal loading conditions at the hip that consider the interdependence of muscle and joint contact forces. The data from these analyses allow a better understanding of the mechanical interactions between muscle and bone structures during two normal activities of daily life. They provide detailed information about the loading of the lower extremities and can therefore be used to define more realistic loading scenarios, consistent with patient activities and muscle activation, to be applied to the femoral joint while assessing the prosthesis stability *in vitro*.

However, the computed muscle and joint forces are specific to the anatomy of the patient thigh bones and to the related lever arms of the adjacent muscles. Femur specimens used in experimental *in vitro* studies are often retrieved from human cadavers and may therefore exhibit considerable anatomical variations. Due to this

inter-specimen variability, it would be necessary to determine for each femur specimen the corresponding musculoskeletal loads to be implemented in an *in vitro* mechanical test set-up. An alternative method would consist in selecting a reference femur to which the vector force coordinates computed for the patient femur could be adapted.

1.4 Stability of hip prostheses

1.4.1 Significance of prosthesis stability

In a healthy joint, musculoskeletal loads are transmitted from the acetabulum to the femur head and from the proximal to the distal femur through an ingenious structure of trabecular bone (Figure 5). According to Wolff's law of bone remodelling, bone structures are formed along load transmission pathways, whereas bone resorption occurs in unloaded areas (Wolff 1892). The orientation of the trabecular bones therefore indicates how forces are transmitted within the bone, particularly in the metaphyseal region.

The implantation of a hip endoprosthesis causes a mechanical disruption of the load bearing structures, leading to an alteration of the original force distribution within the bones. As a result of the joint replacement procedure, mechanical interfaces are created between the acetabular and femoral prosthesis components and the pelvic bone (acetabulum) and femoral cavity, respectively. In the case of a cemented THA, the intra-operative bonding of prosthesis and surrounding bone by means of acrylic bone cement restores the load transfer pathways. The rapid hardening of the cement mantle creates a mechanically stable bone-cement-prosthesis interface and allows, albeit initially at a lower level, a direct post-operative loading of the reconstructed joint.

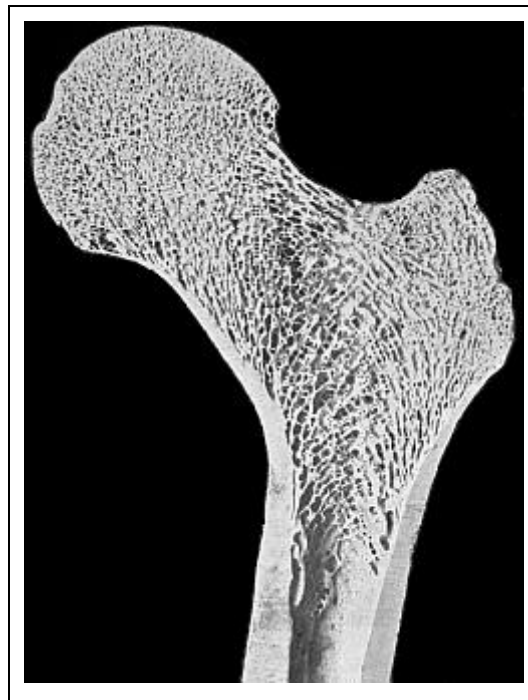


Figure 5 ▲

Longitudinal section of the proximal femur showing the trabecular structure in the metaphyseal region (Source: <http://ilfb.tuwien.ac.at/~daxner/ictam-projekt/my-femur-section-small.jpg>).

In contrast to their cemented counterparts, cementless hip prostheses do not provide an initial bond between the femoral stem and the bone. In fact, the primary stability only relies on the mechanical strength of the bone-prosthesis interface. A long-lasting bond between the components of the reconstructed joint occurs only weeks after the surgical operation, when an extensive bone apposition onto the prosthesis (osteointegration) has taken place. Sufficient initial mechanical stability at the bone-prosthesis interface, with regards to post-operative partial weight-bearing and rehabilitation, is required for an adequate biological integration of the prosthesis and for its long-term performance (Cameron *et al.* 1973; Ducheyne *et al.* 1977; Haddad *et al.* 1987; Morscher E 1987; Soballe *et al.* 1992).

Lack of primary stability is characterised by excessive micro-motions at the bone-prosthesis interface. The impact of micro-movements on the osteointegration process of cementless prostheses has been analysed in experimental investigations (Pilliar *et al.* 1986; Maloney *et al.* 1989; Sugiyama *et al.* 1989; Soballe 1993). In these animal studies, osteointegration was observed in the presence of micro-movements averaging 30 μm , while micro-movements larger than 150 μm were reported to compromise or inhibit the biological integration of the prosthesis. Interface micro-movements beyond the range from 30 μm to 150 μm may promote the formation of a thin layer of fibrous connective tissue around the prosthesis, leading to continuous implant migration and ultimately to aseptic loosening (Pilliar *et al.* 1986; Nistor *et al.* 1991; Engh CA *et al.* 1992).

Bone apposition can be stimulated by covering the implant surface with a bio-active substance such as hydroxyapatite (HA) (Geesink 1989; Geesink and Hoefnagels 1995; Jaffe and Scott 1996; Hayashi *et al.* 1999). The nature of the implant surface may also influence the osseointegration process (Galante *et al.* 1987; Kitamura *et al.* 1999; Laine *et al.* 2000); Implants with grit-blasted or matte surfaces ought to produce interdigitation to the surrounding bone. Such macro-textured implants, however, have shown poor clinical results (Havelin *et al.* 1995), compared to porous-coated prostheses. The optimum pore size to enhance bone ingrowth into porous surfaces has been evaluated between 50 μm and 400 μm (Bobyne *et al.* 1980). The extent of the porous coating depends on the design philosophy of the prosthesis: for hip prostheses that aim to transfer the joint loads in the metaphyseal region of the femur, the porous-coating is limited to the proximal part only, whereas distal anchoring prostheses are fully coated (Engh CA, Sr. and Culpepper 1997).

Although a better clinical outcome has been documented for fully coated than for only proximally coated prostheses (Otani and Whiteside 1992; Otani *et al.* 1995; Kronick *et al.* 1997; Nourbash and Paprosky 1998), the basic requirement in both cases to achieve biological integration is a sufficient primary stability at the bone-prosthesis interface. The fit between the prosthesis and the endosteal cavity of the femur appears to be a critical determinant of implant stability. However, due to the

lower strength of the metaphyseal trabecular bone it may be difficult to achieve a tight fit in the proximal, metaphyseal femur. Diaphyseal fixation is, therefore, often considered an alternative and may provide the necessary resistance to the joint loads in general and to rotational forces in particular (Whiteside *et al.* 1996). A mainly distal anchorage, conversely, may lead to non-physiological load transmission pathways with proximal bone resorption (stress shielding) and eventually aseptic loosening in the long-term (Rosenberg 1989; Plitz 1993).

Stability of femoral components is therefore considered a determinant of the clinical success of cementless total hip endoprostheses (Mjoberg 1991; Kim and Kim 1993; Freeman and Plante-Bordeneuve 1994; Kobayashi S *et al.* 1997). An evaluation of the stability of hip endoprostheses may therefore contribute to predict the long-term outcome of joint reconstructions and to prevent or reduce the risk of joint failure.

1.4.2 Assessment of prosthesis stability

In vivo evaluation

Although the stability of hip prostheses in the early post-operative period has been shown to be essential for the biological integration of the implant in the surrounding bone, there is currently no published method to directly and non-invasively measure the magnitude of the interface micro-movements occurring in THA patients under musculoskeletal loading conditions *in vivo*.

In clinical practice, the stability of hip prostheses can be assessed indirectly by comparing successive plain radiographs of the hip region taken in the anterior-posterior and lateral planes (Hardinge *et al.* 1991; Mulroy *et al.* 1991). On one hand, the stability of the prosthesis can be described qualitatively by the amount of radiolucent lines around the prosthesis which indicate the presence of a fibrous tissue layer characterized by a low mechanical strength. This method is, however, not very accurate, since some radiolucent lines may be overshadowed by the

prosthesis on the radiographs and the extent of the radiolucent lines may thus be underestimated (Reading *et al.* 1999). On the other hand, the migration of the prosthesis within the bone can be assessed by comparing its position relative to the bone on consecutive digitalized radiographs (Malchau *et al.* 1995; Biedermann *et al.* 1999; Krismer *et al.* 1999; Wilkinson *et al.* 2002). For this purpose, a set of landmarks must be defined and identified on both the prosthesis and the bone. Bony landmarks are, however, difficult to localize in a reproducible manner, a fact that considerably limits the measurement accuracy, which has been evaluated to 1 mm. Six months after surgery, an average prosthesis migration of 1.53 mm was reported by Phillips and co-workers (2002) using consecutive digitized radiographs.

The most accurate measurement method to assess the three dimensional interface micro-movements in total hip arthroplasty to date is the Roentgen Stereophotogrammetric Analysis (RSA) technique (Selvik 1990; Valstar *et al.* 2000). The higher accuracy of this method compared to the standard radiographs technique has been made possible by the use of radiographically-opaque tantalum markers as bone and prosthesis landmarks. These small markers (maximum 1mm) are inserted in the bone during the operation. The accuracy of the RSA technique has been evaluated between 0.05 mm and 0.5 mm in translation and between 0.15° and 1.15° in rotation (Karrholm 1989).

Several investigators have used the RSA technique to assess the subsidence of cementless hip prostheses *in vivo* (Mjoberg *et al.* 1986; Wykman *et al.* 1988; Nistor *et al.* 1991; Soballe 1993). Soballe (1993) determined the prosthesis migration 3, 6 and 12 months after surgery and reported a maximum migration of 0.2 mm at 12 months. Nistor and co-workers (1991) reported much higher average migration of up to 2.4 mm three years post-operatively. In these two studies, prosthesis migration was most accentuated directly after surgery and decreased afterwards. Moreover, migration of more than 2 mm within the first two years has been associated with a high risk of joint failure (Ryd 1992; Walker *et al.* 1995). The prognostic value of the *in vivo* measurement of early prosthesis migration with respect to the long-term clinical outcome has been demonstrated (Krismer *et al.* 1999). However, early clinical

failures of hip prostheses may be avoided or minimized through specific pre-clinical *in vitro* evaluations.

Pre-clinical testing of the primary stability in vitro: state of the art

Pre-clinical testing of hip endoprotheses aims at predicting and evaluating the *in vivo* behaviour of different prosthesis designs prior to clinical use. Knowledge of the prosthesis initial stability may provide pertinent information for the development of hip prostheses that allow optimal clinical results in terms of fixation strength. Several investigators have studied the primary stability of hip prostheses *in vitro* (Gebauer *et al.* 1989; Schneider E *et al.* 1989a; Schneider E *et al.* 1989b; Sharkey *et al.* 1990; Burke *et al.* 1991; McKellop *et al.* 1991; Fischer *et al.* 1992; Berzins *et al.* 1993; Harman *et al.* 1995; Naidu *et al.* 1996; Buhler *et al.* 1997; Baleani *et al.* 2000; Claes *et al.* 2000; Speirs *et al.* 2000; Gotze *et al.* 2002; Maher and Prendergast 2002; Pancanti *et al.* 2003). However, different methods were used due to the lack of a standardised protocol with respect to the loading conditions, to the method of load generation and application as well as to the methods of micro-movement measurement.

It has been shown that the loads acting on a reconstructed hip joint considerably affect the stability of hip prostheses and thus their long-term outcome (Bergmann *et al.* 1995; Lu *et al.* 1997; Lu *et al.* 1998). Therefore, *in vitro* tests should attempt to adequately simulate the physiological loading conditions at the hip. This requires a profound knowledge of the mechanical conditions at the hip following total hip arthroplasty. The complex musculoskeletal loading of the proximal hip region has been extensively evaluated and quantified in experimental and analytical studies, as presented earlier (Duda *et al.* 1998a; Bergmann *et al.* 2001a; Heller *et al.* 2001; Stansfield and Nicol 2002). Muscle forces were found to influence considerably the stress behaviour of the femur. Consequently, muscle forces may also affect the initial stability of endoprotheses. Furthermore, the degree of instability, expressed as interface micro-movement magnitudes, may be related to the patient activity.

However, the loads used for *in vitro* testing often represent a major simplification of the loading of the hip occurring in THA patients *in vivo* (Rohlmann *et al.* 1983a; Gebauer *et al.* 1989; McKellop *et al.* 1991; Berzins *et al.* 1993; Buhler *et al.* 1997; Chareancholvanich *et al.* 2002; Gotze *et al.* 2002; Maher and Prendergast 2002). The most common testing configuration consists of vertically loading the head of the prosthesis by the resultant hip contact force only (Gebauer *et al.* 1989; McKellop *et al.* 1991; Speirs *et al.* 2000; Gotze *et al.* 2002; Maher and Prendergast 2002; Pancanti *et al.* 2003). The magnitude and the direction of the contact forces applied in these studies depended on the activities which were simulated (one leg stand, walking, stair climbing) and ranged from about one to four bodyweights. Furthermore, the implanted femur is often potted or clamped distally to resist the load acting at the head of the prosthesis. As a result of the simplified loading regime and of the distal fixation, the stress distribution within the femur may be altered due to the non-physiological bending moments (Rohlmann *et al.* 1983a; Cheal *et al.* 1992; Cristofolini *et al.* 1995; Taylor *et al.* 1996; Simoes *et al.* 2000; Polgar *et al.* 2003).

In some studies, muscle forces have been simulated, in addition to the joint contact force (Burke *et al.* 1991; Callaghan *et al.* 1992; Munting and Verhelpen 1993; Doehring *et al.* 1996; Doehring *et al.* 1999; Simoes *et al.* 2000; Szivek *et al.* 2000; Harrington *et al.* 2002). The load of muscles such as the abductor, the vastus lateralis and the iliotibial band is sometimes modelled. Besides the fact that the source of muscle force data is sometimes not clearly specified, the definition of the load cases varies considerably between the authors and is subjected to controversial discussions (Simoes *et al.* 2000; Szivek *et al.* 2000). Although Pancanti and co-workers (2003) agree on the fact that the forces acting at the head of the prosthesis depend both on the joint reaction and the muscle forces and that muscle forces should be considered when investigating implant biomechanics, they choose, on the basis of preliminary analyses, not to include muscle forces in their loading configuration. However, the authors did not specify which muscles have been considered in their preliminary analyses and how these muscle forces have been determined. On the contrary, Szivek and co-workers (2000) reported an increase in femoral strains when muscle forces were simulated, in addition to the joint contact

force. Based on their experimental data, these authors concluded that loading the femur with the abductor muscles only, as suggested by Stolk and co-workers (2001) using a finite element model of cemented hip prostheses, may underestimate the strains in the femur.

A further point of concern of studies in which muscle forces have been actively simulated is the way these forces are generated and transmitted to the femur. The loading apparatus commonly used in *in vitro* tests consists of a cantilever mechanism which transforms an offset force applied by a universal testing machine into interdependent head and muscle loads. The muscle force magnitudes, which are effectively transmitted to the femur, are generally unknown, since no muscle force transducers to measure the applied muscle forces are incorporated into the testing apparatus and the lever mechanism may be over-constrained. While generating the musculoskeletal loads, the hip contact force is therefore rarely considered the sum of muscle activity and loading due to bodyweight. In fact, these load components are usually treated as mechanically independent variables.

Several studies have been conducted to determine the primary stability of hip prostheses (Gebauer *et al.* 1989; Schneider E *et al.* 1989b; Burke *et al.* 1991; Berzins *et al.* 1993; Buhler *et al.* 1997; Bachus *et al.* 1999; Baleani *et al.* 2000; Chareancholvanich *et al.* 2002; Gotze *et al.* 2002; Maher and Prendergast 2002; Britton *et al.* 2003). The magnitudes and patterns of the micro-movements measured in these studies reflect the variety of the loading configurations that have been realised in the mechanical test set-ups. Furthermore, *in vitro* micro-movements determined with no active simulation of muscle forces were found to be lower than those which occur in patients during the first few months following THA (Karrholm *et al.* 2000; Maher and Prendergast 2002).

1.5 Summary and Goal

Total hip arthroplasty is a well-established surgical procedure by which a degenerated or injured hip joint is replaced by an artificial one fixed in the bone with or without bone cement. In the case of cementless THA, the initial fixation of the prosthesis relies on a press-fit mechanism. The load which acts on a reconstructed joint *in vivo* is determined by the force due to bodyweight and to a large percentage by the forces of the muscles spanning the joint. Whilst the joint contact force can be measured in THA patients *in vivo*, only computer analyses allow an extensive evaluation of the loads exerted by muscle structures. However, the results obtained from computer analyses must be validated against *in vivo* data, in order to allow realistic biomechanical analyses of the hip joint.

Due to their anchorage principle, cementless prostheses should provide sufficient primary stability, which is a prerequisite for a long-lasting fixation through biological integration of the prosthesis in the bone. Post-operative *in vivo* measurements of the subsidence of cementless prostheses within the first months following surgery have been acknowledged as a powerful tool in predicting the long-term clinical outcome of hip joint reconstructions. Knowledge of the initial stability of hip prostheses prior to its clinical release may help predict the *in vivo* performance and to eventually improve the prosthesis design. The primary stability of hip prostheses can be assessed *in vitro* using mechanical test set-ups. Although the effect of muscle forces is increasingly being considered in such pre-clinical tests, there is no consensus in the literature as to how the bone-prosthesis complex should be loaded *in vitro* to better reflect the situation *in vivo*. The question still remains, which muscle groups should be taken into consideration and how such loading configurations should be realised *in vitro*.

Recent analyses of musculoskeletal loading, validated by measurements in THA patients, allow a better understanding of the mechanical interactions between muscle and bone structures and provide detailed information about the loading of the lower extremities during normal activities of daily life. The data from these analyses

describes physiological loading patterns, consistent with patient activities and active muscle groups, to be applied to the femoral joint *in vitro*. However, mechanical load set-ups used to generate the hip loading *in vitro* rarely considered the joint contact force as the sum of muscle and weight loading.

The interface micro-movements registered under such loading conditions are often not consistent with those measured *in vivo*, presumably due to the alteration of the physiological load transmission pathways. It can therefore be hypothesised that a physiological-like loading of hip reconstructions *in vitro* that considers the requirements of force equilibrium and minimal bending stresses of the femur may give rise to more realistic interface micro-movements. Due to the inter-dependence of bodyweight, muscle and hip contact forces and due to the close interaction between these load components, it may be useful to capitalise on a systematic design methodology while implementing such a mechanical loading set-up.

The aim of the present thesis is therefore:

- To introduce simplified, but representative load profiles to be used in the pre-clinical assessment of the primary stability of cementless hip prostheses *in vitro*. These musculoskeletal load profiles should be validated against data measured in total hip arthroplasty patients *in vivo*.
- To implement a mechanical loading device based on the derived load profiles. The design process should yield a set-up that is able to generate and transmit the joint loading in a physiological-like manner.
- To determine the influence of a physiological-like loading on the primary stability of cementless hip prostheses by comparing the load-induced micro-movements obtained with and without active muscle force simulation as well as during different patient activities and load levels.

2 Methods

2.1 Loading conditions for pre-clinical testing of hip implants *in vitro* ♦

Using the musculoskeletal model of the lower extremity developed and validated by Heller and co-workers (2001), it has been possible to determine the forces and moments acting at the reconstructed joint of a THA patient while performing two activities of daily life, walking and stair climbing. Whilst this study used a complex model of the hip musculature with over 30 different lines of muscle action, the physical space limitations and constraints of an *in vitro* test set-up require a reduction of the number of muscle fibres. The model simplification should result in the definition of simplified load profiles that resemble the *in vivo* loading conditions of the “typical THA patient” and considers the interaction between muscle and joint forces.

2.1.1 Simplified musculoskeletal model

Modification of the complex model

The complex representation of the hip muscles from the previously described musculoskeletal model proposed by Heller and co-workers (2001) was grossly simplified in order to reduce the number of muscles (Figure 6). The simplification of the musculoskeletal model was mainly focussed on the so-called “single-joint muscles”, i.e. muscles that solely span the hip joint. In this gross simplification, all fibres of the gluteus muscles with a similar function (gluteus maximus, medius and minimus) were grouped into one simplified “abductor muscle” with a single attachment site. A similar process was applied to the adductor muscles (adductus brevis, magnus and longus), yielding a resultant “adductor muscle” (Table 1).

♦ In cooperation with Markus Heller

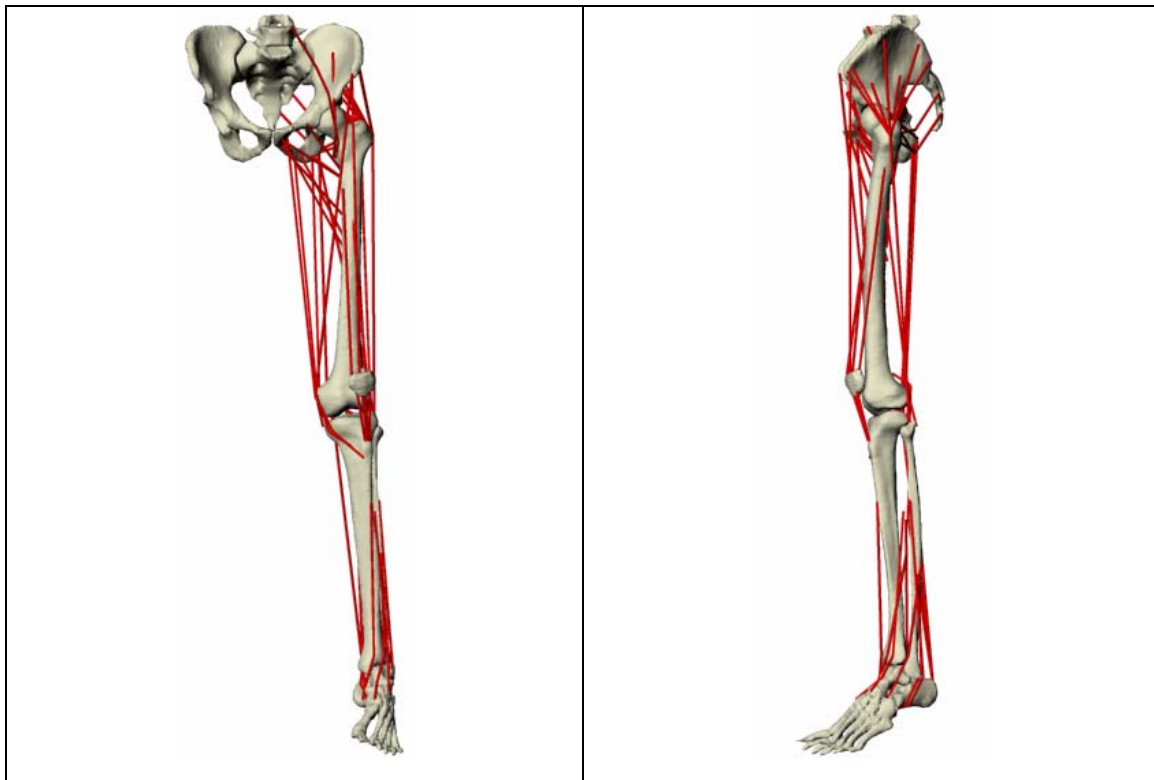


Figure 6 ▲

Complex musculoskeletal model of the lower extremity (See also Appendix A-I).

Muscles that span both the hip and knee joints are commonly referred to as bi-articular or “two-joint muscles”. These two-joint muscles play an important functional role regarding the execution of movements (van Ingen Schenau et al., 1987; van Groenigen and Erkelens, 1994; van Ingen Schenau et al., 1995; Heise et al., 1996; van Bolhuis et al., 1998), and hence were important for deriving the physiological-like loading conditions. From these two-joint muscles, the long head of the biceps femoris, the semitendinosus, the semimembranosus, the rectus femoris, the gracilis and the sartorius, contribute to the hip contact force, but they do not have attachment sites at the proximal femur and therefore exert no direct forces on the bone. Whilst these musculoskeletal structures were included in full detail for the calculation of the musculoskeletal loading conditions throughout the gait cycle, their effect on the proximal femoral loading can be modelled by ensuring an appropriate, physiological-like joint contact force acts on the femoral head, without increasing the complexity of an *in vitro* test set-up.

Table 1 ▼

Modifications of the hip muscles used to derive the Simplified Muscle Model. Muscle fibres which were grouped into one muscle are highlighted. The modifications were restricted to muscles with either an attachment or a wrapping point at the proximal femur. A complete list of the muscles which were included in the simplified model is presented in Appendix II.

Complex Model	Modification	Simplified Model
Gluteus medius	pooled	Abductor
Gluteus minimus		
Gluteus maximus		
Adductor magnus	pooled	Adductor
Adductor longus		
Adductor brevis		
Ilio-tibial tract	unchanged	Ilio-tibial tract
Tensor fascia latae	unchanged	Tensor fascia latae
Iliacus	removed	--
Psoas major	removed	--
Pectineus	removed	--
Gmellus inferior & superior	removed	--
Obturator externus & internus	removed	--
Piriformis	removed	--

In an attempt to further reduce the number of muscles included in the model to the lowest feasible amount, joint contact forces were calculated for a series of different configurations. Muscles that exerted small forces (i.e. muscles from the group of the lateral rotators) were successively removed from the model to such a point that physiological hip joint loading was still calculated. The musculature for the remainder of the lower limb remained as described in the original model (Heller *et al.* 2001).

Validation of the simplified model and calculation of the joint loads

In order to base the simplified load profile on representative data for THA patients, the data sets for the “typical patient” defined by Bergmann and co-workers (2001a; 2001b) were used for the musculoskeletal analyses. Based on these gait data, the inter-segmental resultant joint forces, muscle forces and joint contact forces were computed for the ankle, knee and hip joint using the different configurations of the simplified models of the hip musculature as described before. The whole gait cycle of each walking and stair climbing was analysed in order to establish the conformity of the computed musculoskeletal loading patterns with the hip contact forces of the “typical patient” derived from the *in vivo* measured data. The final simplified load profiles for the proximal femur were determined from the musculoskeletal loading conditions, obtained from the most simplified muscle configuration that resulted in a physiological-like joint loading throughout the gait cycle.

2.1.2 Load profiles for primary stability assessment *in vitro*

Gait cycle and load variation

The magnitude of the forces exerted by the muscles of the human lower extremity usually change depending on the task to be performed. Because the flexion and abduction angles of the femur with respect to the pelvis continuously vary throughout the gait cycle, the directions of the muscle forces in the femur-based coordinate system vary as well. The simulation of a whole gait cycle *in vitro* would therefore not only require a control of the magnitudes of the generated muscle forces, but also a continuously repositioning of the femur relative to the pelvis. This may considerably add to the complexity of *in vitro* mechanical loading models.

Pre-clinical *in vitro* tests of primary stability should preferably analyse the behaviour of implants when these are subjected to the most critical loading conditions within the framework of regular post-operative activities of THA patients. In the case of the hip joint, the loading conditions are defined by the muscular activity and the

inter-segmental forces which result in joint contact forces and moments. Therefore, only the instances of maximum muscular activity and high joint contact force during the activities of walking and stair climbing were selected for realisation in a mechanical loading set-up. The final simplified load profiles for the proximal femur were then determined at these time-points and consisted of the force vectors of the activated muscle groups, the inter-segmental resultant and the hip contact force vectors.

Loads for a representative femur geometry

Composite femora have been used in recent years as substitutes to human bone specimens in experimental analyses of the biomechanical behaviour of hip joint reconstructions (McKellop *et al.* 1991; Harman *et al.* 1995; Kummer *et al.* 1997; Liu *et al.* 2003; Waide *et al.* 2003). These bone substitutes are characterised by a relatively low geometrical variability and resemble human femora with regard to anatomical shape and mechanical stiffness and strength (Cristofolini *et al.* 1996). In this study, composite femora (Model 3103, medium-size, Sawbones Europe AB, Malmö, Sweden) were chosen to define representative load profiles of the proximal femur.

In order to adapt the computed musculoskeletal loads from the patient to the composite femur, a set of three landmarks was defined for each bone. The landmarks were located at the head centre, the greater trochanter, the lateral and the medial epicondyles of each femur (Figure 7). A transformation matrix was determined out of the three-dimensional coordinates of the bony landmarks and used to compute the coordinates of the femoral attachments and wrapping points as well as the vector coordinates of the muscle and joint contact force for the composite femur (Sommer *et al.* 1982). The simplified load profiles adapted to the anatomy of the composite bone were subsequently used to realise a mechanical loading set-up.

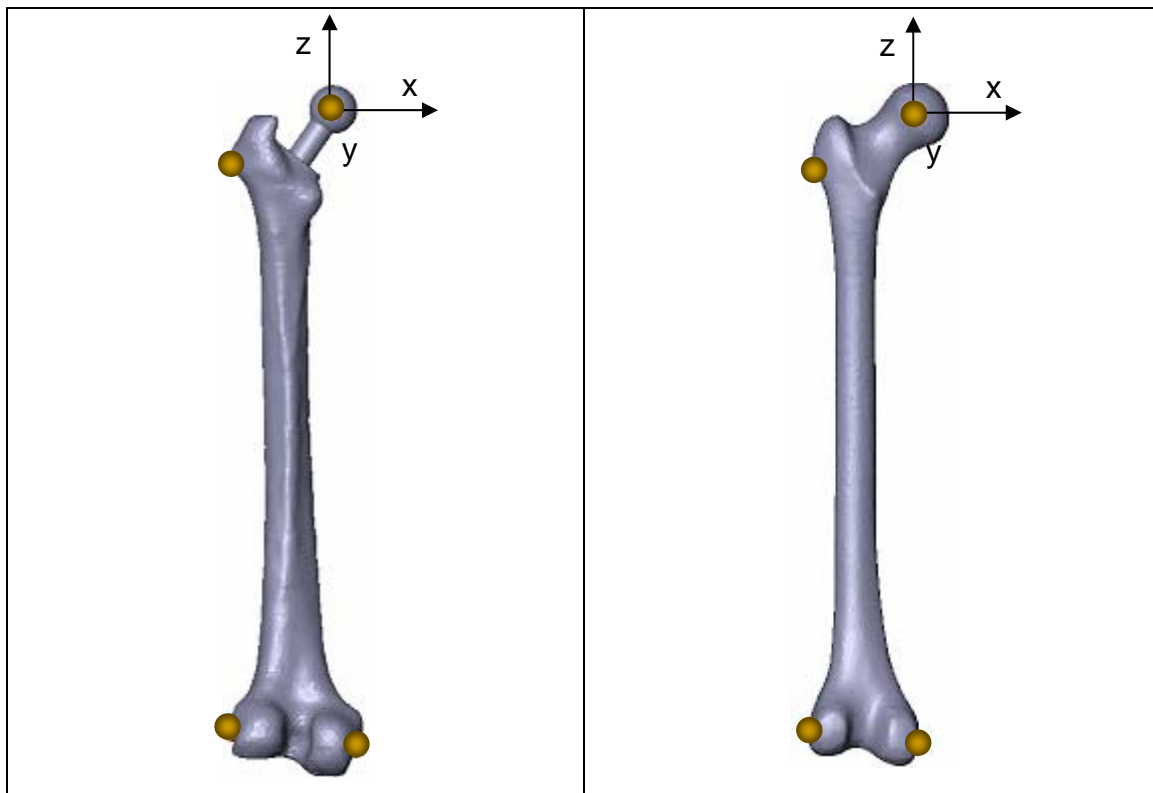


Figure 7 ▲

Femur landmarks used to transform the coordinates of the proximal femur loads from the patient (left picture) to the composite femur (right picture). The landmarks corresponded to readily identifiable anatomical points: the greater trochanter, the medial and the lateral femur epicondyles. The origin of the femur coordinate system was situated at the hip joint centre (centre of the femur head) and the orientations of the axes corresponded to those defined by Bergmann and co-workers (Bergmann et al. 2001a): x-axis oriented in the medio-lateral direction, y-axis in the anterior-posterior direction and z-axis in the proximal-distal direction.

2.2 Mechanical loading set-up

The design process of the mechanical loading set-up was conducted according to a well-established design methodology (Figure 8) (VDI-Richtlinie 2221 1986; Pahl and Beitz 1993). The guidelines defined in this methodology divide the design process into a task clarification, a conceptual, an embodiment and a detail design phase, each consisting of successive, iterative steps. In a first approach, information concerning the task to be performed is collected. This process should lead to an

extensive clarification and definition of the task thus providing a clear set of objectives for the development phase. All the requirements that have been identified and their significance are consigned in a list of requirements and sorted by order of priority (demands, wishes). These requirements are then successively abstracted until the main problems have been identified.

Conceptual design can be described as the process of conceiving ideas and working principles around a given or derived design brief or requirement specification. First, a core function of the planned product is formulated and subsequently divided into sub-functions and modules of lower complexity. A number of concepts are usually generated and evaluated against the brief in order to select the one that would meet the intended performance specification the best. An unambiguous interrelationship between the solutions that have been selected for the different sub-functions is then established, leading to a principle solution which should bring to light the main modules of the product.

The conceptual design phase is followed by an embodiment phase which is a structured development of the chosen concept. In this phase, preliminary design layouts and configurations of the single modules as well as of the whole product are drawn up. The most desirable preliminary layouts are then selected and refined and evaluated against technical and economic criteria. After configurations, shapes, weights and interactions have been determined, detail design of the product can be conducted. At this stage, the data pack required for manufacture is generated.

The design process of the *in vitro* loading set-up was based on the simplified load profiles which were derived from the musculoskeletal analyses and subsequently customised to the composite femur. Additional requirements specific to the assessment of the primary stability of cementless hip endoprostheses were also taken into consideration.

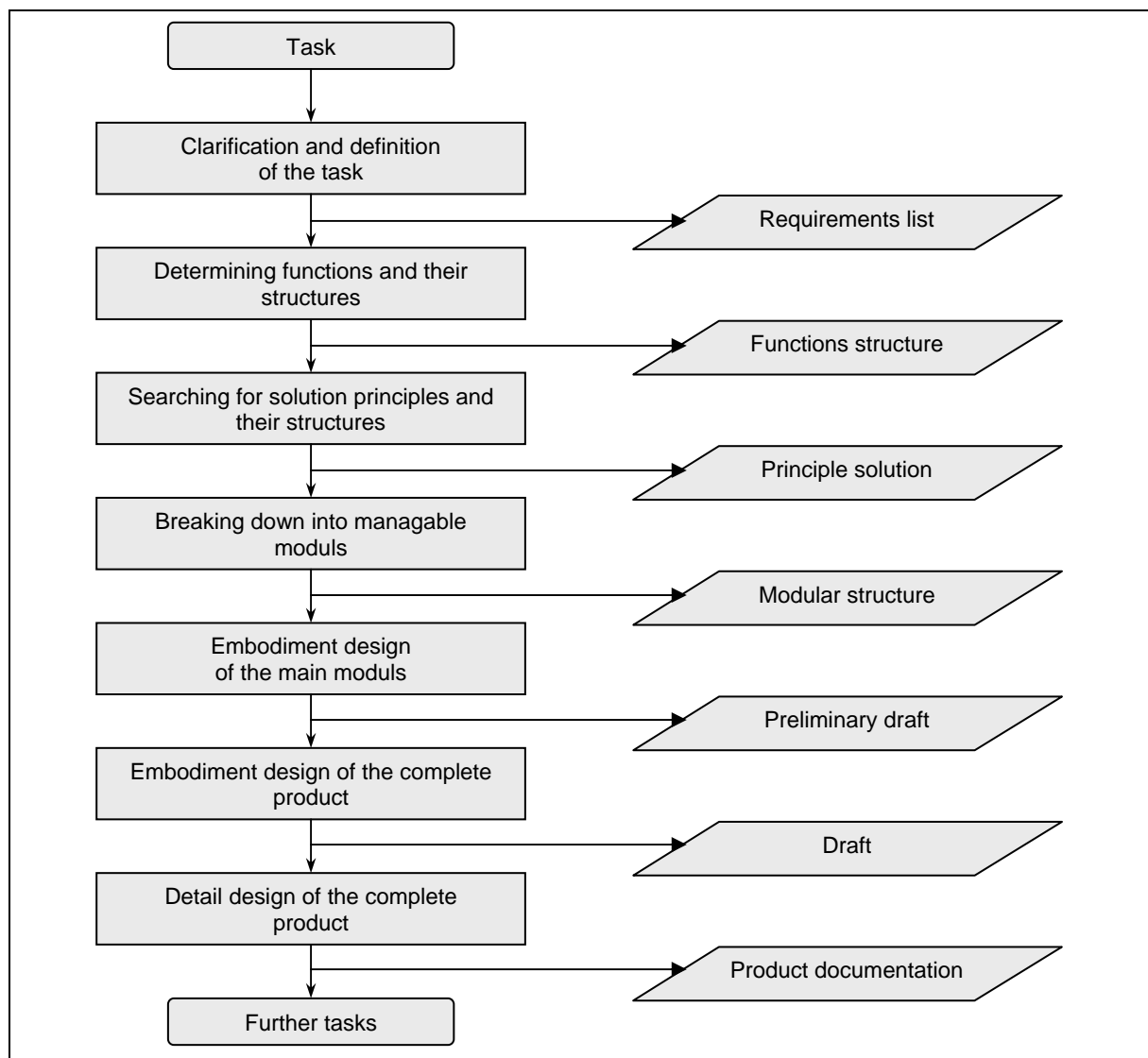


Figure 8 ▲

Steps of the engineering design process (VDI-Richtlinie 2221, 1986).

2.2.1 Requirements and design specification

The requirements to be fulfilled by the mechanical loading set-up were specified and consigned in a list of requirements (Table 2). The main objective of the set-up consisted of applying the previously computed musculoskeletal loads to the proximal femur in such a way that the three dimensional load transfer occurring *in vivo* during activities of level walking and stair climbing can be simulated. More specifically, the forces of the different muscle groups should be synchronously generated and

transmitted to the respective attachments or wrapping points. The resultant contact force at the hip joint should result from the co-action of muscular and inter-segmental loads.

The loading set-up should be used to assess the mechanical performance of different joint reconstruction procedures. In the present case, the primary stability of cementless hip prostheses is to be evaluated. The configuration of the loading set-up should therefore allow measuring the load-induced instability of the joint reconstruction at several points of the bone prosthesis interface, i.e. the mechanism of load transfer and the jig required for this purpose should not interfere with the devices to assess the load-induced relative movements at the bone-prosthesis interface.

Furthermore, the geometry and the dimensions of the set-up should match the space that is available within the existing material testing machine (Model 8871, Instron Corporation). All devices which may be involved in generating and transmitting the muscle forces to the test specimens should be synchronised by the testing machine. Moreover, the configuration of the loading set-up should be transferable to other material testing machines which are commonly used to generate and apply the load of the hip joint.

Table 2 ▼

List of requirements of the mechanical loading set-up.

Nr.	Requirements	Comments, Demand (D) / Wish (W)
	General set-up requirements (G)	
G1	Set-up and material testing machine <ul style="list-style-type: none"> ➤ compatible to the existing testing machine ➤ max. dimensions (mm): 450 x 930 x 400 (W x H x D) ➤ adaptable to other testing machines 	D D W
G2	Handling <ul style="list-style-type: none"> ➤ modular, easy to assemble / disassemble design ➤ robust, low deformations ➤ easy to use (positioning of test specimen) 	D D D
G3	Femur geometry <ul style="list-style-type: none"> ➤ reference femur (medium sized composite femur) ➤ human specimens 	D W
G4	Prototyping <ul style="list-style-type: none"> ➤ use of existing resources ➤ manufacturing at the Charité 	W W
	Load simulation (L)	
L1	Physiological-like loading <ul style="list-style-type: none"> ➤ 3-D force components: up to 2500 N ➤ hip joint force as result of weight and muscle forces ➤ minimum force constraints at hip and knee joint ➤ walking and stair climbing 	D D D D
L2	Simulation of up to five muscle groups <ul style="list-style-type: none"> ➤ muscle force amplitude: up to 2500 N ➤ accurate muscle actuators ($\pm 0.1\%$ peak force) ➤ compatible to primary stability assessment ➤ no interference with movement sensors 	D D D D
L3	Sine loading curve <ul style="list-style-type: none"> ➤ test frequency: 0.25 (to 1Hz) ➤ minimum 1000 load cycles ➤ synchronized with testing machine 	(W) D D
	Safety (S)	
S1	General laboratory safety requirements	D
	Cost (C)	
C1	Minimum costs according to research grant	W

2.2.2 Design and realisation of the set-up

The specifications, which have been defined in the list of requirements, were then abstracted to identify the essential problems and thus the core function of the mechanical loading set-up. The overall function of the set-up was formulated as follows:

“Physiological-like loading of the femur *in vitro*”

The overall function was then broken down into sub-functions, which were divided into two groups. The sub-functions of the first group should generate and apply the weight and muscle forces to the test sample whereas the sub-functions of the second group aimed at positioning and securing the test sample within the set-up in accordance with the specifications of the load profiles. All sub-functions were interconnected through a signal network to a functional unit (Figure 9).

Working principles that fulfilled the identified sub-functions were found and selected with respect to the previously defined requirements (Figure 10). The working principles of all sub-functions were then combined to fulfil the overall function of the mechanical loading set-up. A principle solution of the whole set-up was then created (Figure 11)

The core component of the loading set-up was a commercially available servo-hydraulic material testing machine (Instron 8871, Instron Wolpert GmbH, Darmstadt, Germany) which was used to transform hydraulic energy into mechanical energy. The part of the hip contact loading produced by the inter-segmental force was generated by the testing machine and applied through the plunger. The material testing machine was computer-controlled and its application software was used to set the magnitude and the course of the inter-segmental force.

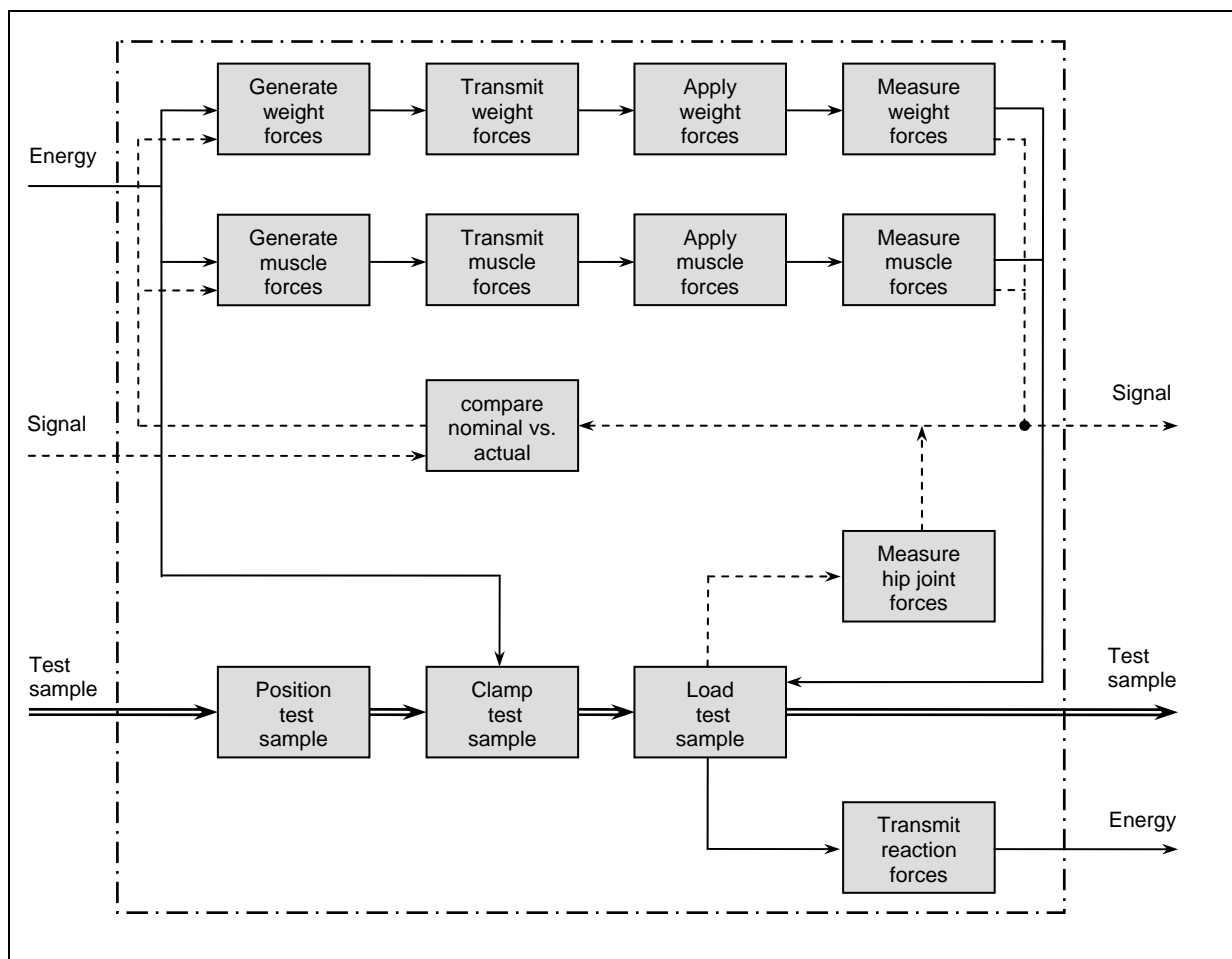


Figure 9 ▲

Function structure of the mechanical loading set-up. Described are the material and energy flows as well as the signal network connecting all components of the in vitro loading set-up.

Muscle forces were generated through four miniature servo-electric motors (PowerCube Drive Unit 70-100, 15 Nm nominal torque, AMTEC GmbH, Berlin, Germany). The muscle force actuators were torque adaptive position control systems with a high positioning accuracy ($\pm 0.02^\circ$) and a high angular velocity ($238^\circ/\text{s}$). The actuators were connected to and synchronized with the testing machine. The triggering signal was the curve progression of the inter-segmental force supplied by the testing machine.

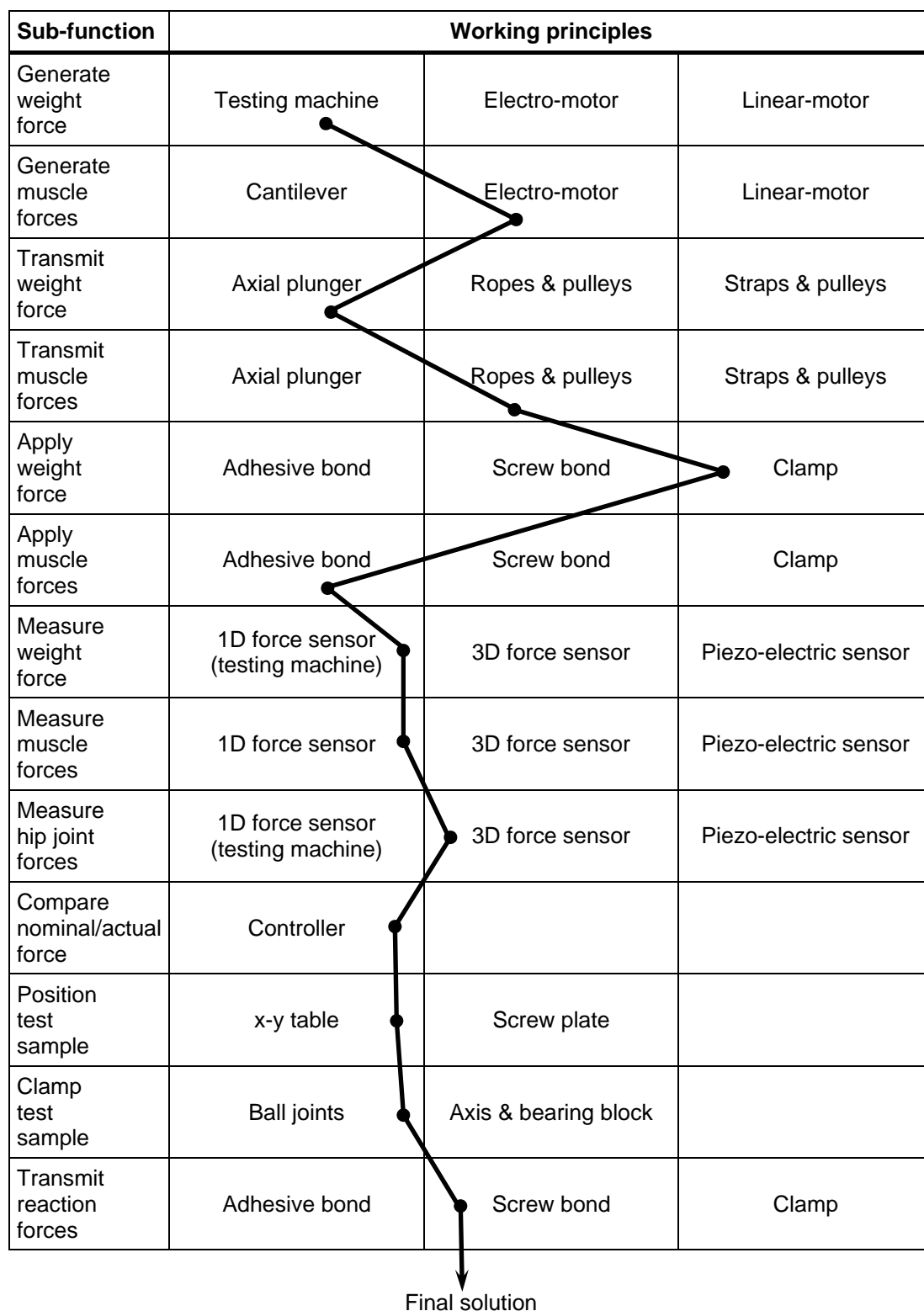


Figure 10 ▲

Morphological chart presenting the working principles of the mechanical loading set-up.

An adjustable, modular frame was designed to replicate the spatial loading of the hip region according to the simplified musculoskeletal model and to transmit these loads from the muscle force actuators to the head of the prosthesis and to the proximal femur. The upper part of the frame consisted of a base-plate that was attached to the crosshead of the testing machine. In addition, perpendicular plates were screwed to the base-plate to carry out the different loading configurations.

The muscle force actuators and the bearings which supported the shafts of the actuators were mounted on the base-plate of the modular frame. The generated muscle forces were transmitted from the actuators by synthetic, stretch-free fibre ropes (LIROS-Hiload, Rosenberger Tauwerk GmbH, Lichtenberg, Germany) that simulated the muscle structures. The loading ropes were passed through pulleys to produce the orientations of the respective muscle force vectors. The pulleys were mounted on the modular frame and their diameters as well as the distance between them were specific to the two activities to be simulated, walking and stair climbing.

The ropes were then anchored at the muscle insertion sites on the femur surface. The effective muscle forces were to be measured through miniature force sensors (OCDZ-3kN, Wazau GmbH, Berlin, Germany). One force sensor was attached to each of the ropes. The actuator, rope and sensor for each muscle force were configured in an independent closed loop control unit. Due to space limitations between the muscle attachment sites and the deviation pulleys, the muscle force sensors were attached on the section of the rope between the pulley and the force actuator. The frictional loss occurring at the pulleys was quantified by correlating the rope forces, which were simultaneously measured on both sides of the pulleys. The calculated coefficients of friction were used to adjust the target values for the muscle forces.

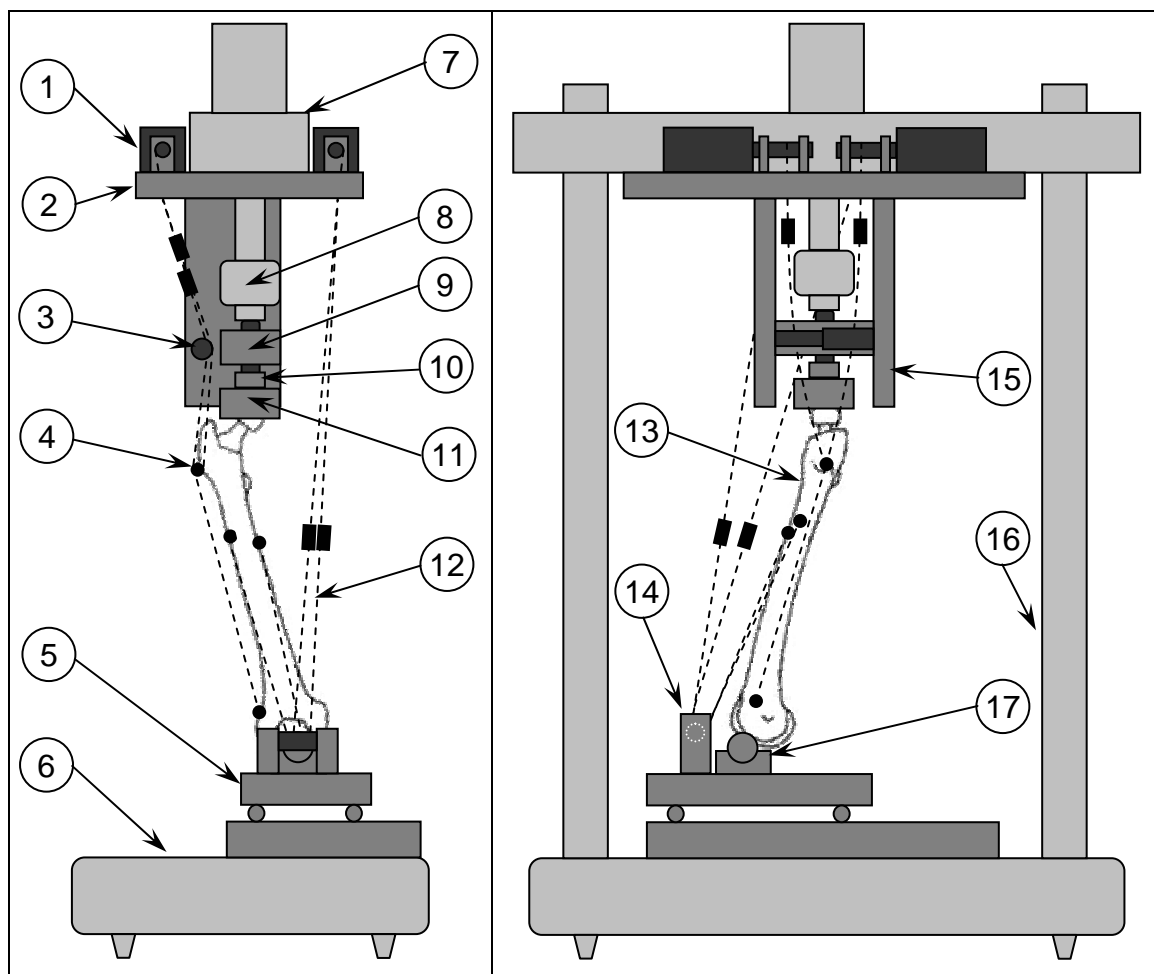


Figure 11 ▲

Principle solution combining the components that fulfil the different sub-functions of the mechanical loading set-up: (1) muscle force actuator, (2) base-plate, (3) proximal deviation pulleys, (4) anchorage point of the fibre rope, (5) x-y table with interlocking bolt, (6) bed of the testing machine, (7) crosshead of the testing machine, (8) plunger of the testing machine with force sensor, (9) force coupler with radial bearing, (10) three dimensional force sensor, (11) holder of the polyethylene cup, (12) loading rope with axial force sensor, (13) femur with prosthesis, (14) distal deviation pulleys, (15) perpendicular plate, (16) frame of the testing machine, (17) distal ball bearing.

The simultaneous action of muscle forces and inter-segmental resultant force resulted in a contact force at the hip joint. The ceramic head of the hip prosthesis was secured by a polyethylene cup that was connected to the plunger of the material testing machine. A three dimensional load cell (9251A, Kistler Instrumente GmbH,

Ostfildern, Germany) was mounted between the cup and the plunger of the testing machine to monitor the components of the hip contact force. In order to protect the testing machine from excessive radial loads, the plunger was decoupled from the polyethylene cup in such a way that predominantly axial loads could be transmitted to the actuator of the testing machine. Radial forces resulting from the three dimensional loading of the prosthesis head were transmitted to the machine bed through the loading frame.

The lower part of the modular frame was mounted on the bed of the servo-hydraulic testing machine and consisted of an adjustable x-y table which allowed variable positioning of the femur for different activities. The orientations of the loading ropes simulating the distally oriented muscle forces were produced by a pair of pulleys mounted on the x-y table. The distal femur was mounted on a ball bearing that exclusively permitted a transfer of forces but not moments (Figure 11)

Software was developed to control the four muscle actuators independently and to synchronise them to the material testing machine (Figure 12). The force synchronisation was achieved by expressing the magnitudes of the muscle forces to be applied by the actuators as a linear function of the inter-segmental resultant force generated by the mechanical testing machine. A force ratio specific to each of the muscle force actuators was determined from the peak muscle and inter-segmental force values derived from the computer analysis. Based on the actual value of the inter-segmental resultant force and the force ratio, the software determined the load which should be exerted by each actuator. The latter then pulled on the loading rope until the target force value was reached.

In addition, the Proportional-Integral-Derivative (PID) controller of each control path could be customised separately. The PID-values were determined iteratively in a preliminary study and saved in an initialising file. Hip joint contact and muscle force signals were recorded with an 8-channel digital data logger (Spider8 & Catman, HBM GmbH, Darmstadt, Germany) and processed with a connected personal computer.

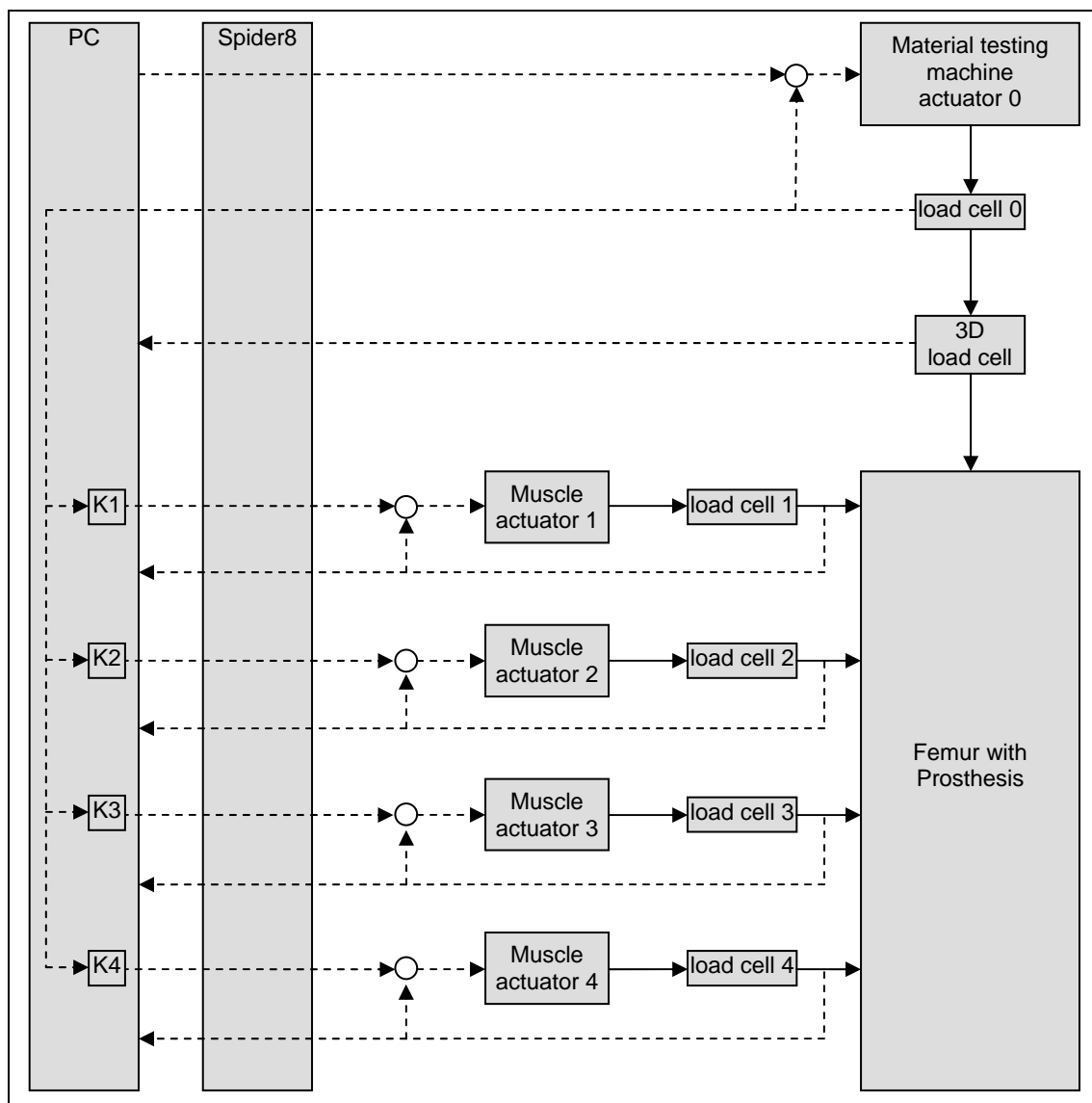


Figure 12 ▲

Operating principle of the custom-made software to control the muscle force actuators. The force applied by the material testing machine is used to synchronise the whole test set-up. The forces generated by the four muscle force actuators are continuously computed from the actual value measured by the load cell of the testing machine and a proportionality factor K specific to each of the muscle force actuators. These factors also take into account the frictional losses at the deviation pulleys of the loading ropes simulating the muscle structures.

2.3 *In vitro* assessment of primary stability

The mechanical loading set-up was then used to evaluate the primary stability of cementless hip prostheses *in vitro* by determining the load-induced relative movements at the interface between the prosthesis and the femur. Furthermore, the influence of the load generation and load transmission procedure to the proximal femur was analysed by comparing the stability of the stem-bone complex when subjected to different loading configurations and to previously published data.

2.3.1 Implants and bones

Implants

Two clinically well-established and successful cementless stems were selected for the comparative analysis of the primary stability *in vitro* (Eyb *et al.* 1993; Malchau *et al.* 1993; Schramm *et al.* 2000; Siebold *et al.* 2001; Aldinger *et al.* 2003): the CLS Spotorno (Size 11.25, Centerpulse Orthopaedics, Wintertuhr, Switzerland) and the Alloclassic SL Zweymueller (Size 4, Centerpulse Orthopaedics). Both stems aim to ensure initial stability through press-fit anchorage. This anchorage concept is characterised by a forced stem insertion into a femoral cavity prepared with slightly smaller dimensions. An accurate preparation of the prosthesis bed and a sufficient pre-stressing of the bone-implant interface are thus essential requirements for a stable press-fit fixation.

Though both stems are based on the press-fit anchorage concept, they rely on different geometrical design parameters to transmit the loads from the pelvis to the femur. The CLS stem is designed to ensure metaphyseal, inter-trochanteric load transmission and to avoid distal stress shielding (Figure 13). Axial ribs in the proximal region of the stem should increase its rotational stability and its overall fixation strength. The triple-tapered collarless stem is manufactured from titanium alloy (Ti6Al7Nb) with a grit-blasted surface. The Alloclassic SL stem, on the other hand, is a straight, collarless prosthesis based on a more distal anchorage concept with a predominantly meta-diaphyseal load transmission (Figure 13). The conical design

should allow a reliable initial fixation, while the grit-blasted surface of this likewise titanium implant should ensure rapid bone ingrowth and a long lasting fixation.

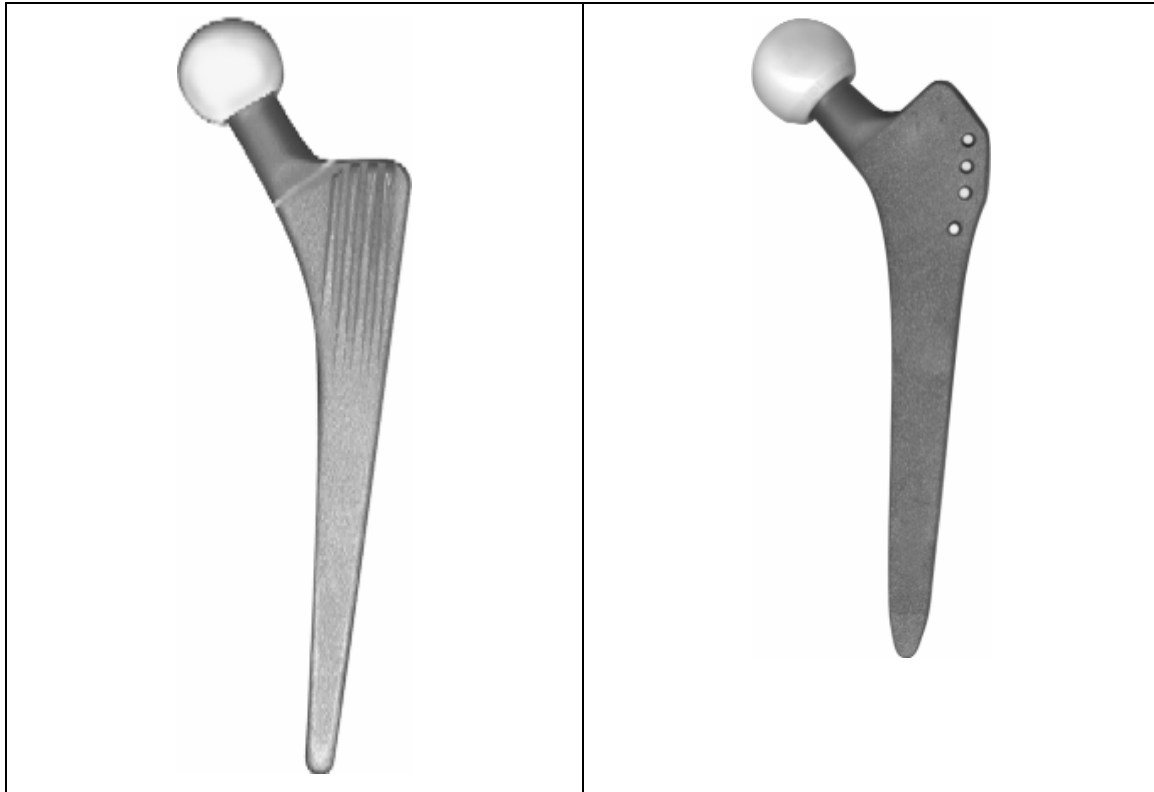


Figure 13 ▲

CLS Spotorno (left) and Alloclassic SL Zweymueller (right) stem.

For the measurement of the 3-D interface micro-movements, five levels with a total of seven single locations were selected on the prosthesis, ranging from the shoulder to the distal tip (Figure 14). The locations were distributed on the anterior, medial and posterior sides of the stem surface and were named after the corresponding level. In the case where a level contained more than one location, the letters a or b were added to differentiate: location 1 at the prosthesis shoulder centrally on the proximal surface of the stem; location 2a on the medial and location 2b on the anterior surface in the proximal stem region. In order to evaluate the rotational movement of the prosthesis, location 2b was positioned slightly medially to the femoral long axis; location 3 on the anterior surface in the middle of the

prosthesis shaft; location 4a on the anterior and location 4b on the posterior surface in the distal prosthesis region; and finally location 5 in the anterior surface at the prosthesis tip. The position of the measurement locations at the stem tip (4a, 4b and 5, Figure 14) were adjusted to the stem geometry because of the different prosthesis lengths.

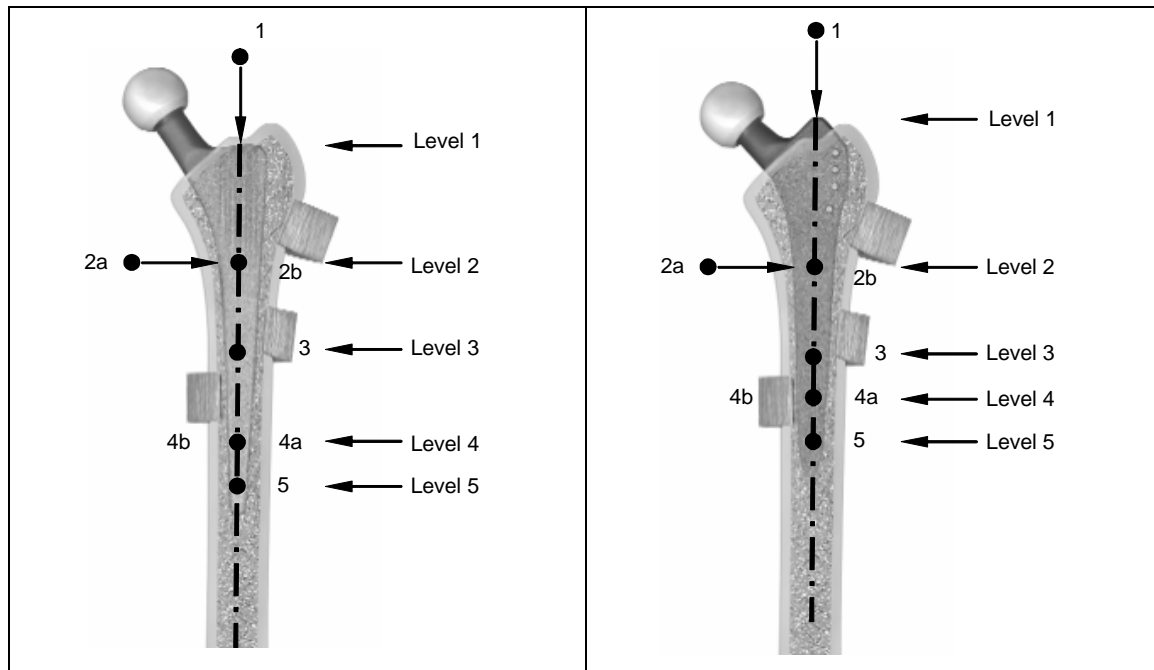


Figure 14 ▲

Locations of interface movement measurement on the surface of the CLS (left picture) and the SL prosthesis (right picture). Muscle attachments and wrapping points on the femur surface as previously determined under 2.1.2 are also represented. The detailed description of the configuration of these points is given in the following section.

In addition, each location of micro-movement measurement was assigned a single, definite orientation in which micro-movement was to be recorded: proximal-distal micro-movements at the locations 0 and 5, medial-lateral micro-movements at 2a and 4b and anterior-posterior micro-movements at 2b, 3 and 4a (Figure 15). The measurement locations were accordingly configured: perpendicularly to the orientation of micro-movement measurement, a planar surface of 4 mm in diameter was created at the locations 2a, 2b, 3 and 4a, while a 3 mm deep hole with a

diameter of 1.5 mm was drilled at the locations 4b and 5. In contrast to the other locations where micro-movements were recorded directly at the prosthesis surface and due to the space limitation, the longitudinal movement of the stem shoulder had to be recorded through a small metal bar screwed at location 1.

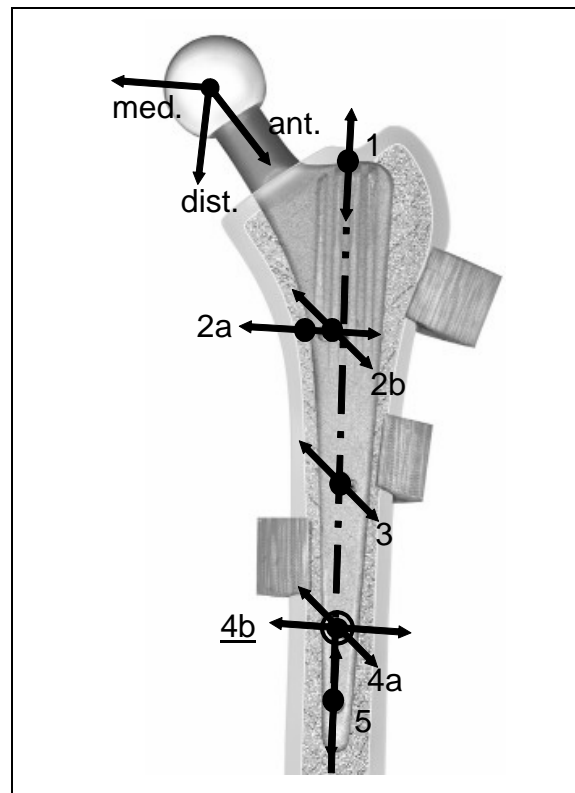


Figure 15 ▲

Orientations of movement measurement at the bone-prosthesis interface for each of the measurement locations.

Bones

To assess the stability of the selected cementless stems *in vitro*, the medium-sized composite femur (Model 3103, Sawbones Europe AB, Malmö, Sweden) used to derive the representative load profiles was chosen (Figure 16). The geometrical and anatomical structure of the composite femur resembles that of humans: polyurethane foam representing the cancellous core of the bone is surrounded by a fibre-reinforced

epoxy resin modelling the cortical bone. This architecture gives the composite femora a uniform mechanical behaviour throughout its length and consequently a structural stiffness comparable to that of human specimens. Moreover, this femur model was chosen to minimise the high inter-specimen variability in mechanical properties often associated with the use of cadaveric bones in experimental biomechanical analyses (Cristofolini *et al.* 1996).

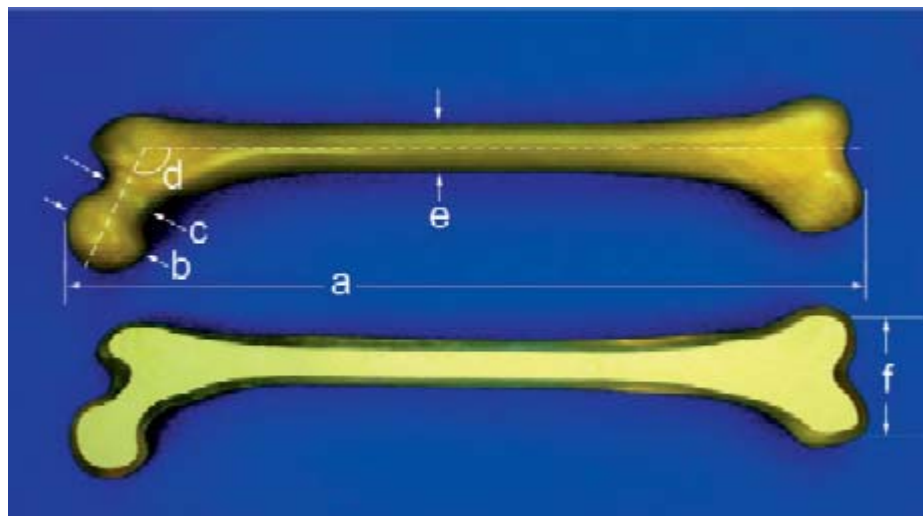


Figure 16 ▲

Composite femur used to assess the primary stability of cementless hip prostheses in vitro. a: 455 mm b: 43 mm c: 33 mm d: 135 degrees e: 28 mm f: 78 mm.

The pre-operative planning process preceding the implantation of the stem was performed by an experienced orthopaedic surgeon according to the manufacturer's recommended procedure. For both stem designs, the size which best fit into the medium-sized femora was determined using corresponding stem templates and standard frontal and lateral radiographs of the composite bones.

A clamping device was designed to enable a precise positioning and thus a reproducible preparation of the femoral cavity and a reproducible stem insertion as suggested by Monti and co-workers (1999) (Figure 17). The accuracy of the positioning of the femora within the clamping device was determined by the inter-

specimen variability of their surface contour and was evaluated to 2 mm. A rough resection of the femoral head was first performed with a conventional handsaw, after the femur was positioned within the clamping device. The clamped femur was then mounted in a Computer Numerically Controlled (CNC) machine for a more accurate preparation procedure compared to the manual procedure. The neck of the femur was milled up to the calcar region and mechanical reaming of the medullary canal was subsequently performed using appropriate chipped-tooth broaches. The orientation of the medullary cavity corresponded to an antetorsion angle of 10°.



Figure 17 ▲

Composite femur in the clamping device used to allow a reproducible preparation.

In order to transmit the muscle forces to the bone, an adhesive bond was created between the loading ropes and the femur, as the use of more invasive fixation devices such as screws was constrained by the low cortical thickness at the sites of muscle insertions. With the femur mounted in the clamping device, an area of approximately 25 mm x 25 mm, which represented the smallest surface to produce a sustainable adhesive joint with respect to the muscle forces to be transmitted, was marked around each of the muscle insertion points. The size of the curved area was limited by the dimensions of the femur and the space required for the devices to record interface movements. Using a small CNC-controlled end mill, a thin layer (maximum 0.5 mm thickness) of the cortical bone was removed (Figure 18), resulting in a homogeneous curved surface. The congruent counterparts to attach the loading ropes consisted of small fabric-based laminate components which were glued onto

the prepared muscle insertion sites with a two-part epoxy resin adhesive (Araldit 2010, Ciba GmbH, Wehr / Baden, Germany).



Figure 18 ▲

Preparation of the muscle attachments and wrapping sites on the femur surface. The femur is clamped in the custom-made device.

In addition, a tapped hole was drilled into the lateral epicondyle of the femur to attach the distal part of the tensor fascia latae and the ilio-tibial band muscles by means of a threaded pin. The distal part of the femur was configured as a ball bearing in order to limit distal joint moments and avoid unpredictable forces. For this purpose, the geometry of the femoral condyles was modified by resecting 10 mm of the distal end of the femur and screwing on a metallic socket into a longitudinal tapped hole.

Cylindrical holes with a diameter of $\varnothing 5$ mm were drilled through the cortical and the cancellous bone at the proximal femur to make the measurement locations on the prosthesis accessible. The transcortical holes also served to mount the displacement sensors which aimed at recording the relative micro-movements at the interface between the bone and the prosthesis. The sensor mounting locations were positioned as close as possible to the bone-prosthesis interface in order to minimise

the effect of the load-induced bone deformation on the relative interface movements. In fact, a sensor mounted on the femur surface at a certain distance of the measurement location may record a movement which consists of a superposition of the real interface movement and the sensor movement due to the load-induced cortical strains (Monti *et al.* 1999).

2.3.2 Mechanical testing

Test specimens

The femoral stems were implanted in the composite bones according to clinical and manufacturer-specific criteria. The prostheses were manually inserted into the reamed medullary cavity of the femora mounted in the clamping device for this purpose. To reach a stable press-fit fixation, the prostheses were impacted with the appropriate hammer to apply comparable forces to those applied intra-operatively by an orthopaedic surgeon. In order to create identical mechanical conditions for all test specimens prior to mechanical testing, the implanted femora were additionally subjected to a pre-loading. Using a material testing machine, the prostheses were pressed into the femoral cavity with an axial force up to a maximal value of 1000 N. The position and the alignment of the prostheses within the bones were evaluated at the end of the implantation procedure and X-rays of the implanted femora in the frontal and sagittal planes were performed in order to detect eventual mal-alignments of the prostheses.

To measure the relative micro-movements at the bone-prosthesis interface, the femora were instrumented at six of the seven measurement locations (2a, 2b, 3, 4a, 4b and 5, Figure 14 and Figure 15) with high-precision linear variable displacement transducers (LVDT WETA1/2mm, accuracy 0.5 μm , HBM GmbH, Darmstadt, Germany). Due to their geometry and dimensions, the LVDTs could not be directly mounted in the transcortical holes. Small plastic jigs were therefore designed to connect the LVDTs and the bones (Figure 19, Figure 20). The custom-made jigs were then press-fit into the undersized transcortical holes to ensure a stable fixation.

The LVDTs were clamped within the jigs by means of screws. The contact between the plunger of the displacement transducers and the surface of the implanted stem was realised through a metal pin of 1 mm in diameter which was screwed in the plunger (Figure 19). Relative shear movements were recorded at the positions 4d and 5 using a metal pin ($\varnothing 1$ mm) perpendicularly connected to the plunger of the LVDT (Monti *et al.* 1999). To avoid collision with the muscle attachment and loading structures, radial movements were recorded at the positions 2a, 2b, 3 and 4a. The influence of the stem roughness on the radial movement was reduced by milling a contact area of $\varnothing 4$ mm (roughness: $2.5 \mu\text{m}$) perpendicular to the transducer plunger.

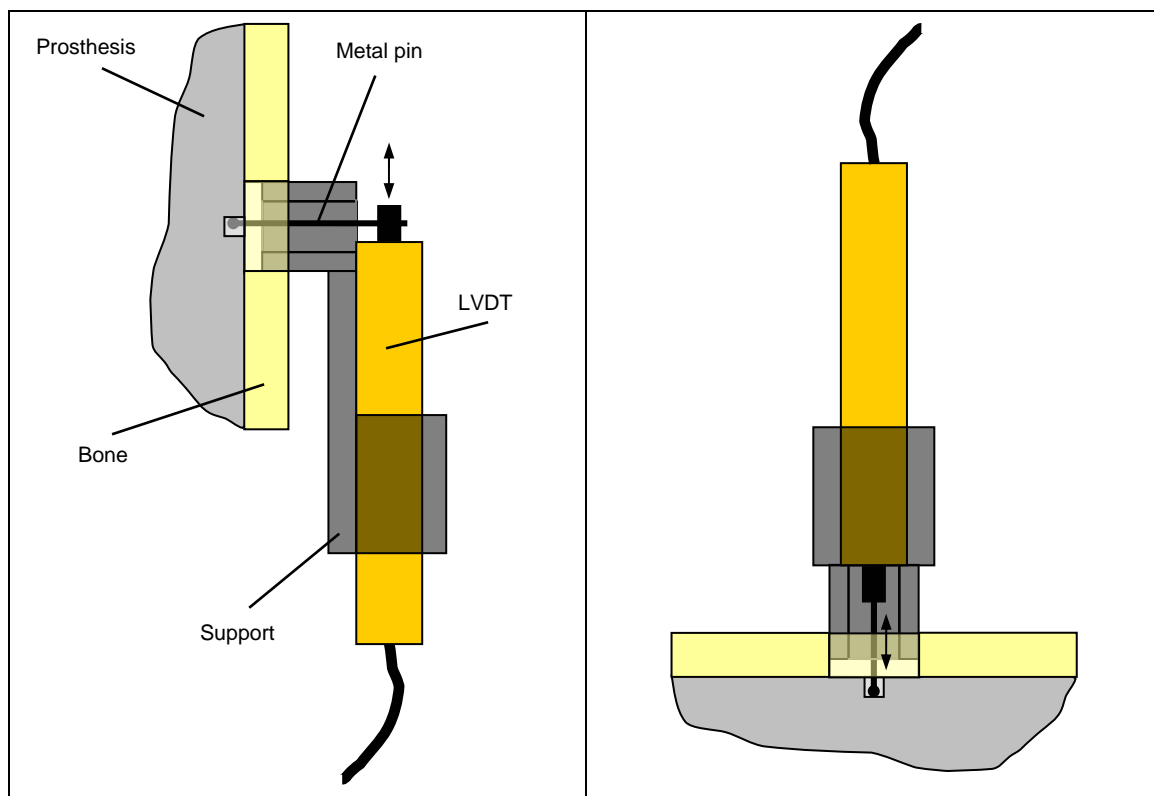


Figure 19 ▲

Principles of measurement of shear (left) and radial (right) interface movements. The movement sensor (LVDT) is mounted on a plastic support which is in turn press-fitted in a transcortical hole in the composite femur. A metal pin connected to the plunger of the LVDT contacts the prosthesis at an area that has been milled for this purpose.

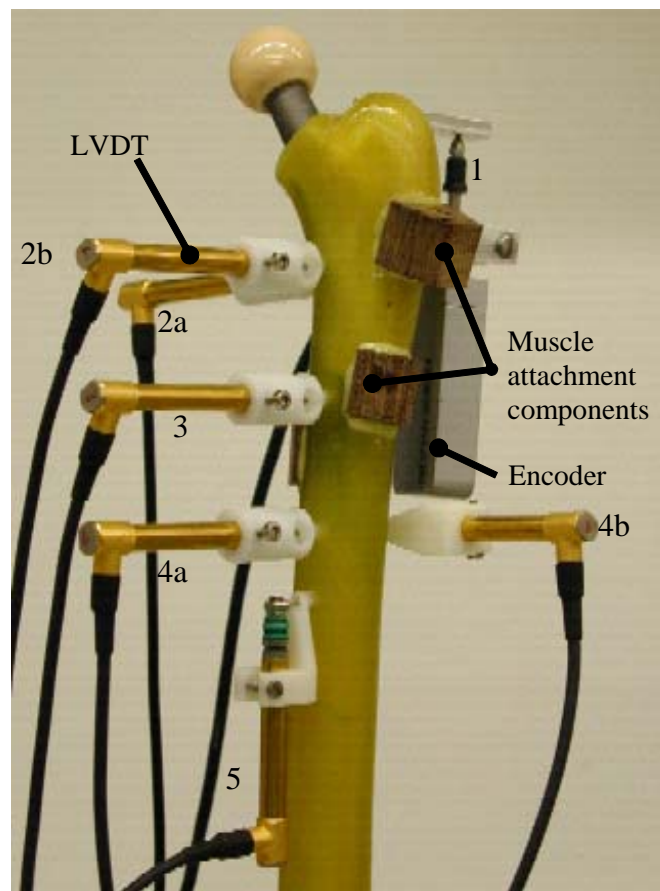


Figure 20 ▲

Composite femur implanted with a cementless hip prosthesis. The prosthesis-bone complex is instrumented with movement sensors to record the load-induced relative movements at the prosthesis shoulder and at the bone-prosthesis interface. The muscle insertion points are represented by small fabric-based laminate components which are glued onto the surface of the femur

In addition to the interface movements at the locations 2 to 5, the axial displacement of the prosthesis shoulder was measured at location 1 by means of an optical linear encoder (MT1271, accuracy 0.2 μm , Heidenhain GmbH, Traunreut, Germany). This encoder was fixed on a metal jig, which allowed an exact adjustment of the encoder with respect to the stem axis. The jig was glued to the anterior side of

the femur at the greater trochanter level and the plunger of the encoder perpendicularly contacted a small metal bar screwed at location 1 (Figure 20). The maximal deviation of the micro-movement measurement devices for repeated measurements was evaluated as 3 μm .

Study design and loading regime

A total of 24 composite femora were used to analyse the influence of active muscle force simulation, load level, patient activity and anchorage principle on the primary stability of cementless hip prostheses *in vitro*. Six femora were randomly assigned to each of the four groups (Table 3). The femora of three of the constituted groups were implanted with the proximal anchoring CLS-stem while the femora of the forth group were implanted with the distal anchoring Alloclassic SL-stem.

Table 3 ▼

Characteristics of the four groups which were included in the analysis of primary stability.

Group	Femora	Activity	Prosthesis	Muscles	%peak load
1	n = 6	Walking	CLS	Yes	50 and 75%
2	n = 6	Stair climbing	CLS	Yes	50 and 75%
3	n = 6	Stair climbing	CLS	No	50 and 75%
4	n = 6	Stair climbing	SL	Yes	50%

Three loading configurations were then defined (Figure 21). In the first configuration, six of the femora implanted with the CLS stem (group I) were subjected to a loading scenario simulating the activity of walking (8° adduction, 1° flexion). The muscular loading was exerted by the tensor fascia latae, the abductor and the vastus lateralis. The second loading configuration represented the activity of stair climbing. In addition to the muscle forces which were active in the walking configuration, forces

representing the ilio-tibial band and the vastus medialis were simulated. These loads were applied on two groups of six femora each and implanted with the CLS-stem (group II) and the Alloclassic SL-stem (group III) respectively. In both the walking and the stair climbing loading configurations, the ceramic head of the prosthesis was horizontally constrained in a polyethylene liner. The distal part of the femur was mounted on a ball bearing surface in order to limit distal joint moments and avoid unpredictable forces (Figure 22).

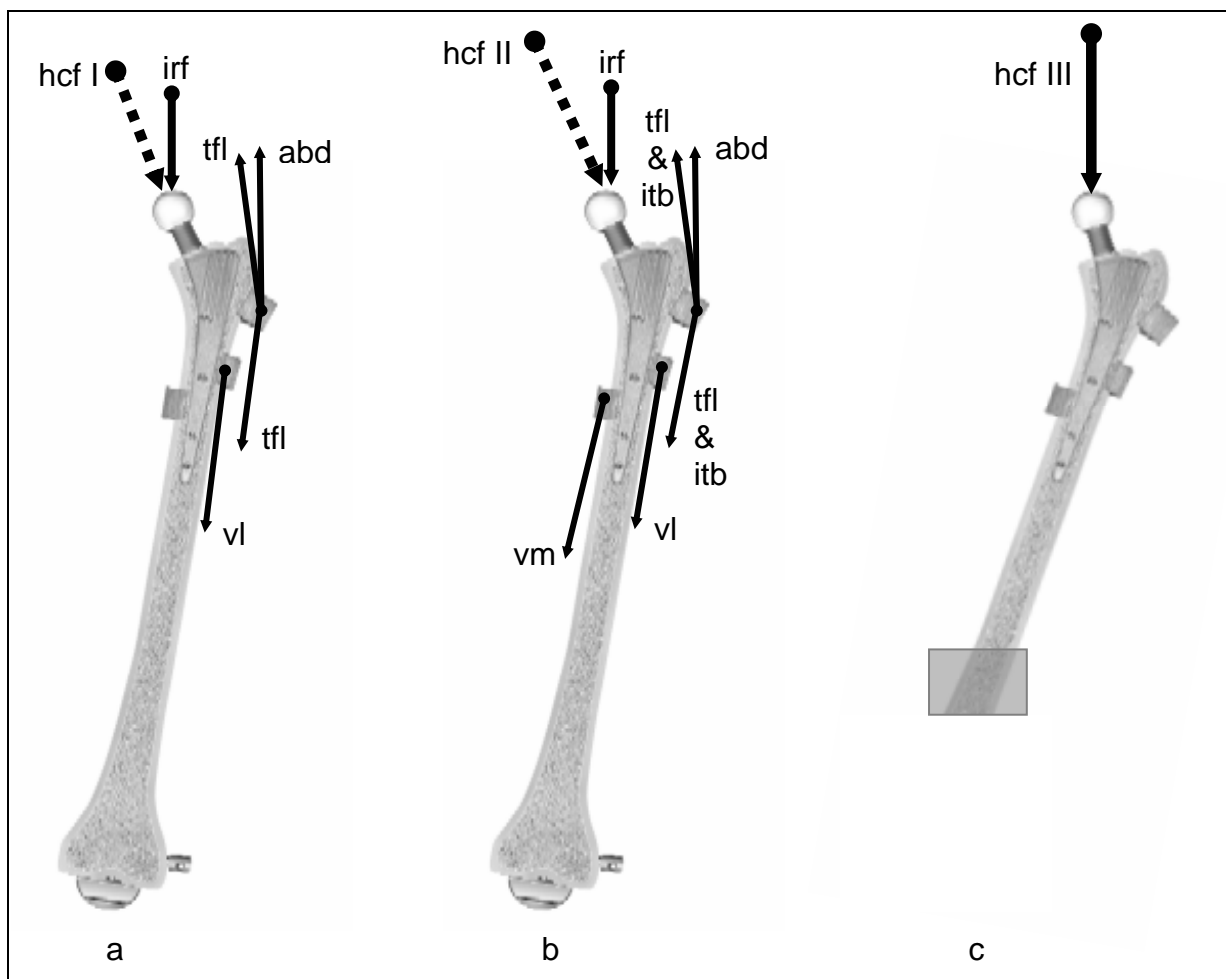


Figure 21 ▲

Loading configurations to analyse the prosthesis stability in vitro: (a) loading configuration representing walking with active simulation of muscle forces (b) loading configuration representing stair climbing with active simulation of muscle forces (c) loading configuration representing stair climbing with the same resultant joint contact force as in (b), but without active simulation of muscle forces. Hcf: hip contact force; irf: intersegmental resultant force; tfl: tensor fascia latae; itb: ilio tibial band; abd: abductor; vm & vl: vastus medialis & lateralis.

For comparison with conventional primary stability tests and to analyse the influence of the active simulation of muscle forces, the remaining six femora implanted with the CLS stem (group IV) were loaded only with the resultant hip contact force measured during stair climbing with active simulation of muscle forces. In this case, the prosthesis head was unconstrained and the femur was fixed with polymethylmethacrylate (PMMA) at a position 300 mm distally of the head.

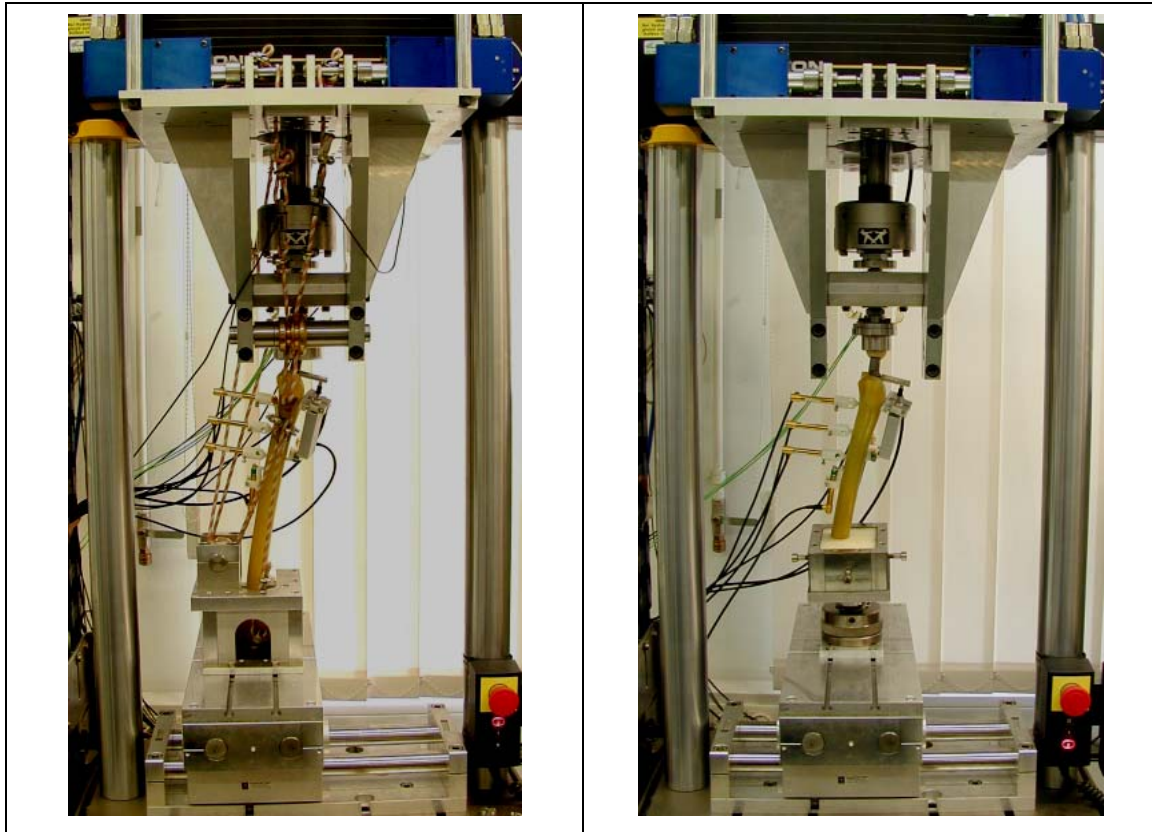


Figure 22 ▲

Test sample in the mechanical loading set-up. Simulation of stair climbing with active muscle forces (left) and with the hip contact force only (right).

Each test specimen was positioned in the mechanical test set-up and the loading ropes were clamped at the prepared muscle attachment sites (Figure 22). The test specimens were loaded successively with 50 and 75 percent of the computed peak loads, corresponding to a joint contact force of 1062 N / 1174 N (walking / stair climbing) and 1593 N / 1761 N respectively; Loads above these levels resulted in mechanical damage of the glued muscle attachment components. The

femora in group IV were loaded only with 50% of the peak load, since the influence of the load level could be determined for the three other groups. For each load level, a sinusoidal load shape with a frequency of 0.25 Hz was applied. The number of loading cycles was limited to 1000: after this, no considerable slope of the displacement-time curve was observed.

Data evaluation and statistical analysis

To determine the primary implant stability, the load-induced relative movements at the bone-prosthesis interface were continuously recorded throughout the testing period. The total interface movements were the summation of the elastic (recoverable) and the plastic (unrecoverable) movement components. The average elastic movement components were evaluated during the last 100 cycles, while the plastic components were determined between cycle 100 and cycle 1000 of the considered load level.

In addition to the interface movements, the vertical movement of the head of the prosthesis was recorded. Furthermore, the forces applied on the femur through the loading ropes as well as the three components of the resultant hip contact force were recorded. In order to evaluate the accuracy of the musculoskeletal loading at the hip *in vitro*, the measured muscle forces and the resultant contact force at the hip joint were compared to default values, which were taken from musculoskeletal analyses validated with *in vivo* measurement data.

Statistical analysis was performed using the Mann-Whitney U test (SPSS 10) to assess significant changes in interface movement magnitudes. Comparisons were established between the interface movements recorded under the loading configurations with and without active simulation of muscle forces, under the walking and stair climbing configurations and for the proximal and distal anchoring stems. Differences were considered statistically significant when the p value was less than 0.05.

3 Results

3.1 Simplified loading conditions

3.1.1 Model simplification and validation

The final, most simplified model which predicted a physiological-like loading of the hip joint consisted of 15 muscles (Figure 23). Similar to the complex model, a reduced number of muscles in the simplified model were simultaneously activated, depending both on the patient activity to be performed and on the considered instant of the gait cycle. The curve progression and magnitudes of the hip contact forces calculated with the simplified musculoskeletal model for a complete gait cycle compared well with the *in vivo* forces for the “typical patient” for both activities (Figure 24).

During the walking cycle, the forces predicted by the simplified model were slightly higher than the *in vivo* forces. The musculoskeletal loading conditions at the hip were characterised by a dominant inferior-superior joint contact force component. The model predicted two force peaks in this component, during early and late stance phase. The largest resultant hip contact force (262% BW) acted at the beginning of the gait cycle. The medio-lateral (max. 84 %BW) and the anterior-posterior (max. 28 %BW) shear force components were considerably smaller than the inferior-superior forces. At the instance of maximum *in vivo* hip contact force, the force calculated with the simplified model of the hip muscles differed by approximately 7% from the *in vivo* value obtained for the “typical patient”.

During stair climbing, the calculated hip joint contact forces slightly overestimated the *in vivo* forces for the “typical patient” during the early stance phase, but underestimated the forces during late stance (Figure 24). Similar to walking, the peak joint contact force at the hip during stair climbing was calculated

during the early stance phase (278% BW). Whilst the peak hip contact forces were generally larger than during walking, the most pronounced difference in amplitude was observed in the anterior-posterior joint contact force. This force component was twice as large during stair-climbing than during walking. The instance of maximum hip contact force coincided with the peak in anterior-posterior force and also represented the load profile for maximum torsion acting on the shaft of the implant. At this instance, the difference between the calculated and the *in vivo* hip contact force of the “typical patient” was approximately 10%.

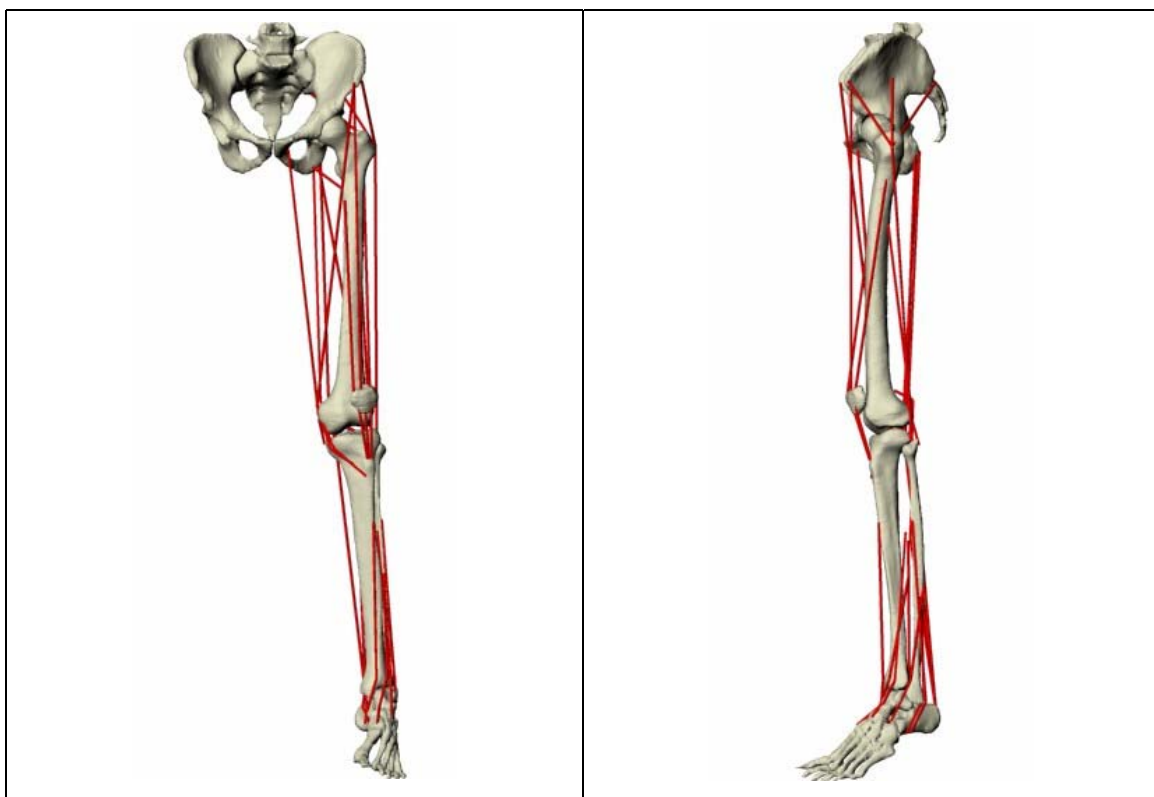


Figure 23 ▲

Frontal and lateral view of the simplified model of the lower extremity which is characterised by a reduced number of muscle fibres, particularly in the proximal femur, compared to the complex configuration (see Figure 6).

During the simplification process it was found that the simplification of the hip muscles to a single abductor and adductor muscle as well as the removal of most muscles with small forces was possible while maintaining physiological-like activation of the remaining muscles and hip joint loads comparable to the *in vivo* data. Whilst

the absolute force magnitudes of ilio-tibial tract and the tensor fasciae latae were found to be low, the forces in the remaining muscles and the hip joint contact forces were drastically increased when these structures were not included in the model. In fact, hip contact forces of more than 5 times body weight during walking, and up to 7 times body weight (BW) during stair climbing were calculated.

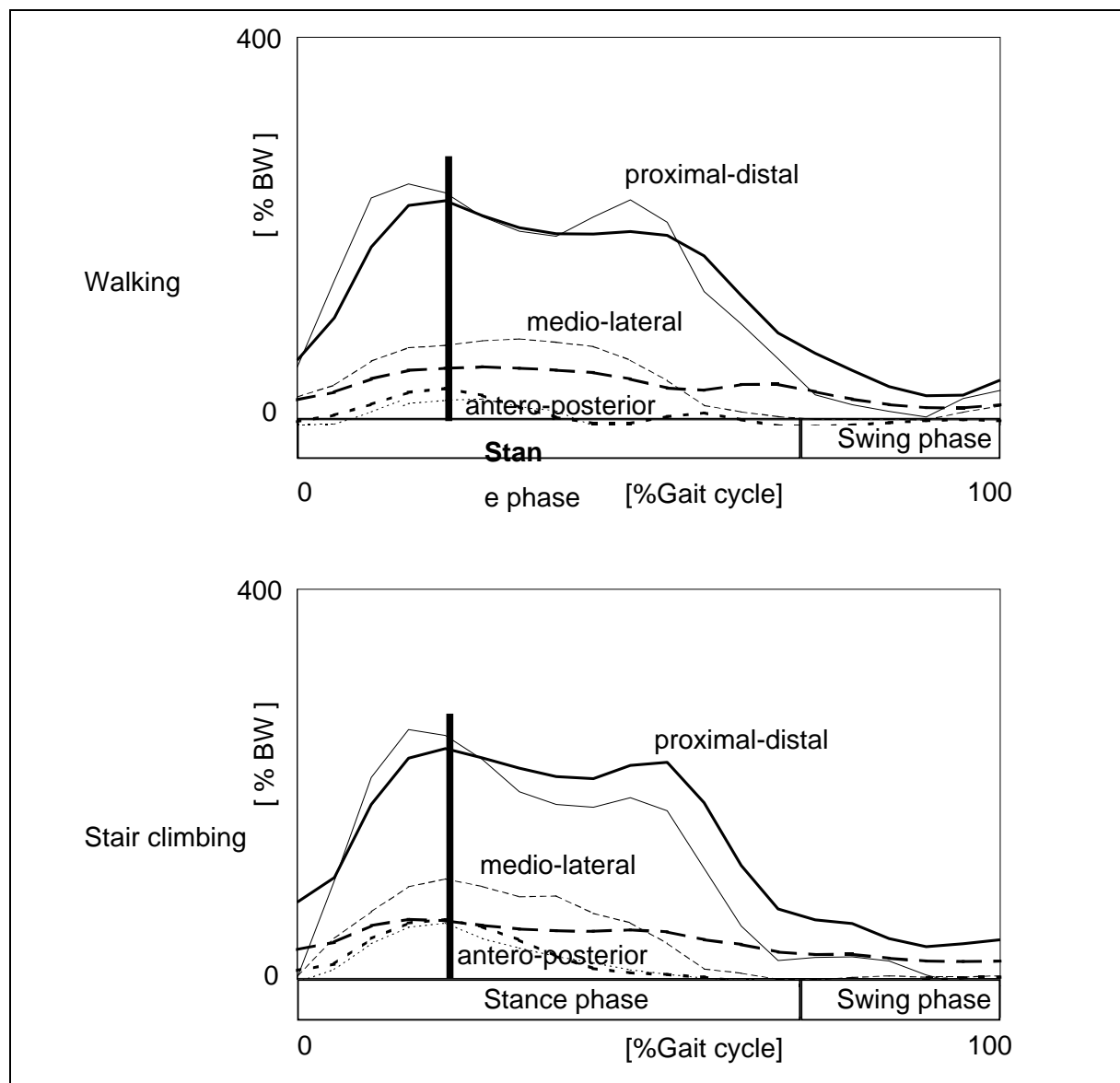


Figure 24 ▲

Components of the hip joint force during walking (top) and stair climbing (bottom): computed (thin lines) and *in vivo* (thick lines) values. BW: Body Weight

3.1.2 Load profiles for *in vitro* testing

At the instant of the measured peak resultant contact force (early stance phase at 25% gait cycle) during walking, the largest muscle forces were computed for the abductor (104 %BW), the vastus lateralis (95 %BW) and the tensor fasciae latae (19 %BW). At the same instant, the largest contribution to the hip contact force from the group of the two joint hip muscles came from the semimembranosus (60% BW). A higher activity of the muscles spanning both the hip and knee joint, i.e. the rectus femoris (max. 80% BW), the gracilis (max. 27% BW) and the sartorius (max. 14% BW) was observed, particularly at the end of the stance phase and during the swing phase of the cycle. The largest forces in the gastrocnemi, which attach at the distal femur, were also found towards the end of the stance phase (up to 31% BW).

Analysis of the muscle activity during stair climbing showed that the peak force in the abductors was increased by about 10% compared to walking (114% BW). Most importantly, the anterior-posterior component of the abductor force was increased more than 6-fold. The largest muscle forces during stair climbing were calculated for the vastus lateralis (137% BW) and the vastus medialis (270% BW). Whilst a considerable peak force in the two joint semitendinosus muscle (115% BW) was found during early stance phase, activity of the muscles spanning both hip and knee joint was observed mainly during the late stance and swing phase, with only small force magnitudes (up to 29% BW).

Based on the musculoskeletal loading conditions determined for the complete gait cycles of both activities, the simplified load profile for the proximal femur was then generated for the single instant of maximum *in vivo* hip contact force in each of the walking and the stair climbing cycles. For the two selected instances, a total of five muscles exerted forces at the proximal femur (Figure 25): the abductor muscle inserting at point P1 with a proximally-oriented force vector, the ilio-tibial tract and the tensor fascia latae wrapped at point P1 and divided into a proximally- and a distally-orientated part, the vastus lateralis inserting at point P2 and the vastus medialis inserting at point P3, both with distally-orientated force vectors.

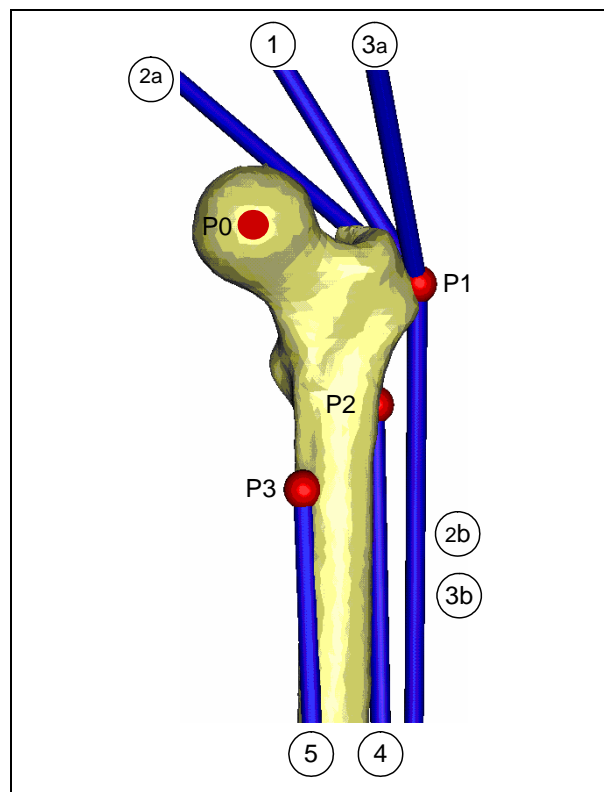


Figure 25 ▲

Activated muscles derived from the simplified model at the instance of maximum in vivo joint contact force. 1: abductor 2a: Ilio-tibial tract, proximal part; 2b Ilio-tibial tract, distal part; 3a: tensor fascia latae, proximal part; 3b tensor fascia latae, distal part; 4: vastus lateralis; 5: vastus medialis; P0: hip joint center; P1-P3: wrapping and attachment sites of the muscles.

The directions of the muscle force vectors were identical for the patient and for the composite femur. Only the positions of the attachments and wrapping points on the surface of the composite femur were relocated to match the local geometry. The lowest position adjustment was observed for the z-coordinates (inferior-superior direction, maximum 2.6 mm), followed by the x-coordinates (medio-lateral direction) with up to 4.2 mm (Table 4). Conversely, adjustments of up to 6.9 mm were necessary for the y-coordinates in the anterior-posterior direction. This resulted in an

increase in hip joint contact force magnitude of 7% for the walking and 10% for the stair climbing configuration.

Table 4 ▼

Three dimensional coordinates of the attachments and wrapping points of the active forces at the instance of maximum in vivo loads with respect to the patient and the Sawbones femur.

Patient femur	Coordinates [mm]		
Points	x	y	z
P0	0.0	0.0	0.0
P1	-67.8	-12.0	-35.4
P2	-49.4	-5.0	-79.5
P3	-18.8	8.8	-106.2

Sawbones femur	Coordinates [mm]		
Points	x	y	z
P0	0.0	0.0	0.0
P1	-69.9	-6.7	-32.8
P2	-53.1	1.9	-77.3
P3	-23.0	15.8	-104.6

The derived simplified model for the proximal femur of the “typical patient” consisted of a set of three active muscles during walking: the abductor, the tensor fascia latae and the vastus lateralis (Table 5). During stair climbing, the ilio-tibial tract and the vastus medialis were additionally activated (Table 6). The proximal and the distal part of both the tensor fascia latae and the ilio-tibial tract transmitted their force at a common wrapping point (P1). Due to their similar loading mechanism, these two muscles were therefore resolved to a single, two-part force vector to simplify the implementation into a mechanical *in vitro* loading set-up. In the same manner, two-joint muscles which were activated at the instance of maximal *in vivo* joint contact

force and the inter-segmental resultant force were also resolved to a single force acting at the joint centre, in addition to the load due to bodyweight.

Table 5 ▼

Vector coordinates of the active forces at the instance of maximum in vivo loads with respect to the patient femur. The forces are derived from the simplified model of a THA patient. The numbers in the brackets refer to the representation of the force components in Figure 25.

Walking, Patient femur

Force	x [N]	y [N]	z [N]	Resultant	Acts at Point
Hip contact	-451.4	-274.2	-1916.1	1987.6	P0
Intersegmental resultant & two-joint muscle	93.6	-141.3	-1082.6	1095.8	P0
Abductor (1)	484.9	35.9	723.1	871.4	P1
Tensor fascia latae, proximal part (3a)	60.2	97.0	110.4	158.8	P1
Tensor fascia latae, distal part (3b)	-4.2	-5.9	-158.8	159.0	P1
Vastus lateralis (4)	-7.5	154.7	-776.6	791.9	P2

Stair climbing, Patient femur

Force	x [N]	y [N]	z [N]	Resultant	Acts at Point
Hip contact	-504.6	-515.7	-2010.9	2136.4	P0
Intersegmental resultant & two-joint muscle	207.6	-254.4	-1154.8	1200.6	P0
Abductor (1)	596.6	245.1	722.5	968.5	P1
Ilio-tibial tract, proximal part (2a)	89.4	-25.5	108.9	143.2	P1
Ilio-tibial tract, distal part (2b)	-4.3	-6.8	-143.0	143.2	P1
Tensor fascia latae, proximal part (3a)	26.4	41.7	24.7	55.2	P1
Tensor fascia latae, distal part (3b)	-1.7	-2.6	-55.3	55.4	P1
Vastus lateralis (4)	-18.7	190.6	-1149.7	1165.5	P2
Vastus medialis (5)	-74.9	337.0	-2273.0	2299.1	P3

Table 6 ▼

Vector coordinates of the active forces at the instance of maximum in vivo loads with respect to the composite Sawbones femur. The forces are derived from the simplified model of a THA patient. The numbers in the brackets refer to the representation of the force components in Figure 25.

Walking, Sawbones femur

Force	x [N]	y [N]	z [N]	Resultant	Acts at Point
Hip contact	-749.8	-75.4	-1985.4	2123.6	P0
Intersegmental resultant & two-joint muscle	-162.4	-16.8	-1172.3	1183.6	P0
Abductor (1)	517.6	-28.8	700.5	871.4	P1
Tensor fascia latae, proximal part (3a)	69.8	87.4	112.6	158.7	P1
Tensor fascia latae, distal part (3b)	-11.5	3.5	-158.6	159.0	P1
Vastus lateralis (4)	-34.0	199.2	-765.7	791.9	P2

Stair climbing, Sawbones femur

Force	x [N]	y [N]	z [N]	Resultant	Acts at Point
Hip contact	-987.1	-319.1	-2107.0	2348.5	P0
Intersegmental resultant & two-joint muscle	-225.4	-141.9	1272.1	1299.7	P0
Abductor (1)	639.4	174.4	706.2	968.5	P1
Ilio-tibial tract, proximal part (2a)	92.7	-36.0	103.1	143.2	P1
Ilio-tibial tract, distal part (2b)	-10.9	1.6	-142.8	143.2	P1
Tensor fascia latae, proximal part (3a)	29.5	38.9	25.7	55.2	P1
Tensor fascia latae, distal part (3b)	-4.3	0.7	-55.2	55.4	P1
Vastus lateralis (4)	-59.9	257.1	1135.2	1165.5	P2
Vastus medialis (5)	-158.2	470.3	-2244.9	2299.1	P3

3.2 Mechanical loading set-up

3.2.1 Evaluation of the set-up

Both the simulated muscle forces and the resulting force at the head of the prosthesis exhibited a similar time dependent progression during walking and stair climbing. The loading and unloading cycles of all muscle force actuators were synchronous and the peak resultant hip contact force occurred at the time of maximum muscle activity (Figure 26). No drift of the simulated muscle forces occurred during the whole test period.

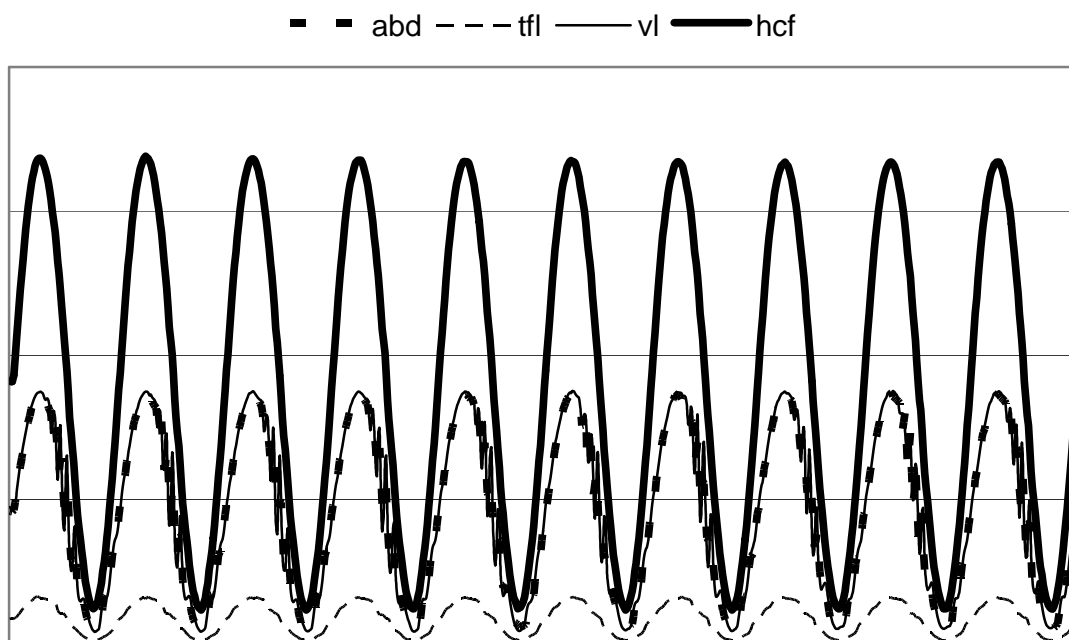


Figure 26 ▲

Curve progression of the simulated muscle forces and the resultant joint contact force at the head of the prosthesis. abd: abductor muscle; tfl: tensor fascia latae; vl: vastus lateralis; hcf: hip contact force.

Although both the ceramic head of the prosthesis and the distal part of the femur were secured in the test set-up by means of a polyethylene cup and a ball bearing respectively, the position of the implanted femur remained constant throughout the testing time. During the loading phase, however, the femur experienced a slight backwards rotation, particularly in the loading configuration representing stair climbing. In the subsequent unloading phase, the femur was rotated to its initial position. The cyclical rotation of the instrumented femur was coupled with minor bending deformations. Despite this, no interference was observed between the loading ropes and the sensors recording the load-induced micro-movements at the bone-prosthesis interface. The most important deformation was observed at the x-y table at the instance of maximum musculoskeletal loading. Due to the combined action of the hip contact force and the reaction forces at the deviation pulleys of the distally orientated muscles, the base plate of the x-y table was subjected to perceptible bending deformations.

At the 50% load level, the generated muscle forces could be applied via the loading ropes to the instrumented femur mounted in the testing machine. However, occasionally at the 75% load level and for almost every femur at the 100% load level a mechanical damage of the adhesive bonds connecting the loading ropes to the femur occurred. The most frequent failure was observed for the attachment site of the abductor muscle at the greater trochanter. An analysis of the failed bonds showed that the interface between the two-part adhesive and the femur was more vulnerable than the one between the adhesive and the laminate components used to attach the loading ropes.

3.2.2 Accuracy of load simulation

In order to evaluate the accuracy of the muscle forces which were generated by the muscle force actuators and subsequently applied to the test specimen, the forces measured in the loading ropes were analysed. A comparison between the measured forces and the corresponding computed target issued from the musculoskeletal analysis values showed moderate differences in magnitude. The median deviation at

the instance of maximum loading during walking did not exceed 2.1% (Table 7). In general, the measured muscle forces were slightly higher than the computed values. However, the differences were within the accuracy of the force sensors and were therefore not significant.

Similar values were detected for the muscle forces measured during the activity of stair climbing. In this case also, the applied forces were up to 1.6% higher than the computed values, except for the vastus medialis where a median deviation of -11.7% was detected, indicating that the applied force was lower than the computed value (Table 7). In general, the deviations detected during stair climbing tended to be higher than those detected during walking.

Table 7 ▼

Average error of the in vitro applied/measured muscle forces with respect to computed values at the instance of maximum loading (peak of the sinusoidal curve) during walking and stair climbing. A positive deviation indicates that the generated force exceeds the target force, and vice versa.

Muscle	Median deviation (range) [%]	
	Walking	Stair climbing
Abductor	0.4 (-0.1 ; 1.0)	0.5 (-1.1 ; 0.8)
Ilio-tibial tract & tensor fascia latae	-	0.9 (-0.2 ; 1.6)
Tensor fascia latae	1.1 (0 ; 2.1)	-
Vastus lateralis	0.4 (-0.1 ; 1.0)	0.9 (-0.8 ; 1.4)
Vastus medialis	-	-11.7 (-13.6 ; 4.0)

The hip contact force was computed based on the force components measured at the prosthesis head and also compared with the target value. The resultant hip joint force at the head during walking averaged $967 \text{ N} \pm 10 \text{ N}$ and was 4% lower than the computed target value (Table 8). Increasing the load level from 50 to 75% also

led to an increased deviation with respect to the computed values. In this case, a 8% lower resultant force was registered at the head of the prosthesis.

Comparable errors were registered in the stair climbing configuration. The resultant hip joint force computed from the three force components measured at the head of the prosthesis *in vitro* were below the target values issued from the musculoskeletal analyses, both at the 50 and at the 75% load levels (Table 8). The mean error at the instance of maximum muscle force averaged 5% and 9% at the 50% and at the 75% load levels respectively.

Table 8 ▼

Magnitudes and directions of the hip contact forces measured at the head of the prosthesis for the load cases walking (hcf I) and stair climbing (hcf II) with active simulation of muscle forces, and stair climbing with no active simulation of muscle forces (hcf III). The numbers in parentheses indicate the percentage of the measured values to the calculated target values from Table 5 and Table 6, with respect to the load level (50 or 75% of the peak loads).

	Hip contact forces measured <i>in vitro</i>			
	Magnitude [N], mean \pm SD (% calculated value)		Direction [°], mean \pm SD	
	50% load level	75% load level	Adduction	Flexion
Hcf I	967 \pm 10 (46)	1414 \pm 27 (67)	17 \pm 0.3	4 \pm 0.4
Hcf II	1051 \pm 26 (45)	1555 \pm 10 (66)	20 \pm 1.9	6 \pm 1.4
Hcf III	1051 \pm 0.1 (45)	1555 \pm 0.4 (66)	20	6

In the loading configuration with no active simulation of muscle forces, the hip contact force measured during stair climbing with active simulation of muscle forces was directly applied to the head of the prosthesis and controlled by the load cell of the material testing machine. Consequently, the measured-to-computed force ratio was in both cases identical. Moreover, the direct application of the hip joint force

through the actuator of the testing machine led to a much lower standard deviation obtained in the configuration without active simulation of muscle forces (0.1 to 0.4N).

In addition to its magnitude, the direction of the hip contact force applied *in vitro* was derived from the force components measured at the prosthesis head. The resultant force which acted at the head of the prosthesis exhibited, with $17^\circ \pm 0.3^\circ$ for walking and $20^\circ \pm 1.9^\circ$ for stair climbing, lower adduction angles compared to the *in vivo* values (21° and 25° respectively). Larger deviations were registered for the flexion angles of the hip contact forces. While a lower angle value was determined for stair climbing ($6^\circ \pm 1.4^\circ$ vs. 9°), the flexion angle of hip contact force during walking ($4^\circ \pm 0.4^\circ$) was larger than the *in vivo* value (2°).

3.3 Primary stability

3.3.1 Implantation procedure

A machined reaming of the medullary canal was performed in order to minimise the influence of the canal preparation procedure on the quality of the prosthesis bed. Most of the femora exhibited a homogeneous distribution of the reamed cancellous bone structure within the medullary cavity. In the femora which were implanted with the metaphyseal anchoring prostheses (CLS), however, the cancellous bone was completely removed in parts of the diaphyseal cavity of the femur.

In spite of the slight variations in the surface contour of the composite femora which affected the positioning of the femora within the clamping device, a good match between the positions of the transcortical holes and the positions of the measurement locations on the stem surface could be observed after implantation. All measurement locations were therefore accessible as planned, even after pre-loading the implanted femora in the testing machine prior to mechanical testing, since no considerable displacement of the loading actuator occurred.

The assessment of the X-rays of the implanted femora showed that all prostheses achieved a good alignment in the femur (Figure 27). No varus (twisted inward) or valgus (twisted outward) alignment of the prosthesis occurred. Furthermore, a tight fit could be observed both in the metaphyseal and the diaphyseal regions with the Alloclassic SL stem, while the CLS stem exhibited a metaphyseal tight fit and, as expected, an unobstructed tip in the medullary canal.



Figure 27 ▲

Anterior-posterior X-rays of a CLS (left) and a SL prosthesis (right) implanted in a composite femur.

3.3.2 Muscle force simulation and interface movements

In order to analyse the influence of the mode of generating and transmitting musculoskeletal loads to the proximal femur when assessing the primary stability of cementless hip prostheses, the plastic and elastic interface movements recorded during stair climbing with and without active simulation of muscle forces were compared. Under the loading regime with no active simulation of muscle forces, i.e. when the implanted femur was loaded only by the resultant joint contact force applied

to the unconstrained prosthesis head, similar magnitudes of plastic movements were recorded at almost all measurement locations (Figure 28, bottom).

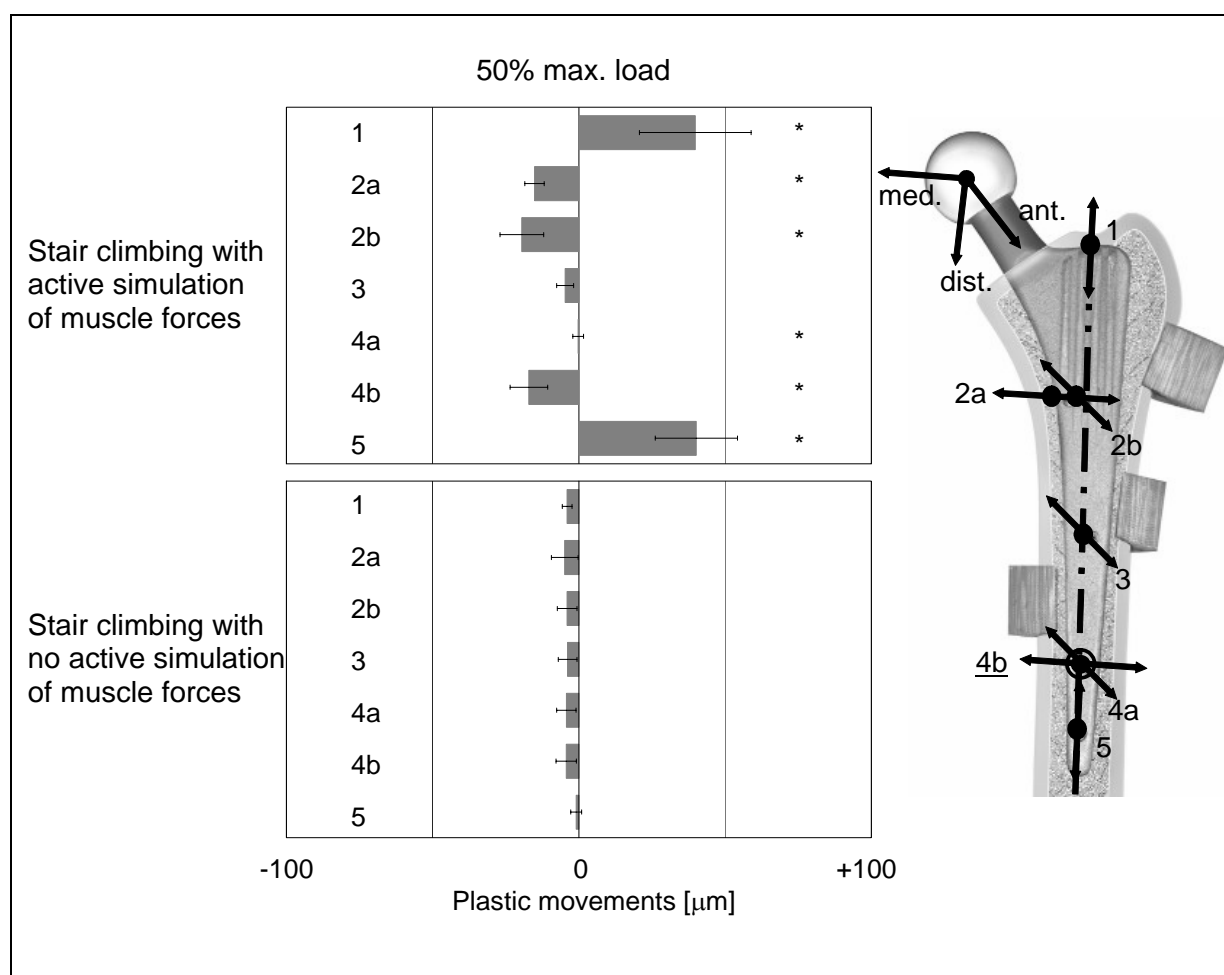


Figure 28 ▲

Plastic interface movements measured during stair climbing with (top) and without (bottom) active simulation of muscle forces at a 50% load level. The directions of micro-movements at the seven locations are defined as follows: proximal-distal movements at locations 1 and 5, medio-lateral movements at 2a and 4b and anterior-posterior movements at 2b, 3 and 4a. The coordinate system at the prosthesis head shows the positive orientation in each measurement direction. The transducer readouts at locations 1 and 5 resulted from the superposition of the longitudinal movement and the medio-lateral tilt of the stem. * $p < 0.05$.

According to the directions of the plastic movements at the measurement locations, the prosthesis was subjected to a slight valgus tilt in the medio-lateral plane and no substantial distal migration occurred at the stem tip level. In fact, the

movement transducers at locations 1 and 5 exhibited negative values, suggesting a proximally-orientated plastic movement of the stem. Overall, the plastic movements at any measurement location under 50% of the peak force without active simulation of muscle forces did not exceed $5 \pm 5 \mu\text{m}$ (Table 9).

Table 9 ▼

Values of the plastic and elastic interface movements recorded during stair climbing with (left) and without (right) active simulation of muscle forces at a 50% load level.

Location	Interface micro-movements at 50% max. load (mean (SD)) [μm]			
	Active simulation of muscle forces		No active simulation of muscle forces	
	plastic	elastic	plastic	Elastic
1	40 (19)	9 (2)	-4 (2)	-5 (2)
2a	-15 (3)	-9 (3)	-5 (5)	-5 (1)
2b	-20 (7)	-50 (5)	-4 (3)	-1 (0)
3	-5 (3)	-8 (3)	-4 (3)	-0 (0)
4a	0 (2)	1 (2)	-4 (3)	-1 (0)
4b	-17 (6)	-9 (3)	-4 (3)	-1 (1)
5	40 (14)	14 (3)	-1 (2)	-3 (3)

Under the active simulation of muscle forces, the prostheses exhibited a different pattern and magnitude of plastic movements. In this case, a larger range of plastic movements was observed among the different measurement locations (Figure 28, top). The largest plastic movements at the 50% load level averaged $40 \pm 14 \mu\text{m}$ and were recorded principally in the longitudinal direction. In addition, the prosthesis experienced a pronounced plastic posterior movement at location 2b ($20 \pm 7 \mu\text{m}$, Table 9) which indicated rotation of the implant within the bone. Although a lateral movement of the prosthesis also occurred in this case, it did not represent the predominant component. At most of the locations, the plastic movements recorded during stair climbing with active simulation of muscle forces were significantly larger than in the load configuration with the hip contact force only (Figure 28).

The patterns of the elastic movement components followed that of their plastic counterparts. Again, significantly smaller elastic movement magnitudes were recorded with the femur loaded with the hip contact force only, compared to those registered under active simulation of muscle forces (Figure 29); the largest elastic movements measured under these two loading regimes averaged $7 \pm 2 \mu\text{m}$ and $50 \pm 5 \mu\text{m}$ respectively (Table 9).

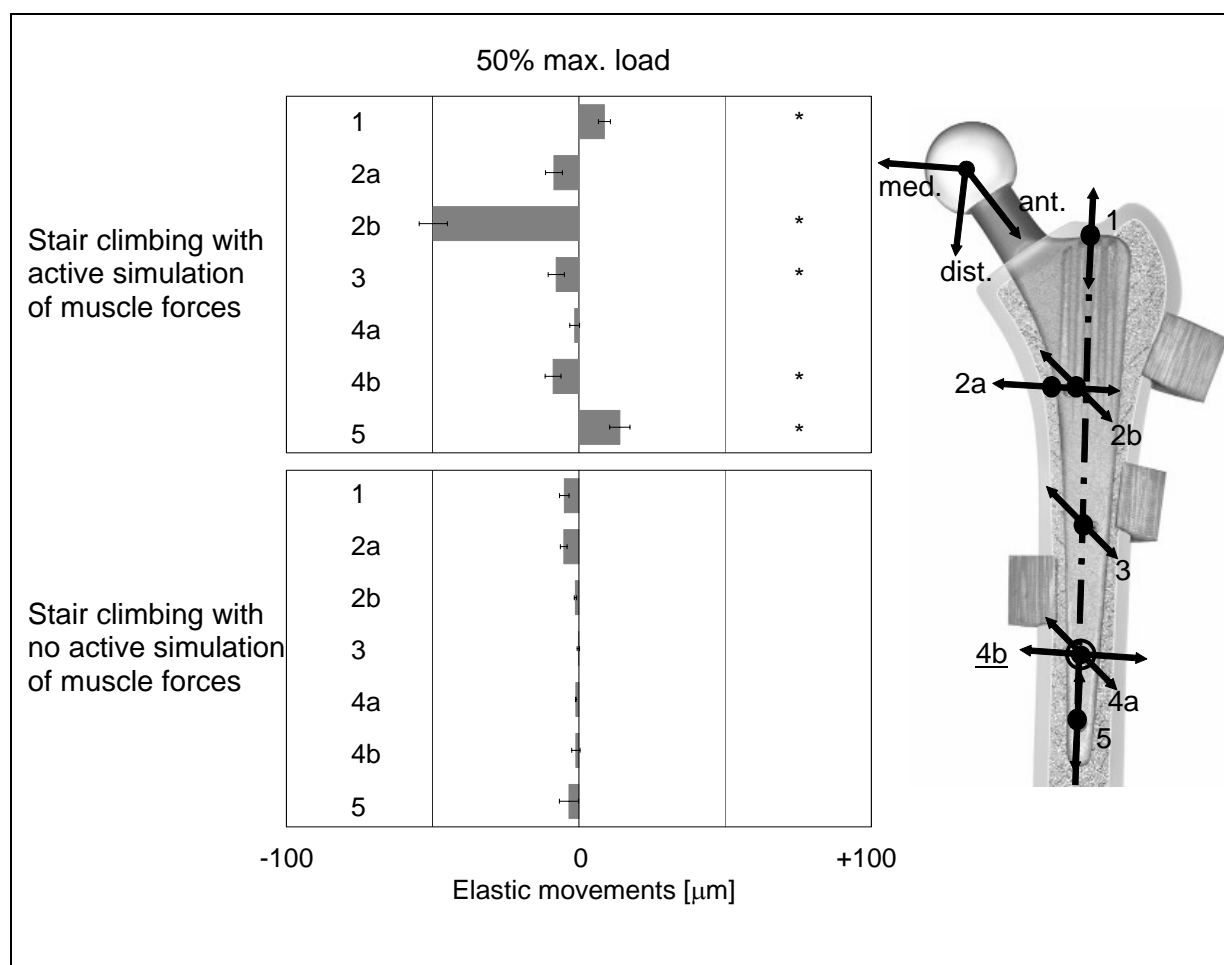


Figure 29 ▲

Elastic interface movements measured during stair climbing with (top) and without (bottom) active simulation of muscle forces at a 50% load level. The directions of micro-movements at the seven locations are defined as follows: proximal-distal movements at locations 1 and 5, medio-lateral movements at 2a and 4b and anterior-posterior movements at 2b, 3 and 4a. The coordinate system at the prosthesis head shows the positive orientation in each measurement direction. The transducer readouts at locations 1 and 5 resulted from the superposition of the longitudinal movement and the medio-lateral tilt of the stem. * $p < 0.05$.

Raising the magnitudes of the applied forces from 50 to 75% of the peak loads led as expected to an increase in the plastic movement components, but not to different patterns of interface movements, both for the loading configuration with and without active simulation of muscle forces (Compare Figure 28 and Figure 30).

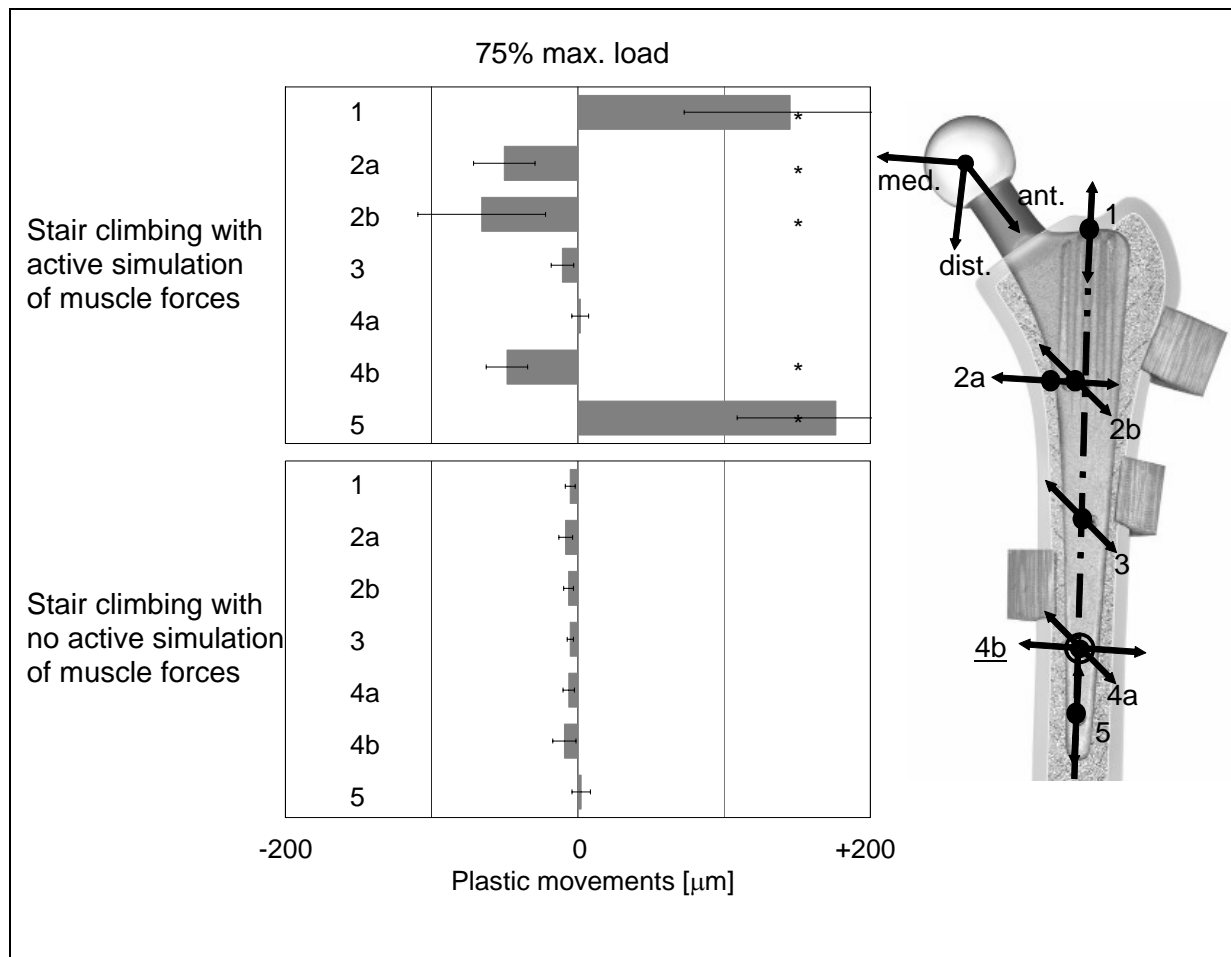


Figure 30 ▲

Plastic interface movements measured during stair climbing with (top) and without (bottom) active simulation of muscle forces at a 75% load level. The directions of micro-movements at the seven locations are defined as follows: proximal-distal movements at locations 1 and 5, medio-lateral movements at 2a and 4b and anterior-posterior movements at 2b, 3 and 4a. The coordinate system at the prosthesis head shows the positive orientation in each measurement direction. The transducer readouts at locations 1 and 5 resulted from the superposition of the longitudinal movement and the medio-lateral tilt of the stem. * $p < 0.05$.

However, the increase in plastic movement magnitude was more pronounced when muscle forces were actively simulated. In that case, the plastic movements at the end of the 75% load level averaged $177 \pm 68 \mu\text{m}$ in the longitudinal direction of the femur at location 5 and $66 \pm 44 \mu\text{m}$ in the posterior direction at location 2b (Table 10). Although the plastic movements with no active simulation of muscle forces reached a magnitude of $-9 \pm 8 \mu\text{m}$ after raising the load level to 75%, they were still far below the values experienced when muscle forces were actively stimulated. Even at this higher load level, the pronounced rotational plastic movement observed at location 2b under active simulation of muscle forces did not occur by applying the hip contact force only. Under this loading regime, the most pronounced plastic movement was registered in the lateral direction.

Table 10 ▼

Values of the plastic and elastic interface movements recorded during stair climbing with (left) and without (right) active simulation of muscle forces at a 75% load level.

Location	Interface micro-movements at 75% max. load (mean (SD)) [μm]			
	Active simulation of muscle forces		No active simulation of muscle forces	
	plastic	elastic	plastic	Elastic
1	145 (73)	12 (5)	-5 (3)	-6 (2)
2a	-50 (21)	-5 (1)	-8 (5)	-7 (2)
2b	-66 (44)	-28 (10)	-6 (3)	-1 (1)
3	-11 (8)	-6 (2)	-5 (2)	-0 (0)
4a	2 (6)	1 (1)	-6 (4)	-1 (1)
4b	-49 (14)	-1 (2)	-9 (8)	-1 (2)
5	177 (68)	7 (8)	2 (6)	7 (5)

Contrary to the plastic movement components, the elastic components experienced no increase as a result of raising the musculoskeletal forces from 50 to 75% of the peak values (Compare Figure 29 and Figure 31). In the loading configuration with active simulation of muscle forces, the largest elastic movements at the 75% load level averaged $28 \pm 10 \mu\text{m}$, whereas applying the hip contact force

only led to maximum elastic movements of $7 \pm 2 \mu\text{m}$ (Table 10). However, when comparing both loading configurations, significant differences in elastic movement magnitudes could be seen between single measurement locations, particularly in the metaphyseal region.

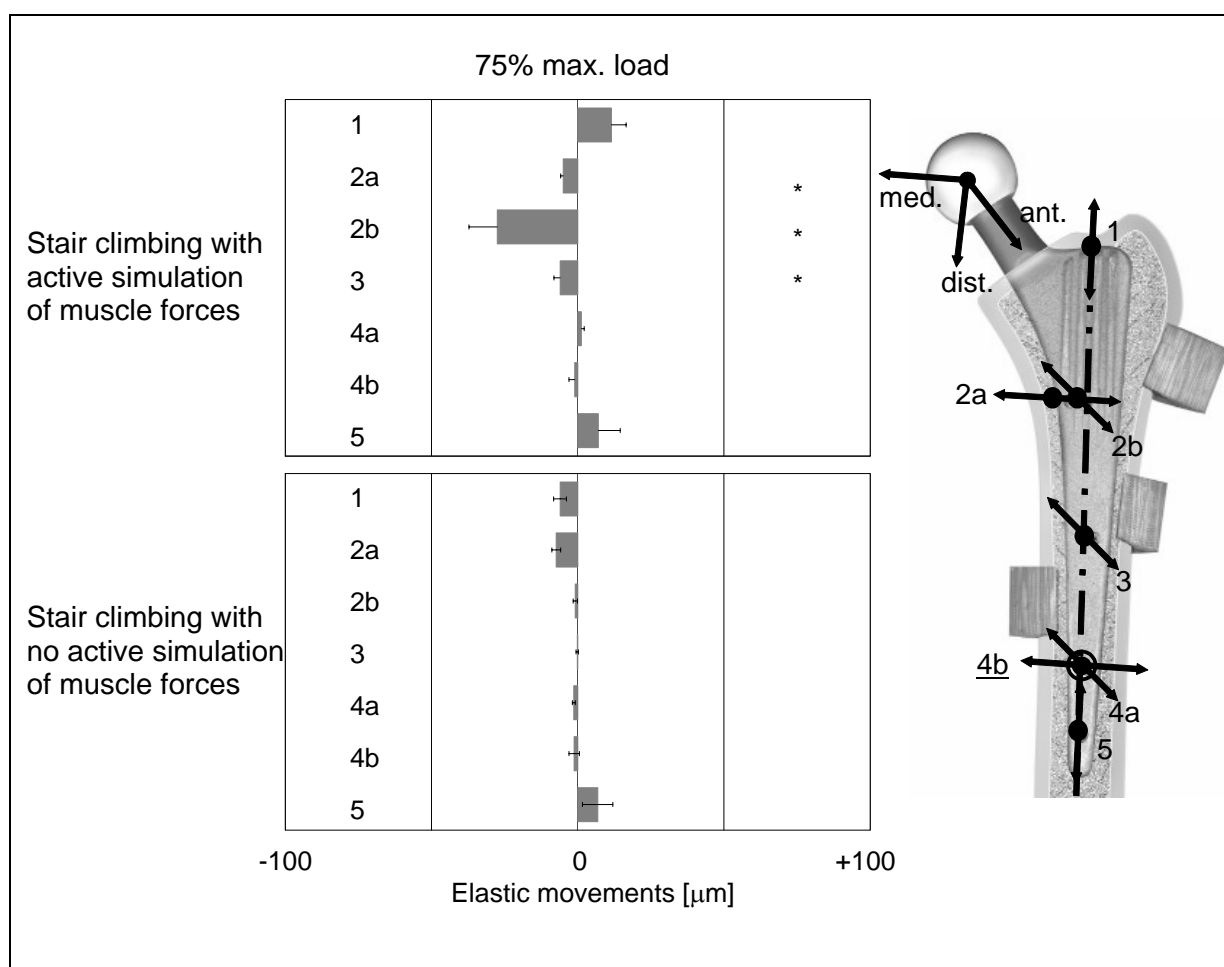


Figure 31 ▲

Elastic interface movements measured during stair climbing with (top) and without (bottom) active simulation of muscle forces at a 75% load level. The directions of micro-movements at the seven locations are defined as follows: proximal-distal movements at locations 1 and 5, medio-lateral movements at 2a and 4b and anterior-posterior movements at 2b, 3 and 4a. The coordinate system at the prosthesis head shows the positive orientation in each measurement direction. The transducer readouts at locations 1 and 5 resulted from the superposition of the longitudinal movement and the medio-lateral tilt of the stem. * $p < 0.05$.

In addition to the load-induced relative movements at the bone-prosthesis interface, the subsidence of the head of the prosthesis throughout the testing period was analysed. In both loading regimes, the head of the prosthesis was subjected to considerable subsidence within the first one hundred loading cycles (Figure 32). During the following loading cycles, the subsidence of the prosthesis head occurred more gradually, to reach a somewhat steady state with minimal slope at the end of the loading period. The relative subsidence between load cycle 100 and load cycle 1000 with no active simulation of muscle forces averaged $248 \pm 150 \mu\text{m}$, whereas the active muscle force simulation led to an averaged subsidence of $109 \pm 40 \mu\text{m}$. Whilst the interface movements exhibited smaller magnitudes, particularly in the longitudinal direction of the femur, the subsidence of the head of the prosthesis occurring under the action of the hip contact force alone was significantly larger than under the additional simulation of muscle forces.

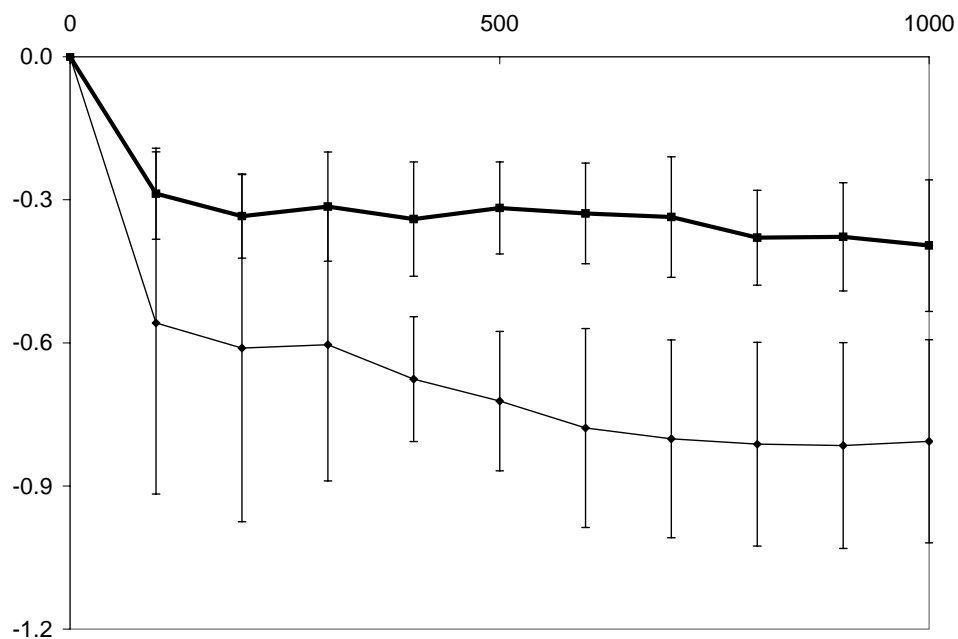


Figure 32 ▲

Subsidence of the head of the prosthesis for the loading configurations with (thick line) and without (thin line) active simulation of muscle forces at the 50% load level for 1000 loading cycles.

In conclusion, the prostheses in both loading configurations exhibited similar elastic and plastic movement patterns at both the 50% and at the 75% load level. Increasing the bone-implant loading by 25% led to an increase in plastic interface movement magnitudes of almost 100%, particularly during stair climbing with active simulation of muscle forces. Conversely, elastic movement components were in general less affected by the load increase. Even though different movement patterns could still be observed between the loading configurations at the higher load level, fewer locations exhibited significant differences in magnitude of elastic movements. Loading the implanted femur with the hip contact force only provoked up to a 2.3-fold subsidence of the prosthesis head as compared to the loading regime with active simulation of muscle forces.

3.3.3 Patient activity and interface movements

The interface movements measured with the bone-prosthesis complex loaded with muscle forces simulating the activity of stair climbing of THA patients were compared to those determined from the loading configuration representing level walking. Walking and stair climbing induced different magnitudes and patterns of plastic movements at the bone prosthesis interface. During walking, plastic movements in the posterior and in the lateral directions were relatively small compared to those seen in the longitudinal (proximal-distal) direction (Figure 33). Moreover, the pronounced plastic posterior movement at location 2b indicating a rotation of the implant within the bone as observed during stair climbing did not occur.

The largest plastic interface movements registered in the walking configuration when loaded with 50% of the peak force were always lower than $-20 \pm 10 \mu\text{m}$ compared to $40 \pm 19 \mu\text{m}$ during stair climbing (Table 11). As already observed when loading the implanted femur with the hip contact force only, a proximally-orientated plastic movement of the prosthesis occurred at locations 1 and 5, while the part of the prosthesis below the metaphyseal region tended to move laterally due to a tilt in the anterior plane.

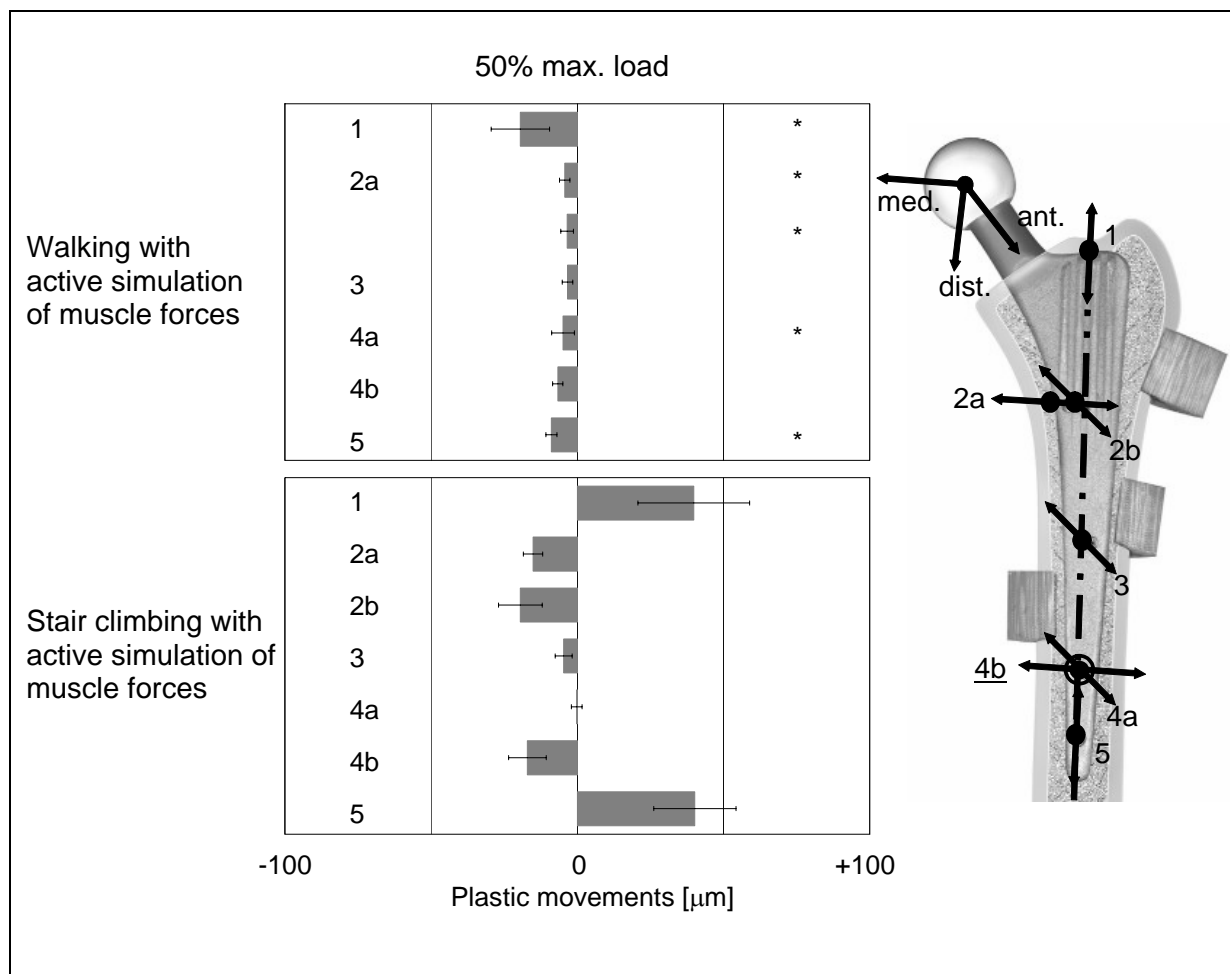


Figure 33 ▲

Plastic interface movements measured during walking (top) and stair climbing (bottom) with active simulation of muscle forces at a 50% load level. The directions of micro-movements at the seven locations are defined as follows: proximal-distal movements at locations 1 and 5, medio-lateral movements at 2a and 4b and anterior-posterior movements at 2b, 3 and 4a. The coordinate system at the prosthesis head shows the positive orientation in each measurement direction. The transducer readouts at locations 1 and 5 resulted from the superposition of the longitudinal movement and the medio-lateral tilt of the stem. * $p < 0.05$.

The pattern of the elastic movements occurring during walking at the 50% load level resembles that of the plastic movements for the same activity. Except for the tip of the prosthesis, with up to $16 \pm 8 \mu\text{m}$, comparatively smaller elastic movements were registered at all other measurement locations on the stem surface as during stair climbing, where a peak elastic movement of $50 \pm 5 \mu\text{m}$ was measured at

location 2b (Table 11). Therefore, the elastic interface movements measured when stair climbing was simulated were significantly larger than in the walking load configuration at almost all locations (Figure 34).

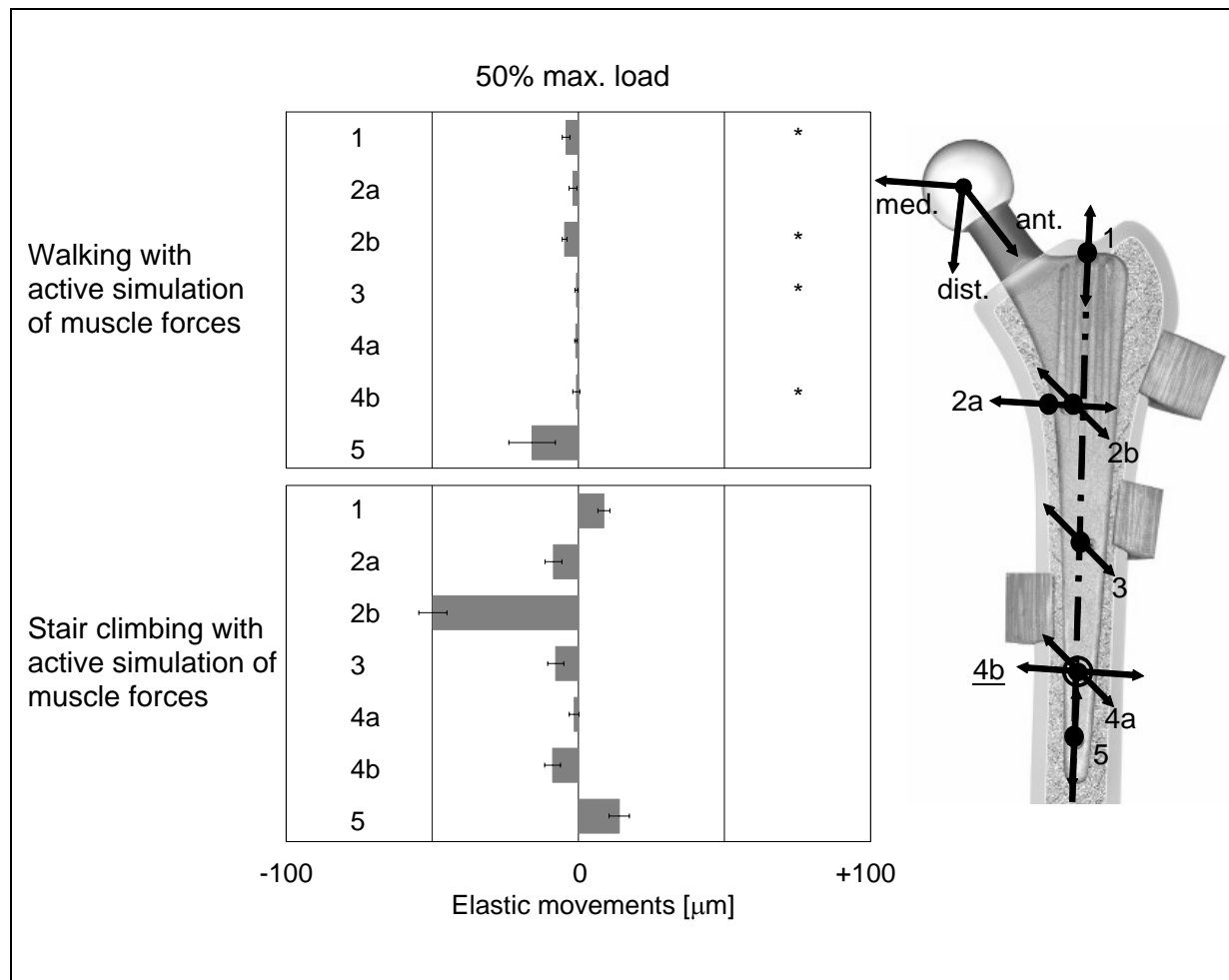


Figure 34 ▲

Elastic interface movements measured during walking (top) and stair climbing (bottom) with active simulation of muscle forces at a 50% load level. The directions of micro-movements at the seven locations are defined as follows: proximal-distal movements at locations 1 and 5, medio-lateral movements at 2a and 4b and anterior-posterior movements at 2b, 3 and 4a. The coordinate system at the prosthesis head shows the positive orientation in each measurement direction. The transducer readouts at locations 1 and 5 resulted from the superposition of the longitudinal movement and the medio-lateral tilt of the stem. * $p < 0.05$.

Table 11 ▼

Values of the plastic and elastic interface movements recorded during walking (left) and stair climbing (right) with active simulation of muscle forces at a 50% load level.

Location	Interface micro-movements at 50% max. load (mean (SD)) [μm]			
	Walking		Stair climbing	
	plastic	elastic	plastic	elastic
1	-20 (10)	-4 (1)	40 (19)	9 (2)
2a	-4 (2)	-2 (1)	-15 (3)	-9 (3)
2b	-4 (2)	-5 (1)	-20 (7)	-50 (5)
3	-3 (2)	-1 (1)	-5 (3)	-8 (3)
4a	-5 (4)	-1 (0)	0 (2)	1 (2)
4b	-7 (2)	-1 (1)	-17 (6)	-9 (3)
5	-9 (2)	-16 (8)	40 (14)	14 (3)

Regarding the activity of stair climbing, the effect of increased loads on the stability of a cementless prosthesis under a load regime representing level walking was analysed. The plastic interface movements recorded at the different locations at the end of the 75% load level exhibited a similar distribution as observed at the end of the 50% level (Figure 35). The largest plastic interface movement did not exceed $36 \pm 19 \mu\text{m}$ and was oriented proximally. Even though these movement magnitudes represented almost a 2-fold increase, they were significantly lower than the peak values measured during stair climbing ($177 \pm 68 \mu\text{m}$, Table 12).

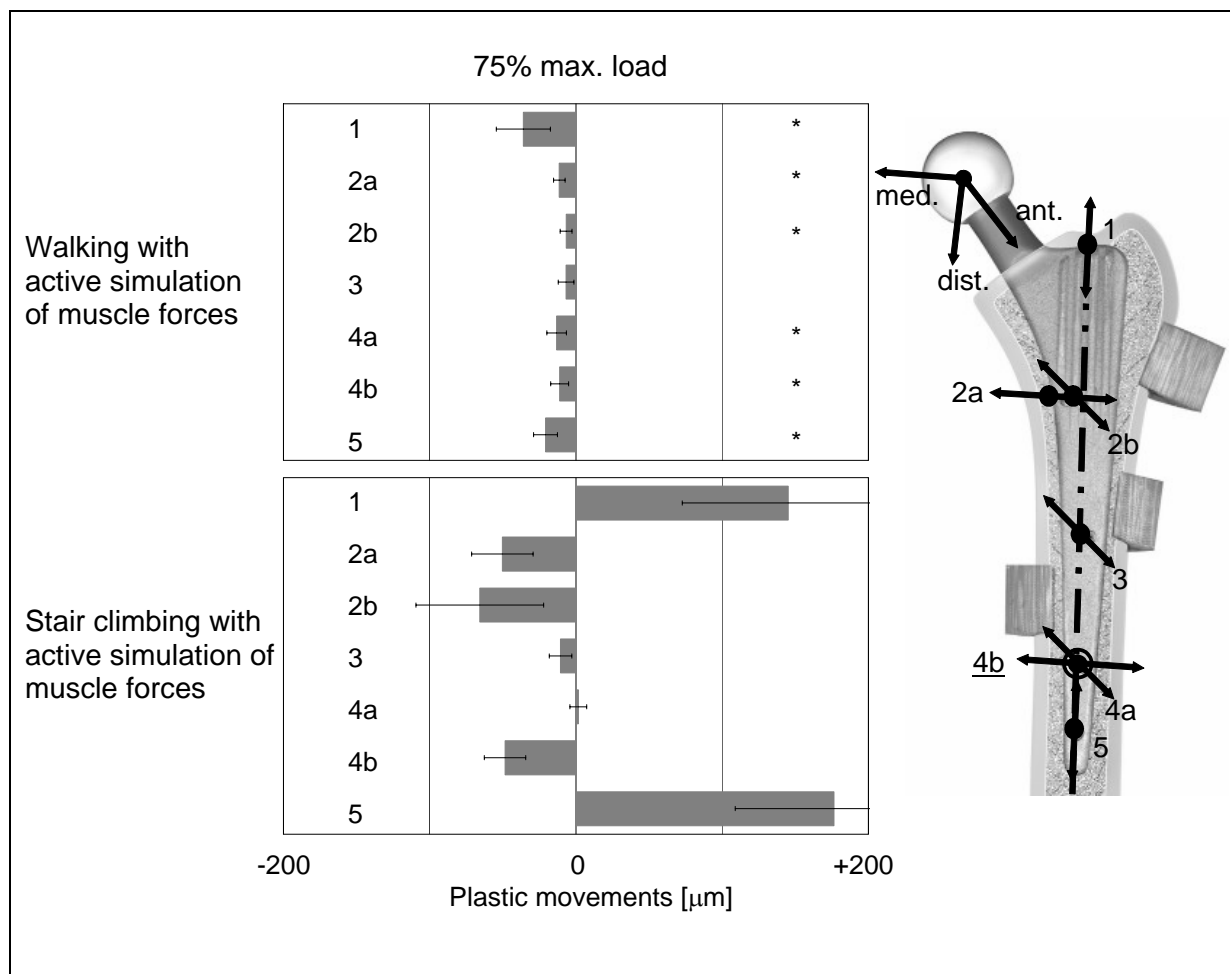


Figure 35 ▲

Plastic interface movements measured during walking (top) and stair climbing (bottom) with active simulation of muscle forces at a 75% load level. The directions of micro-movements at the seven locations are defined as follows: proximal-distal movements at locations 1 and 5, medio-lateral movements at 2a and 4b and anterior-posterior movements at 2b, 3 and 4a. The coordinate system at the prosthesis head shows the positive orientation in each measurement direction. The transducer readouts at locations 1 and 5 resulted from the superposition of the longitudinal movement and the medio-lateral tilt of the stem. * $p < 0.05$.

As observed for the loading regime representing stair climbing, the elastic interface movements during walking reacted minimally to increased loads (Figure 36). While the largest elastic movements at the 50% load level averaged $16 \pm 8 \mu\text{m}$, loading the bone-implant complex with 75% of the peak loads produced similar peak elastic interface movements, averaging $17 \pm 6 \mu\text{m}$. With increasing loads, fewer

measurement locations exhibited significant differences in elastic interface movements between the walking and the stair climbing configurations.

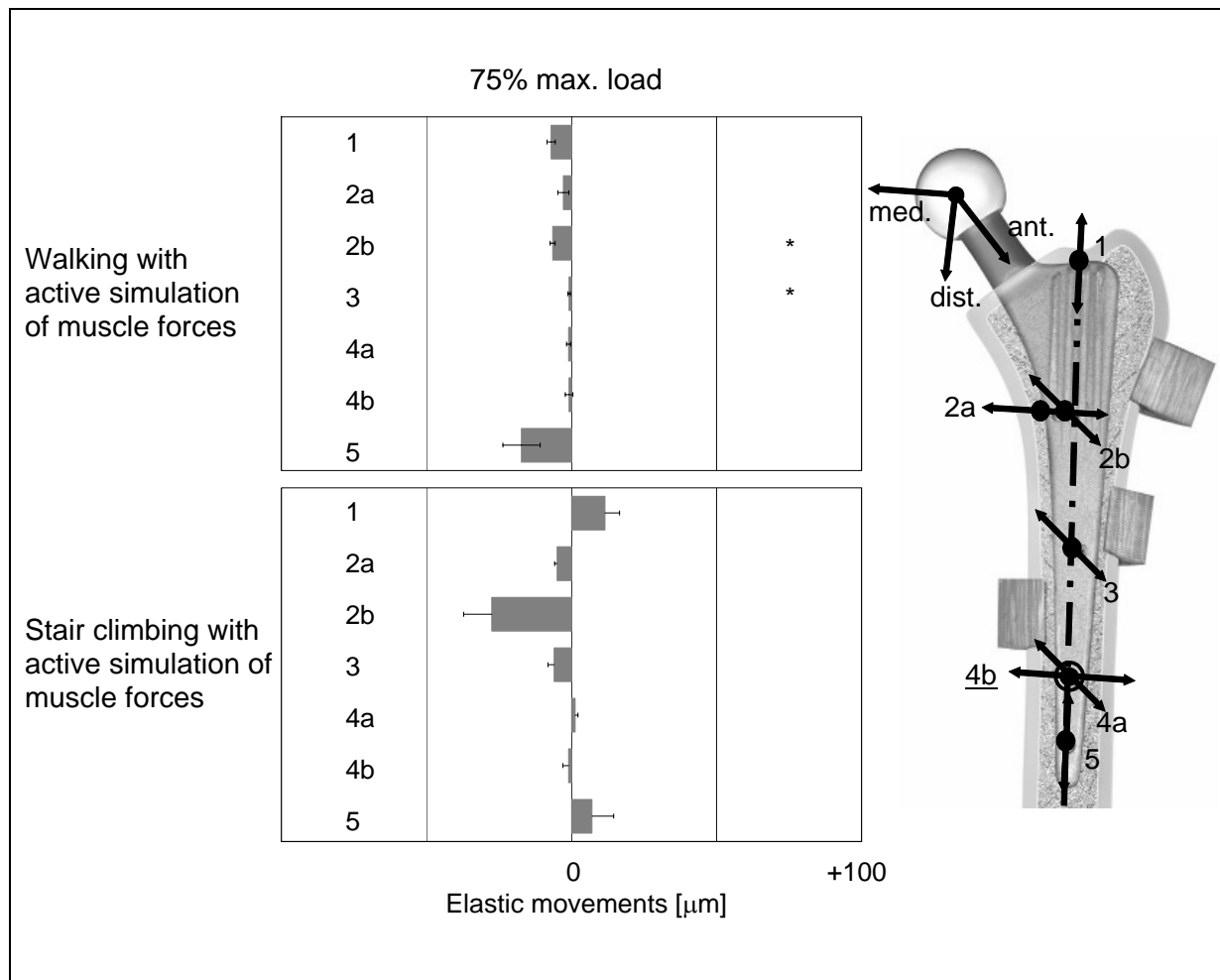


Figure 36 ▲

Elastic interface movements measured during walking (top) and stair climbing (bottom) with active simulation of muscle forces at a 75% load level. The directions of micro-movements at the seven locations are defined as follows: proximal-distal movements at locations 1 and 5, medio-lateral movements at 2a and 4b and anterior-posterior movements at 2b, 3 and 4a. The coordinate system at the prosthesis head shows the positive orientation in each measurement direction. The transducer readouts at locations 1 and 5 resulted from the superposition of the longitudinal movement and the medio-lateral tilt of the stem. * $p < 0.05$.

Table 12 ▼

Values of the plastic and elastic interface movements recorded during walking (left) and stair climbing (right) with active simulation of muscle forces at a 75% load level.

Location	Interface micro-movements at 75% max. load (mean (SD)) [μm]			
	Walking		Stair climbing	
	plastic	elastic	plastic	elastic
1	-36 (19)	-7 (1)	145 (73)	12 (5)
2a	-11 (4)	-3 (2)	-50 (21)	-5 (1)
2b	-7 (4)	-7 (1)	-66 (44)	-28 (10)
3	-7 (5)	-1 (0)	-11 (8)	-6 (2)
4a	-13 (7)	-1 (1)	2 (6)	1 (1)
4b	-11 (62)	-1 (1)	-49 (14)	-1 (2)
5	-21 (6)	-17 (6)	177 (68)	7 (8)

The results presented above demonstrated that stair climbing and level walking generate different patterns and magnitudes of relative movements at the bone-prosthesis interface. Stair climbing exhibited significantly larger plastic movements and therefore appeared to be more critical than walking. Under this loading regime, the prosthesis was subjected to a dominant distal movement and a characteristic posterior movement of the stem in the metaphyseal area. Similar to stair climbing, elastic movement components were less pronounced during walking and varied little with increased loading.

3.3.4 Anchorage principle and interface movements

The interface movements of a proximally- and of a distally-anchoring stem loaded in the stair climbing configuration with active simulation of muscle forces were evaluated. After 1000 loading cycles, both stem designs exhibited similar plastic movement patterns, with the prosthesis moving mainly in the distal direction and exhibiting a characteristic rotational movement around the longitudinal axis as

indicated by the pronounced anterior-posterior movement at location 2b (Figure 37). In addition, both stems experienced a slight tilt in the frontal plane and relatively small interface movements were registered in the anterior-posterior direction.

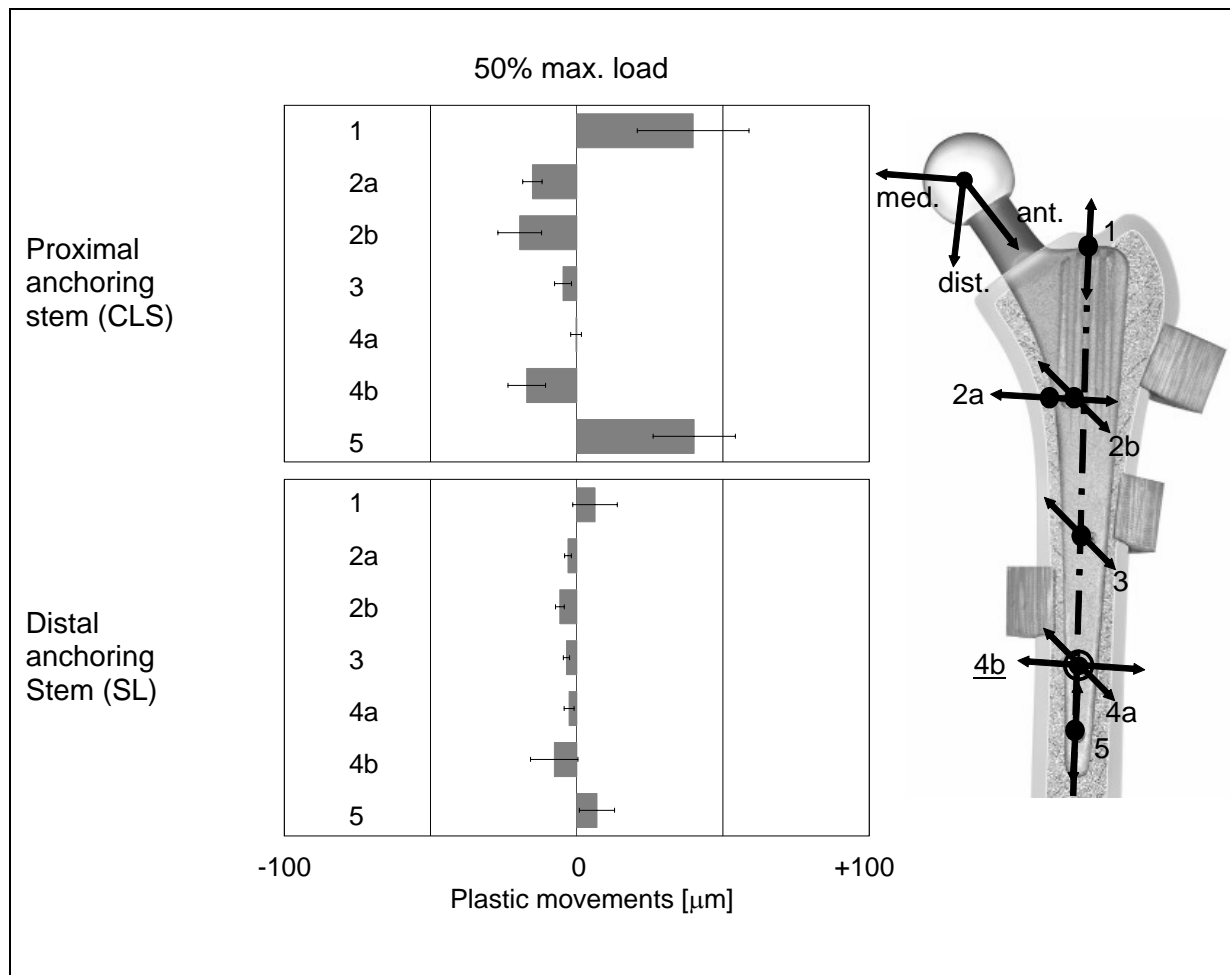


Figure 37 ▲

Comparison of the plastic interface movements measured for a proximal (top) and a distal (bottom) anchoring stem during stair climbing with active simulation of muscle forces at a 50% load level. The directions of micro-movements at the seven locations are defined as follows: proximal-distal movements at locations 1 and 5, medio-lateral movements at 2a and 4b and anterior-posterior movements at 2b, 3 and 4a. The coordinate system at the prosthesis head shows the positive orientation in each measurement direction. The transducer readouts at locations 1 and 5 resulted from the superposition of the longitudinal movement and the medio-lateral tilt of the stem. * $p < 0.05$.

However, the proximal anchoring CLS-stem exhibited higher plastic interface movements than the distal anchoring Alloclassic SL stem, particularly for the proximal-distal movement components (locations 1 and 5) and for the medio-lateral and the anterior-posterior movement components in the metaphyseal region (locations 2a and 2b); the maximum plastic movements averaged $40 \pm 19 \mu\text{m}$ and $7 \pm 6 \mu\text{m}$, respectively (Table 13). Comparable ratios were observed for the posterior-oriented movement at location 2b. In this case, the average plastic rotational movement was $-20 \pm 7 \mu\text{m}$ for the CLS stem and $-6 \pm 2 \mu\text{m}$ for the Alloclassic SL.

Table 13 ▼

Values of the plastic, elastic and plastic/cycle interface movements recorded for a proximal (left) and a distal (right) anchoring stem during stair climbing with active simulation of muscle forces at a 50% load level.

Location	Interface micro-movements at 50% max. load (mean (SD)) [μm]					
	Proximal anchoring stem			Distal anchoring stem		
	plastic	elastic	plastic/cycle	plastic	elastic	plastic/cycle
1	40 (19)	9 (2)	2 (0)	6 (8)	16 (5)	4 (2)
2a	-15 (3)	9 (3)	2 (1)	-3 (1)	3 (1)	1 (0)
2b	-20 (7)	50 (5)	12 (6)	-6 (2)	12 (2)	3 (3)
3	-5 (3)	8 (3)	2 (1)	-4 (1)	4 (1)	1 (0)
4a	0 (2)	1 (2)	1 (0)	-3 (2)	3 (1)	1 (0)
4b	-17 (6)	9 (3)	2 (1)	-8 (8)	9 (5)	2 (1)
5	40 (14)	14 (3)	5 (3)	7 (6)	11 (6)	2 (2)

The elastic movement components were also compared for each of the measurement locations (Figure 38). Contrary to the plastic movement components, the elastic components exhibited not only similar patterns, but also magnitudes. Except for the elastic movement of the CLS stem at location 2b in the metaphyseal region, which averaged $50 \pm 5 \mu\text{m}$, the elastic movement components at the different measurement locations were comparable for both stem designs and did not exceed $16 \pm 5 \mu\text{m}$. In addition to the total elastic and total plastic interface movements, the

plastic movement following each loading cycle was assessed (Table 13). Although the plastic movements per loading cycle were in both cases small compared to the elastic and total plastic movements, they tended to be higher with the proximally anchoring CLS-stem. Furthermore, the largest plastic movement per loading cycle was also registered in the metaphyseal region of the stem.

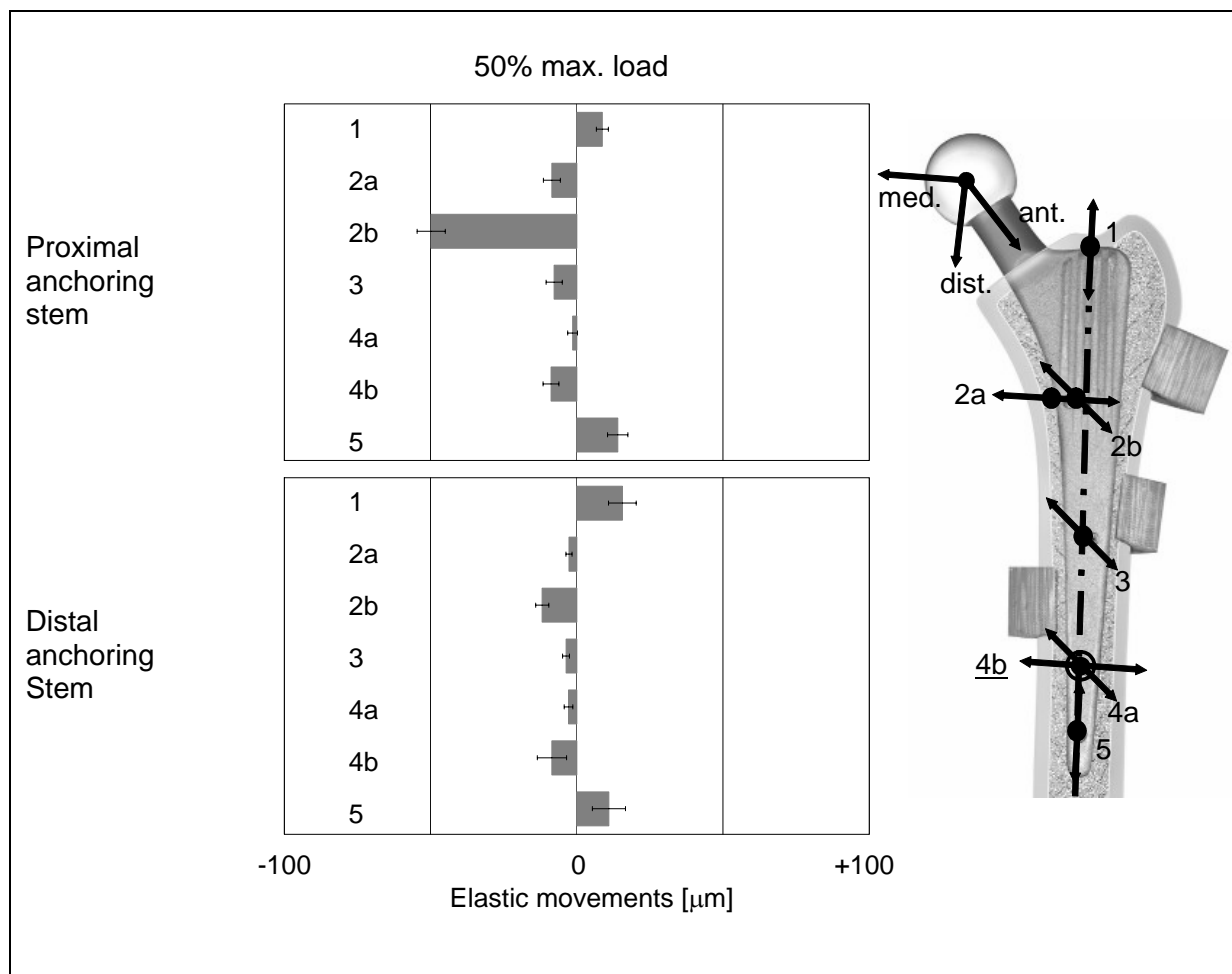


Figure 38 ▲

Comparison of the elastic interface movements measured for a proximal (top) and a distal (bottom) anchoring stem during stair climbing with active simulation of muscle forces at a 50% load level. The directions of micro-movements at the seven locations are defined as follows: proximal-distal movements at locations 1 and 5, medio-lateral movements at 2a and 4b and anterior-posterior movements at 2b, 3 and 4a. The coordinate system at the prosthesis head shows the positive orientation in each measurement direction. The transducer readouts at locations 1 and 5 resulted from the superposition of the longitudinal movement and the medio-lateral tilt of the stem. * $p < 0.05$.

4 Discussion

The aim of this study was threefold: First, to introduce simplified, but representative, load profiles of the proximal femur that have previously been derived from the complex model of the human lower extremity and validated against *in vivo* measured hip joint forces; Second, to design and implement an experimental loading device able to simulate a physiological-like loading of the proximal femur based on the presented, validated load profiles. Finally, to determine the influence of the simplified load profiles on the primary stability of cementless hip prostheses in order to evaluate the relevance of the mechanical loading set-up with respect to a standardised pre-clinical loading procedure *in vitro*.

Based on gait analysis and hip contact force data recorded in THA patients with telemeterised hip prostheses *in vivo*, it has been possible to compute the musculoskeletal loads acting at the proximal femur and hence to derive validated, simplified loading configurations. The implemented mechanical device mimics the three dimensional loading of the proximal femur that occurs during walking and stair climbing, with a special emphasis on the active simulation of muscle forces according to the *in vivo* situation. The results of the primary stability analysis suggest that the new, physiological-like loading set-up presented in this study allows a more realistic pre-clinical evaluation of the interface micro-movements of cementless hip prostheses *in vitro*. Such a loading procedure should therefore be taken into consideration in pre-clinical primary stability analyses of hip prostheses prior to clinical release.

4.1 Primary stability of cementless prostheses

4.1.1 Influence of active simulation of muscle forces

It is well-accepted that the loading conditions to which the bone-prosthesis complex is subjected *in vivo* have a major influence on the stability of a joint reconstruction (Bergmann *et al.* 1995). Furthermore, the importance of physiological loading conditions in relation to mechanical testing of total hip prostheses *in vitro* has been demonstrated by several authors (Cristofolini *et al.* 1995; Lu *et al.* 1997; Duda *et al.* 1998b; Simoes *et al.* 2000; Szivek *et al.* 2000). However, there is no consensus in the literature as to how the femur-prosthesis complex should be loaded *in vitro* to yield an initial mechanical stability which best reflects that occurring in THA patients *in vivo*. Due to a lack of standardised musculoskeletal loading conditions, the load configurations typically employed in the pre-clinical evaluation of the primary stability of hip prostheses *in vitro* represented a major simplification of the actual *in vivo* situation.

Some studies restrictively examined the torsional stability of femoral stems by applying a pure torque moment to the prosthetic head (Gustilo *et al.* 1989; Nunn *et al.* 1989; Sugiyama *et al.* 1989; Phillips TW *et al.* 1990; Baleani *et al.* 2000; Effenberger *et al.* 2001). Although the anterior-posterior component of the resultant contact force at the hip joint exerts a considerable torsional moment upon the prosthesis (Bergmann *et al.* 1995), additional compressive and bending loads are also transmitted to the cortical bone. Therefore, the rotational movements of the prosthesis occurring under complex *in vivo* loading situations may be also affected by the axial and the tilt movement components. Furthermore, prostheses with sufficient fixation strength in rotation may exhibit poor stability under axial loading. Even though the assessment of the torsional stability is often used to quantitatively compare various prosthesis designs and implantation techniques, this method may, however, provide only a partial description of the overall stability of the prosthesis (Hua and Walker 1994).

In other studies, the loading of the hip joint has been reduced to the resultant joint contact force which was directly applied to the prosthesis head (Gebauer *et al.* 1989; McKellop *et al.* 1991; Berzins *et al.* 1993; Hua and Walker 1994; Buhler *et al.* 1997; Gotze *et al.* 2002; Maher and Prendergast 2002). Whilst loading the bone-prosthesis complex by the hip contact force alone might create critical stresses in the shaft of the femoral component, it might not induce critical micro-movements at the implant-bone interface. In fact, the overestimated bending moments (Taylor *et al.* 1996; Duda *et al.* 1997; Duda *et al.* 1998a; Szivek *et al.* 2000) might cause locking of the prosthesis within the medullary canal of the femur, which may hinder further prosthesis movement. The patterns of interface movements observed under a loading configuration consisting of the hip contact force alone are thus often characterised by a predominance of radial over axial movement components (McKellop *et al.* 1991; Hua and Walker 1994; Gotze *et al.* 2002). Therefore, the movement data obtained under such oversimplified loading conditions may well overestimate the primary stability which will actually be achievable in THA patients *in vivo*.

In addition to the resultant joint contact force applied to the head of the prosthesis, abductor muscles are occasionally simulated in experimental loading set-ups (Rohlmann *et al.* 1983b; Schmotzer *et al.* 1992; Cristofolini *et al.* 1995; Szivek *et al.* 2000; Gillies *et al.* 2002; Harrington *et al.* 2002). In these cases, the forces exerted by the abductor muscles are transmitted to the femur through a cantilever system. Even though the projection of the muscle force vectors in the frontal plane as well as the distal constraining of the femur may alter the physiological load transmission pathways, the inclusion of adductor muscles in mechanical loading set-ups contributes to reduce the bending moments in the femur and therefore represents a better approximation of the physiological loading conditions.

Experimental and finite element studies have been conducted to investigate the effects of the modelling of additional lateral muscle loads (Schmotzer *et al.* 1992; Cristofolini *et al.* 1995; Szivek *et al.* 2000; Stolk *et al.* 2001). Most of the investigations carried out in this context focussed on the strain distribution in an intact

femur under different loading configurations. Whilst the abductor-only configuration has been considered adequate to reproduce *in vivo* loading by Cristofolini and co-workers (1995), Szivek and co-workers (2000) strongly recommended loading the hip joint with a configuration that incorporates muscles such as the vastus lateralis and the ilio-tibial band for a more physiological loading. In a finite element analysis to predict mechanical failure of cemented hip prostheses Stolk and co-workers (2001) found that the action of structures such as the ilio-tibial tract and vasti had small influence on cement stresses when compared to the influence of the abductors. However, it could be questioned whether the results obtained for a cemented prosthesis with respect to the long-term mechanical failure can be extrapolated to analyses regarding the initial stability of hip prostheses in general and cementless prostheses in particular. Furthermore, it can be expected that the effect of additional lateral muscles might be more noticeable when validated and balanced musculoskeletal loads would be implemented. In fact, Britton and co-workers (2003) examined the effect of including muscle forces on the migration of cemented femoral prostheses and came to the conclusion that *in vitro* fatigue tests should include loading of lateral muscles to provide increased confidence in the results by stabilising the femoral component during the test.

In this study, a mechanical loading set-up based on validated load data was used to determine the initial stability of cementless hip prostheses *in vitro*. The load-induced interface movements obtained using the mechanical loading set-up with active simulation of muscle forces were compared to those obtained by only applying the resultant joint contact force to the prosthesis head. The movement magnitudes and patterns were dramatically different when muscle forces were not actively simulated, i.e. when the femur-prosthesis complex was loaded with the joint contact force only. Under this loading regime, significantly lower interface micro-movements were recorded, particularly in the longitudinal direction of the prosthesis, even though the head of the prosthesis experienced a considerable higher distal subsidence. The discrepancy between distal interface movements and subsidence of the head of the prosthesis suggested that the prosthesis-femur complex was subjected to bending loads. As a result of the bending moments caused by the joint contact force, the

angulations of the femur and a lack of lateral stabilisation through muscle structures, the prosthesis inevitably underwent a valgus tilt expressed in pronounced lateral movements. These findings compared well with those reported in studies using a similar load configuration (McKellop *et al.* 1991; Hua and Walker 1994; Gotze *et al.* 2002).

Even though lateral interface movements also occurred when muscle forces were actively simulated, the prostheses were principally subjected to axial, longitudinal movements, which can be associated with the predominantly compressive stressing of the femur resulting from the physiological-like load transmission. Due to the long lever arm of the reference metal bar screwed at the prosthesis shoulder (Figure 20), the effective longitudinal movement of the prosthesis may have been overlapped or overshadowed by the movement components resulting from the medio-lateral tilt of the prosthesis. This may have lead to the shift in direction occasionally observed at the shoulder and at the tip of the prosthesis, suggesting that the prosthesis was moving out of the femur. This phenomenon seemed to be less pronounced with increasing axial migration of the stem, as observed during stair climbing with active simulation of muscle forces.

The primary stability of the cementless CLS prosthesis has been evaluated *in vitro* by various investigators (Schneider E *et al.* 1989b; McKellop *et al.* 1991; Buhler *et al.* 1997). The experiments were conducted with both composite and cadaveric femora. None of the previous investigators actively simulated muscle forces. The load level (hip contact force up to 300% BW), test frequency (up to 1 Hz) and number of loading cycles (up to 5000) were considerably higher than in the present study. Although the direction of the applied hip contact force was, in some cases, parallel to the longitudinal axis of the prosthesis, the reported micro-movements were comparable with our findings under active simulation of muscle forces but at a much lower load level: up to 70 μm / 30 μm (plastic / elastic) and 400 μm / 50 μm were measured in the longitudinal direction of the prosthesis by Buhler and co-workers (1997) and McKellop and co-workers (1991) respectively.

Even though a limited number of loading cycles was simulated, the relative plastic movements measured in the present study between femur and prosthesis, particularly during stair climbing, seemed to better approximate the short-term patient data: retrospective measurements from standard radiographs of THA patients exhibited a median CLS stem migration of 200 μm after a one year follow-up period (Krismer *et al.* 1999). The hip joint reconstructions that were included in the retrospective analysis were clinically stable with a mean survival rate of 94% after 10 years. Comparable, and in some cases higher migration (up to 800 μm per year) and survival rates (86 - 100% at six years) have been observed in patients with other stem designs (Donnelly *et al.* 1997).

Since elastic movement components may play a more important role for the biological osseointegration process (Pilliar *et al.* 1986; Spotorno *et al.* 1987; Maloney *et al.* 1989; Buhler *et al.* 1997), it may therefore be necessary to differentiate between elastic and plastic movement components. As expected, the elastic movement components measured in this study exhibited similar patterns as the plastic components. The elastic interface movements were, at all locations, lower than 150 μm , a threshold-value with regard to osseointegration (Pilliar *et al.* 1986). The maximal elastic movements averaged 50 μm and were registered in the metaphyseal region, which may therefore be a more critical region with respect to osseointegration.

In the configuration loaded with 75% of the maximal load under active simulation of muscle forces, total plastic movements higher than 150 μm were recorded in the longitudinal direction. Increasing the load by 25% led to a more than fourfold increase in relative plastic movements, in contrast to the elastic movements which experienced no significant increase. A similar increase in prosthesis movement was observed in the study of Buhler and co-workers (1997), in which the primary stability of the cementless CLS-Spotorno prosthesis was also analysed.

4.1.2 Influence of patient activity

The patterns and magnitudes of the contact forces and moments acting at a reconstructed hip joint have been found to depend on the type of motor task performed by the total hip arthroplasty patient (Bergmann *et al.* 1993; van den Bogert *et al.* 1999; Bergmann *et al.* 2001a). Due to the close relationship between the loading of the hip joint and the mechanical stability of joint reconstructions, it can be expected that the micro-movements to which hip joint prostheses are subjected *in vivo* also vary with the patient activity. The definition of the loading configuration to be used in pre-clinical *in vitro* testing should therefore be geared to the load magnitudes, the type of loading, the frequency of the activities and therefore the number of load cycles to which an implant will be exposed during its service life.

The current study has focussed on the musculoskeletal loading conditions/primary stability during two common activities of daily life, i.e. walking and stair climbing. It has been shown that walking is the activity which occurs most frequently in THA patients (Morlock *et al.* 2001) and results in considerable hip contact forces *in vivo* (Bergmann *et al.* 1993; Bergmann *et al.* 2001a). A comparison of the peak loads measured at the hip joint *in vivo* further demonstrates that stair climbing represents an activity during which the highest forces and the highest torsional loading on the shaft of the prosthesis occur, except for extreme and uncommon situations such as stumbling (Wroblewski 1979; Harris *et al.* 1991; Bergmann *et al.* 1993; Bergmann *et al.* 2001a). At the same time, stair climbing is one of the five most frequent activities in the daily life of a THR patient (Morlock *et al.* 2001). Whilst these two activities can represent only a fraction of the total activity of a typical THA patient, the selection seems to be appropriate within the context of standardised pre-clinical testing of prosthesis stability. In fact, cementless hip prostheses are primarily required to exhibit a sufficient mechanical strength within the first months following surgery, a period in which patients are allowed only partial weight-bearing on the limb until secondary stabilisation through osseointegration has taken place. However, the clinical effect/benefit of partial load bearing is still

controversially discussed in the literature (Rao *et al.* 1998; Kishida *et al.* 2001; Woolson and Adler 2002).

In this study, elastic and plastic interface movements were recorded for a loading configuration representing level walking and stair climbing with active simulation of muscle forces. Independent from the magnitude of the applied loads, stair climbing activities induced a significantly higher instability at the bone-prosthesis interface than walking. Although the prosthesis experienced a more pronounced tilt during stair climbing than during walking, distal stem migration was dominant. In addition to the pronounced distal migration, the prosthesis underwent a characteristic backwards twisting (retroversion) when subjected to stair climbing loads. This characterisation of the prosthesis movement agreed well with the load distribution that has been reported for THA patients during stair climbing (Bergmann *et al.* 1995).

Comparable interface movement patterns resulting from different loading configurations have also been reported by other investigators (Phillips TW *et al.* 1990; Phillips TW *et al.* 1991; Fischer *et al.* 1992; Rubin *et al.* 1993; Naidu *et al.* 1996; Chareancholvanich *et al.* 2002). Based on the hip joint forces measured in THA patients *in vivo* by Kotzar and co-workers (1991), Chareancholvanich and co-workers (2002) determined the spatial micro-movements between the prosthesis and the femur under loading conditions representing the stance phase of level walking and stair climbing. In their study, larger rotational micro-movements were recorded during stair climbing than during walking, as also observed in the present study. However, the differences in movement magnitudes were less pronounced for the translational than for the rotational movement components compared to the findings of the present study. This was presumably due to the non-physiological loading of the implanted femora which consisted of the resultant hip contact force only. In a finite element analysis study, Pancati and co-workers (2003) analysed the primary stability of a cementless prosthesis loaded with hip joint contact forces measured in four THA patients while performing nine different activities (Bergmann *et al.* 2001a). Compared to walking, stair climbing produced significantly higher average relative micro-movements.

The findings in this study confirm that torsional moments occurring during stair climbing considerably affect the initial stability of cementless prostheses more than walking and may thus jeopardise the biological integration of the prosthesis in the surrounding cancellous bone. In the context of the post-operative gradual allowance of weight bearing, it appears reasonable, as suggested by other authors (Phillips TW *et al.* 1990; Phillips TW *et al.* 1991; Naidu *et al.* 1996), to encourage THA patients to limit such motor tasks which could lead to a high torsional loading of the bone-prosthesis interface, at least for the first three months.

4.1.3 Influence of anchorage principle

In addition to the musculoskeletal loads (Bergmann *et al.* 1995) and the quality of the host bone (Kobayashi *et al.* 2000), the stability of a joint reconstruction has been shown to also be influenced by the geometric design of the prosthesis (Callaghan 1992; Speirs *et al.* 2000). Different press-fit fixation systems have been developed to afford a sufficient initial stability of the prosthesis by enhancing the fit between the implant and the endosteal cavity and thus to ensure an optimal load transfer. Although cementless prostheses should be stabilised through proximal fit within the metaphyseal region in order to avoid secondary proximal bone loss because of stress-shielding, hip prostheses relying on diaphyseal fixation are also used, especially in revision hip arthroplasty. Distal fixation with cortical contact is thought to provide a better resistance to rotational forces than fixation in the relatively weak metaphyseal region of the femur and therefore enhance the initial torsional stability of cementless femoral components (Kendrick *et al.* 1995; Otani *et al.* 1995; Whiteside *et al.* 1996; Dorr *et al.* 1997; Nourbash and Paprosky 1998). In an experimental study, Whiteside and co-workers (1996) compared the rotational stability of prostheses using different fixation techniques. Based on their results, the authors came to the conclusion that prosthesis designs which allowed a tight distal fit in addition to neck retention had the lowest micro-movements at the interface.

In order to evaluate the influence of the anchorage principle on the primary stability of cementless hip prostheses, a proximal, metaphyseal (CLS Spotorno) and

a distal, meta-diaphyseal (Alloclassic SL Zweymueller) anchoring stem were investigated. Both stems were subjected to a loading regime representing stair climbing, since this activity is thought to produce the highest loads during daily activities with the exception of stumbling incidents (Bergmann *et al.* 2001a; 2004). Under this loading regime, the prostheses experienced high axial forces coupled with considerable retroversion torque forces. The generated patterns of interface movements of both prosthesis designs reflect this load distribution: The prostheses principally migrated distally along their longitudinal axis and experienced a retroversion twist. The active simulation of muscle forces contributed to reduce the commonly observed tilt of the stem in the frontal and lateral planes with an eventual clamping of the implant within the medullary cavity (Schneider E *et al.* 1989b; Gotze *et al.* 2002).

Although similar patterns of elastic movements were observed in both the metaphyseal and the meta-diaphyseal anchoring prostheses, the latter showed reduced plastic deformations. Due to its straight, conical design and its meta-diaphyseal anchoring principle, the Alloclassic SL stem achieved a better fixation in the medullary canal with extensive contact to the surrounding impacted cancellous bone. With the CLS stem, the bone-implant contact was restricted to the metaphyseal femur region. Therefore, the irreversible, plastic interface movements and, consequently, the overall initial migration of the CLS stem were higher than those of the Alloclassic SL stem. With the increasing number of loading cycles, however, the CLS stem migration was gradually reduced and the stem stabilized. This corresponded to the clinical observation in THA patients with cementless stems during the initial post-operative weeks (Delaunay *et al.* 1998; Delaunay and Kapandji 1998; Davies *et al.* 1999; Ornstein *et al.* 2000).

Both plastic and elastic movements of the implants may compromise the biological integration of the prosthesis in the bone. For both stem designs, plastic movements were relatively small and may therefore be less critical for the stability at the bone-implant interface *in vivo*. Elastic movements were generally larger and varied, as expected, from one measurement location to another. The largest elastic

movements were observed in the metaphyseal, inter-trochanteric femur region, which is commonly associated *in vivo* with a substantial post-operative bone turnover: Comparison between pre- and post-operative Bone Mineral Density (BMD) measurements in retrospective analyses conducted in THA patients with stable cementless Alloclassic SL Zweymueller and CLS Spotorno stems revealed a greater decrease of bone mass in the proximal Gruen zones I and VII (lateral trochanter major and medial calcar region respectively) than in the more distal zones III, IV, V (lateral cortex, stem tip and medial cortex region respectively) (Korovessis *et al.* 1997; Sabo *et al.* 1998; Zerahm *et al.* 1998; Gibbons *et al.* 2001).

In spite of the differences in movement magnitudes, both the CLS Spotorno and the Alloclassic SL Zweymueller stems show excellent long term clinical results (Eyb *et al.* 1993; Schramm *et al.* 2000; Traulsen *et al.* 2001; Weissinger and Helmreich 2001; Garcia-Cimbrelo *et al.* 2003; Pieringer *et al.* 2003). In this *in vitro* study, interface movements were measured using composite bones to minimise the impact of bone material properties. Although larger movement magnitudes may be expected in human specimens and under higher loads, the amounts of elastic movement components occurring *in vivo* appear not to be detrimental to the osteointegration process of the stem. Stem discriminations which rely on relatively small differences in interface movements therefore need to be critically viewed. In fact, statistical differences in movement magnitude may be overshadowed by biological consequences of the different fixation principles. Additional parameters such as the quality of the host bone, the surgical approach and the accuracy of the medullary canal preparation may be taken into consideration to evaluate the initial stability of different stem design concepts (Noble *et al.* 1988; Capello 1990; Bourne and Rorabeck 1998; Dorr *et al.* 1998; Zerahm *et al.* 1998).

Initial plastic movements (migration) of up to $177 \pm 68 \mu\text{m}$ were measured *in vitro* for the clinically successful CLS-stem. Subsidence of the stem in the early post-operative period therefore seems to be unavoidable, at least for a straight stem. Despite these initial plastic movements, current well-established stems may already minimize initial elastic movements with respect to osseointegration. Further design

improvements should increasingly focus on the secondary mechanical stability by preventing continued stem migration.

This analysis suggests that the anchoring principle of cementless prostheses influences their primary stability. Whilst patterns of interface movements seem to be determined by the mode of application and transmission of the musculoskeletal loads, elastic and plastic movement magnitudes depend on the shape and the anchorage concept of the stem. Although early migration was more accentuated with the metaphyseal than with the meta-diaphyseal anchoring stem, both designs showed comparable, low elastic interface movements which may explain their good long term clinical results. A metaphyseal, trabecular anchoring stem might be expected to show increased initial migration in comparison to a more distal anchoring stem. The extent of migration will certainly be influenced by the bone quality. In that respect, the anchoring principle should match the available bone quality, i.e. in the presence of proximal bone defects or low-strength trabecular, osteoporotic bones, diaphyseal anchorage should be preferred to metaphyseal anchorage.

4.2 Discussion of the methods

4.2.1 Muscle model and load profiles

The musculoskeletal model of the human lower extremity which has been used in the present study to derive the loading conditions at the hip joint has considered the complex anatomical features of the hip joint as well as the specificities of total hip arthroplasty patients (Heller *et al.* 2001). Based on CT-data from the Visible Human (National Library of Medicine, Bethesda, USA), individual models of four THA patients were customised and subsequently used to compute the muscle and joint contact forces acting at the hip joint. Confidence in the results was obtained from the relatively low errors between the calculated joint contact forces with those measured in the same patients during gait analysis *in vivo*. The model could therefore be considered adequate to define representative load data for patients with a total hip

joint replacement that can be used in the framework of primary stability assessment *in vitro*.

Previous studies have, however, suggested that there is an intra-individual as well as a considerable inter-individual variability in the musculoskeletal loading conditions at the hip between several repetitions of an activity in a single patient or between different patients (Bergmann *et al.* 2001a; Heller *et al.* 2001; Stansfield and Nicol 2002). In order to avoid the simplified load profile only reflecting the loading characteristics of an individual patient, the musculoskeletal loads presented in this study were derived for a “typical patient”. The data for the “typical patient” were obtained by averaging the gait data of up to four of the six examined THR patients for which *in vivo* measured hip contact forces were also available, using a dedicated averaging method (Bergmann *et al.* 2001a; Bergmann *et al.* 2001b).

In order to derive the musculoskeletal loads for a pre-clinical test, two concurrent requirements had to be met: On one hand, only a limited complexity in terms of the number of muscles included was acceptable in order to be able to realise those conditions for an *in vitro* set-up. On the other hand, however, the loading had to result in a mechanical environment which closely resembled the physiological loading conditions at the hip. Therefore, a simplified model of the hip muscles was derived from a complex model of the human lower extremities that had been validated against *in vivo* data (Heller *et al.* 2001). This musculoskeletal model was used to determine the muscle and joint contact forces for a “typical patient”. The resulting musculoskeletal load profile derived for pre-clinical testing achieved both a physiological-like loading environment, shown by an error less than 10%, but also simplified the muscle activity to a maximum of four muscles – a scenario that has been shown to be achievable in an *in vitro* test set-up. A limitation of this approach, however, is that the simplified testing conditions are derived from a numerical model which by itself is based on some assumptions (Heller *et al.* 2001; Stansfield *et al.* 2003).

The characteristics of the musculoskeletal loading conditions of the “typical patient”, obtained with the simplified model of the hip muscles were comparable to those found for the individual hip patients using complex muscle models. The loading conditions for the two activities included in this study differed both in respect to the force magnitudes as well as in respect to the type of the loading conditions. The load levels during stair climbing were generally higher than those during walking. The instances of maximum loading during walking and stair climbing were characterised by the strong activity of the abductors and the quadriceps muscles (vasti, rectus femoris). Since the hip was more flexed during stair climbing, the muscle activity in the abductor led to a doubling of the anterior-posterior joint contact force component at the hip. Because of the torsional loads acting on the prosthesis shaft during stair climbing, it is considered a critical activity for fixation of the implant (Bergmann *et al.* 1995; O'Connor *et al.* 1996; Shelley *et al.* 1996; Aamodt *et al.* 2001). The musculoskeletal loads associated with this activity were therefore included in the load profile developed in this study.

Activity of the tensor fasciae latae and the ilio-tibial tract was also observed. Whilst the tensor fasciae latae and the ilio-tibial tract are two joint structures without direct attachments at the proximal femur, they can exert forces as they are wrapped around the greater trochanter (Duda *et al.* 1998a) and thereby act to minimise the bending moments in the femur (Pauwels 1951; Rohlmann *et al.* 1980; Rohlmann *et al.* 1982). The step-wise simplification process of the hip muscles revealed that these structures had to be included to maintain physiological loading conditions throughout the full movement cycles. Although the physiological recruitment of muscles is rather complex, the activity of the muscles as described above is also in agreement with typical muscle activity profiles derived from EMG data (Sutherland DH 2001).

The loading profiles for the *in vitro* testing were restricted to the forces and moments occurring at the instant of maximum muscular activity and high joint contact forces. On one hand, the simulation of a complete gait cycle would have unnecessarily added to the complexity of the mechanical *in vitro* loading set-up. On the other hand, analyses of the femoral straining have shown peak strains at this time

point (Stolk *et al.* 2001) and it was therefore hypothesised that peak interface micro-movements would be associated with this time point. The coordinates of all force components were transferred to the composite femur by an osteometric scaling procedure using coordinates of bony landmarks (Sommer *et al.* 1982). Due to the differences in anatomy between patient and composite femur, the scaling process led to variations in the position of the muscle attachment and wrapping sites with respect to the origin of the femur coordinate system (femoral head centre) which in turn resulted in increased joint contact forces. However, these changes in hip joint were still within the range of the inter-individual variability (Bergmann *et al.* 2001a; Heller *et al.* 2001; Stansfield *et al.* 2003) and would in a worst case lead to an over- rather than an underestimation of the actual *in vivo* loading conditions.

4.2.2 Mechanical loading set-up

The musculoskeletal analyses conducted in order to derive representative load profiles for pre-clinical testing of primary stability *in vitro* have confirmed the fact that the loads acting at the hip joint are the result of complex interactions between the forces exerted by muscles spanning the joint and forces due to bodyweight. The interdependency of the load components involved in the generation of the resultant contact force at the hip joint have been found to be of increased importance in the context of simplified loading scenarios which consider only a limited number of soft tissue structures. In fact, a simplified model of the hip musculature is more sensitive to alterations caused by one of the loading components. A mechanical loading set-up that aims at mimicking the loading scenario occurring *in vivo* should therefore reflect these interactions and interdependency, albeit at a more simplified level of complexity.

An established design methodology consisting of several iterative steps was used to help identify the major requirements of the mechanical *in vitro* loading set-up and implement it. Even though each step of this systematic approach was not completed, this method allowed the determination of the main requirements of the mechanical loading set-up and to specify its core function. By subdividing the latter

into sub-functions, suitable working principles were then found and used to elaborate a principle solution that fulfilled the identified requirements. This procedure allowed exploring a wide range of possible solutions, before choosing those which matched best the task to be accomplished.

The components of the set-up as well as the set-up in its entirety fulfilled the previously defined requirements for a physiological-like loading procedure *in vitro*. The servo-electrical actuators used to generate the computed muscle forces exhibited a good dynamic behaviour that could be individually adapted by changing the coefficients of the respective PID-controllers. The generated muscle forces were therefore able to synchronously follow the force applied by the material testing machine which provided a triggering signal for all force actuators. Using synthetic loading ropes, it has been possible to adequately transmit the generated muscle forces from the actuators to the femur. Despite the distance separating some muscle force actuators (vastus lateralis and medialis) from their insertion points on the femur surface, no substantial stretching of the ropes was observed. Through the above-mentioned disposition, it was therefore possible to group all muscle force actuators to a spatial unit attached to the crosshead of the material testing machine that can also be adapted and incorporated into other testing machines.

A point of concern, however, was the interface between the laminate components used to anchor the loading ropes and the femur. Due to space limitation and the local cortical thickness, only a small surface around the insertion sites on the femur could be used for the adhesive bond. As a consequence, mechanical damage of the two-part epoxy bond occasionally occurred when loading the femur with the peak loads. In the present validation study, the results obtained at the load levels representing 50% and 75% of the peak loads allowed differentiation between the loading configurations that were analysed. However, the application of the peak loads may be required in certain circumstances, in which case alternative adhesives and material combinations should be taken into consideration.

The three dimensional loading of the proximal femur was made possible through a system of pulleys with different diameters which were mounted on an adjustable modular frame. To simulate the load profiles corresponding to the different activities, it was only necessary to change the set of pulleys and to adjust the distance between them by means of spacing sleeves. Whilst no considerable deformation of the frame supporting the pulleys of the proximally oriented muscle forces was observed, the x-y table on which the distal part of the femur and the pulleys of the distally oriented muscles were mounted experienced a noticeable, cyclical deflection. However, this elastic deformation had a limited impact on the dynamics of the set-up, since the control path of each muscle actuator unit was customised to accommodate the elasticity of the support. From the perspective of providing a mechanically more stable set-up, the x-y table could, however, be replaced by a simple base-plate screwed on the machine bed allowing only a discrete positioning of the distal femur within the set-up.

In order to evaluate the accuracy of the load simulation *in vitro*, the forces measured in the loading ropes were analysed. Although the closed loop control paths of the muscle structures have been configured to take the deflection of the distal support into account, some discrepancies could still be observed between the measured and the target force values. However, the median errors were relatively small and within the measurement accuracy of the miniature force sensors attached to the ropes. Due to the fact that the deflection of the support tended to stretch the loading ropes, the effective forces were slightly higher than the target values. Only the force magnitudes measured in the vastus medialis during stair climbing exhibited significantly larger median errors and were smaller than the target values, a fact that could be related to the comparatively long fibre rope and to a much higher frictional loss at the pulley. The accuracy of the muscle force simulation may therefore be increased by minimising the deflection of the distal support and the friction at the pulleys.

The components of the hip contact forces were measured *in vitro* throughout the testing period by means of a dedicated three-dimensional force sensor connected

to the head of the prosthesis. A resultant hip joint force was then computed from these components and compared to the *in vivo* measured values. As a result of the variations registered for the actively simulated muscle forces in both the walking and stair climbing configuration, a reduction in hip contact force of up to 9% was occasionally recorded at the prosthesis head. Furthermore, the variations in direction registered for the hip contact force could be attributed to the small rotation of the implanted femur under load. Even though the median errors of the hip contact force were above those created by the direct application of the joint force by the material testing machine, the indirectly-generated hip contact force compared well with the values measured *in vivo*.

4.2.3 Testing protocol for prosthesis stability

Quantitative assessment of the primary stability of cementless prostheses *in vitro* involve many steps ranging from the implementation of a mechanical set-up to generate and apply the required loads, to the devices used to record the load-induced interface micro-movements. Each single step of the testing protocol can be considered a potential source of variability which may affect the measurements (Harman *et al.* 1995; Monti *et al.* 1999) and should therefore be as standardised as possible to enhance the accuracy of the results obtained experimentally.

A main concern in primary stability testing *in vitro* is related to the difficulty obtaining anatomically similar cadaver femora which are also free of any pathological abnormalities. Geometrical variations of the femur anatomy are associated with changes in magnitude and orientation of the musculoskeletal loads acting at the hip joint. Commercially available synthetic composite femora (Model 3103, Sawbones Europe AB, Malmö, Sweden) were therefore used in the present study to define representative load profiles of the proximal femur and thus to avoid re-definitions of the load profiles to accommodate individual femur anatomies. Further advantages of composite femora over human specimens are lower inter-specimen variability of the mechanical properties and the ready availability and the ease of handling (Cristofolini *et al.* 1996). Due to the fact that synthetic femur models are widely used as

mechanical surrogates in orthopaedic research both for experimental and finite element analyses (McKellop *et al.* 1991; Szivek and Gealer 1991; McNamara *et al.* 1994; Flahiff *et al.* 1995; Kummer *et al.* 1997; McNamara *et al.* 1997; Lee *et al.* 1998; Pugh *et al.* 1998; Sakai *et al.* 2000; Heiner and Brown 2001; Waide *et al.* 2003), basing validated and representative load profiles on them may also facilitate comparisons between different studies.

In addition to the anatomical similarity, composite femora should also exhibit mechanical properties comparable to those of human specimens in order to be suitable for the analysis of primary stability *in vitro*. Furthermore, composite femora need to be structurally equivalent to humans. The composite femora used in this study consisted of a fibre-reinforced epoxy resin and polyurethane foam representing the cortical and the cancellous bone respectively. Cristofolini and co-workers conducted an experimental validation study in which axial, bending and torsional stiffness as well as the strain distribution of whole composite and human femora were compared (Cristofolini *et al.* 1996). The composite femora were shown to fall within the range of the human specimens and exhibited a significantly lower inter-specimen variability. Since cementless hip prostheses rely on medullary press-fit anchorage, their stability depends on the mechanical quality of the cancellous bone. Szivek and co-workers (1991; 1993) found that the mechanical properties of the polyurethane foam used to model the cancellous bone were within the range of the values reported for human femora, but showed larger inter-specimen variations. Whilst synthetic composite femora represent a useful tool to compare the primary stability of different prosthesis designs, a direct comparison of the micro-movements determined using these femur analogues with *in vivo* data should however be considered with caution.

A further possible source of error in primary stability assessment is the positioning of the prosthesis within the medullary canal which is in turn related to the accuracy of the canal preparation and the implantation procedure. Mal-alignment of the prosthesis commonly resulting in a varus position has been associated with poor outcomes in total hip arthroplasty. Although a varus alignment has been reported to have no adverse effect on the clinical outcome of patients who received the

prostheses used in the present study, the Alloclassic Zweymueller and the CLS Spotorno (Khalily and Lester 2002; Schneider U *et al.* 2002), an attempt was undertaken to make the implantation procedure as accurate as possible and to achieve a neutral positioning of the prostheses. Reaming of the medullary canal was therefore performed using a CNC machine, after the femur has been clamped in a dedicated custom-designed device and positioned within the CNC machine. It has thus been possible to prepare the prosthesis bed in a reproducible manner. Due to occasional surface in-homogeneities of the composite bones, slight variations in position were observed when mounting the femora into the clamping device. However, this had no major impact on the final alignment of the prostheses within the femur as documented in the two-plane X-rays taken after implantation.

Because the biological integration of the femoral component of total hip joint reconstructions is related to the local mechanical conditions, neither micro-movement measurements at a single location nor computed global motions may sufficiently describe the events at the interface (Gustilo *et al.* 1989; Sugiyama *et al.* 1989; Phillips TW *et al.* 1991). The findings of this study confirm the assumption that relative micro-movements at the bone-prosthesis interface vary from region to region (Schneider E *et al.* 1989a; Harman *et al.* 1995; Buhler *et al.* 1997). Since it is technically not possible to examine all locations, experimental analyses should concentrate on the most relevant regions and movement components. In this study, focus was made on six single measurement locations. The locations were selected to cover the proximal, intermediary and distal regions of the prostheses and, at the same time, to minimize the closeness to the muscle attachment and wrapping sites. With the exception of one transducer which was mounted between the attachment sites of the vastus lateralis and medialis, all the remaining transducers were relatively far from the muscle attachment sites. It can therefore be assumed that muscle forces exerted a more global effect on the relative prosthesis movements by influencing the overall stress of the femur. Another distribution of the measurement points may result in different movement magnitudes, but not necessarily different movement patterns.

The method of movement measurement was configured in such a way that the distance between the attachment point of the measurement device on the femur surface and the point of measurement at the interface was as small as possible. In fact, the devices supporting the measurement transducers were mounted in transcortical holes directly at the locations of micro-movement measurement, thus minimizing the influence of bone deformation on the transducer readouts. Furthermore, the diameter of the local holes used to fix the sensors was selected as small as possible to avoid modifications of the mechanical behaviour of the bone (Monti *et al.* 1999). Only the transducer for recording the movement of the prosthesis shoulder was attached at the greater trochanter, because of the space limitation near the head of the prosthesis. Due to the long lever arm of the reference metal bar screwed at the prosthesis shoulder, the effective longitudinal movement of the stem may therefore have been overlapped or overshadowed by the movement components created by the medio-lateral tilt of the prosthesis. This may have led to the shift in direction occasionally observed at the prosthesis shoulder and at the tip of the prosthesis, suggesting that the prosthesis was moving out of the femur. This phenomenon seems to be less pronounced with increasing axial migration of the stem, as observed during stair climbing with active simulation of muscle forces.

The duration of the cyclical loading of the femur to assess the primary stability of cementless prostheses *in vitro* should consider the distribution observed in total hip patients *in vivo* (Morlock *et al.* 2001). In contrast to failure testing which may simulate up to one million loading cycles, *in vitro* testing of primary stability of cementless prostheses should meet two concurrent requirements. Due to the fact that bone remodelling processes around the prosthesis can not be taken into consideration in such an experimental *in vitro* set-up, the test period on the one hand should be limited to the phase preceding these processes, i.e. within the first 6 to 12 weeks following surgery (Gebauer *et al.* 1989; Phillips TW *et al.* 1990). On the other hand, however, the number of loading cycles should be sufficiently high to differentiate between prosthesis designs. In this study, 1000 loading cycles were therefore simulated for each loading configuration. This restriction was determined by preliminary tests and results of other investigators that documented no considerable

migration of the prosthesis afterwards (Hua and Walker 1994; Buhler *et al.* 1997). In addition, restrictions on activity are usually recommended to THA patients in the early post operative period in order to prevent overloading, thus limiting the number of loading cycles.

4.3 Conclusion

The present study has demonstrated the applicability and the relevance of a new, physiological-like loading concept with respect to the *in vitro* assessment of the primary stability of cementless total hip prostheses.

The mechanical loading set-up of the proximal femur presented in this study is based on balanced loading configurations that mimic the three dimensional loading of the proximal femur including the active contribution of muscle forces as it occurs *in vivo*. Moreover, the simulated loads were derived from a complex musculoskeletal model of the lower extremity validated against joint contact forces measured in total hip arthroplasty patients while performing two common daily tasks: level walking and stair climbing. Although the number of active muscles was reduced to be able to manage the complexity of the *in vitro* test set-up, the extracted simplified load cases are, in terms of the resultant hip contact force and muscle activity, comparable to the complex loading situation *in vivo*.

When used to evaluate the primary stability of cementless hip prostheses, the implemented physiological-like loading set-up better approximated the load-induced micro-movements at the femur-prosthesis interface with respect to the *in vivo* data. Furthermore, the loading set-up produced patterns and magnitudes of interface micro-movements consistent with the simulated patient activity and allowed differentiation between prostheses with distinctive anchorage principles. The analyses suggested that active simulation of muscle forces considerably affects the primary stability of cementless hip endoprostheses. Compared to level walking, stair climbing activities induced a higher mechanical instability at the bone-prosthesis interface. The interface micro-movements occurring during this activity may

compromise the necessary osseointegration process. Pre-clinical *in vitro* tests should therefore simulate stair climbing and include the active role of muscles in the assessment of initial prosthesis stability, otherwise interface micro-movements may be underestimated and the primary stability overestimated.

5 Consequences

Improvements in bio-material sciences, prosthesis design and intra-operative handling have lead to a significant reduction in the clinical rate of total hip arthroplasty (THA) failure due to prosthesis breakage (Dall *et al.* 1993; Malchau *et al.* 2002). Since then, pre-clinical analyses in total hip arthroplasty have mainly focussed on the evaluation and optimisation of the mechanical conditions at the interface between the prosthesis and the surrounding cancellous bone. In this respect, particular attention is dedicated to the post-operative fixation strength of the bone-prosthesis complex which has been identified as a critical parameter for the biological integration of cementless prostheses (Pilliar *et al.* 1986; Morscher E 1987; Sugiyama *et al.* 1989; Soballe 1993).

5.1 Pre-clinical analysis of primary stability *in vitro*

The significance of retrospective *in vivo* measurements of post-operative early implant migration in predicting the long-term outcome of hip prostheses has been already documented by several authors using Stereophotogrammetric Analyses (Mjoberg *et al.* 1986; Wykman *et al.* 1988; Karrholm 1989; Nistor *et al.* 1991; Soballe 1993). Pre-clinical evaluations of the implant stability *in vitro* can help reduce the percentage of THA failures *in vivo* due to poor initial fixation. The appropriateness of such *in vitro* testing procedures relies on their ability to generate patterns and magnitudes of interface movements comparable to those measured retrospectively in THA patients.

In this thesis a new approach in the pre-clinical assessment of the primary stability of cementless hip prostheses has been presented and evaluated. The implemented mechanical loading set-up was based on musculoskeletal loads that have been previously validated against data measured in THA patients *in vivo*. The

results of the study suggest that a physiological-like loading of the proximal femur which enables active simulation of muscle forces is a prerequisite for a more realistic evaluation of the initial stability of cementless hip prostheses *in vitro*. The presented testing procedure and evaluation protocol therefore represent a major contribution in the definition of a standardised test protocol for the assessment of primary stability of cementless prostheses *in vitro*, with particular emphasis on the loading scenario. A successful definition of such a standard would contribute to detection of hip prostheses with a likelihood of inferior *in vivo* performance and thus increase the long-term outcome *in vivo* by improving their design prior to clinical release (Vander Sloten *et al.* 1993; Morscher EW 2003).

5.2 Clinical use

From a clinical perspective, the findings of this study illustrate the influence of the anchoring principle and strengthen the role of the patient activity on the mechanical stability at the bone-prosthesis interface after cementless THA.

Due to the often inferior quality of the bone stock in the proximal femur region in terms of mechanical strength of cancellous bone, metaphyseal prostheses may tend to show larger initial migrations than diaphyseal prostheses. Therefore, a sufficient fit and fill of the medullary canal should be ensured in order to reduce the amount of initial migration (Gebauer *et al.* 1990; Eingartner *et al.* 1997). If required, a more diaphyseal, cortical anchorage that bypasses the low strength region should be employed.

The motor tasks performed by total hip arthroplasty patients after surgery determine the micro-movements at the bone-prosthesis interface. Regardless of the method of prosthesis anchorage, the activity of stair climbing generated the highest instability at the bone-prosthesis interface. Stair climbing should therefore be carefully considered in the framework of post-operative rehabilitation as well as in the process of resuming to normal daily life activities.

Literature

Aamodt A, Lund-Larsen J, Eine J, Andersen E, Benum P and Husby OS (2001): Changes in proximal femoral strain after insertion of uncemented standard and customised femoral stems. An experimental study in human femora. *J Bone Joint Surg Br* 83(6): 921-9.

Aldinger PR, Thomsen M, Mau H, Ewerbeck V and Breusch SJ (2003): Cementless Spotorno tapered titanium stems: excellent 10-15-year survival in 141 young patients. *Acta Orthop Scand* 74(3): 253-8.

Amstutz HC (1985): Arthroplasty of the hip. The search for durable component fixation. *Clin Orthop*(200): 343-61.

Andrews JG and Mish SP (1996): Methods for investigating the sensitivity of joint resultants to body segment parameter variations. *J Biomech* 29(5): 651-4.

Bachus KN, Bloebaum RD and Jones RE (1999): Comparative micromotion of fully and proximally cemented femoral stems. *Clin Orthop*(366): 248-57.

Baleani M, Cristofolini L and Toni A (2000): Initial stability of a new hybrid fixation hip stem: experimental measurement of implant-bone micromotion under torsional load in comparison with cemented and cementless stems. *J Biomed Mater Res* 50(4): 605-15.

Baleani M, Cristofolini L and Viceconti M (1999): Endurance testing of hip prostheses: a comparison between the load fixed in ISO 7206 standard and the physiological loads. *Clin Biomech (Bristol, Avon)* 14(5): 339-45.

Bergmann G, Deuretzbacher G, Heller M, Graichen F, Rohlmann A, Strauss J and Duda GN (2001a): Hip contact forces and gait patterns from routine activities. *J Biomech* 34(7): 859-71.

Bergmann G, Gandini R and Ruder H (2001b): Averaging of strongly varying signals. *Biomed Tech (Berl)* 46(6): 168-71.

Bergmann G, Graichen F and Rohlmann A (1993): Hip joint loading during walking and running, measured in two patients. *J Biomech* 26(8): 969-90.

Bergmann G, Graichen F and Rohlmann A (1995): Is staircase walking a risk for the fixation of hip implants? *J Biomech* 28(5): 535-53.

Bergmann G, Graichen F and Rohlmann A (2004): Hip joint contact forces during stumbling. *Langenbecks Arch Surg* 389(1): 53-9.

Berzins A, Sumner DR, Andriacchi TP and Galante JO (1993): Stem curvature and load angle influence the initial relative bone- implant motion of cementless femoral stems [published erratum appears in *J Orthop Res* 1995 Jan;13(1):151]. *J Orthop Res* 11(5): 758-69.

Biedermann R, Krismer M, Stockl B, Mayrhofer P, Ornstein E and Franzen H (1999): Accuracy of EBRA-FCA in the measurement of migration of femoral components of total hip replacement. Einzel-Bild-Rontgen-Analyse- femoral component analysis. *J Bone Joint Surg Br* 81(2): 266-72.

Bjorklund L (1998): The Bone and Joint Decade 2000-2010. Inaugural meeting 17 and 18 April 1998, Lund, Sweden. *Acta Orthop Scand Suppl* 281: 67-80.

Bobyn JD, Pilliar RM, Cameron HU and Weatherly GC (1980): The optimum pore size for the fixation of porous-surfaced metal implants by the ingrowth of bone. *Clin Orthop*(150): 263-70.

Bourne RB and Rorabeck CH (1998): A critical look at cementless stems. Taper designs and when to use alternatives. *Clin Orthop*(355): 212-23.

Brand RA, Crowninshield RD, Wittstock CE, Pedersen DR, Clark CR and van Krieken FM (1982): A model of lower extremity muscular anatomy. *J Biomech Eng* 104(4): 304-10.

Brand RA, Pedersen DR, Davy DT, Kotzar GM, Heiple KG and Goldberg VM (1994): Comparison of hip force calculations and measurements in the same patient. *J Arthroplasty* 9(1): 45-51.

Brand RA, Pedersen DR and Friederich JA (1986): The sensitivity of muscle force predictions to changes in physiologic cross-sectional area. *J Biomech* 19(8): 589-96.

Breusch SJ, Aldinger PR, Thomsen M, Ewerbeck V and Lukoschek M (2000): [Anchoring principles in hip endoprostheses. I: Prosthesis stem]. *Unfallchirurg* 103(11): 918-31.

Britton JR, Walsh LA and Prendergast PJ (2003): Mechanical simulation of muscle loading on the proximal femur: analysis of cemented femoral component migration with and without muscle loading. *Clin Biomech (Bristol, Avon)* 18(7): 637-46.

Buhler DW, Berlemann U, Lippuner K, Jaeger P and Nolte LP (1997): Three-dimensional primary stability of cementless femoral stems. *Clin Biomech (Bristol, Avon)* 12(2): 75-86.

Burke DW, DO OC, Zalenski EB, Jasty M and Harris WH (1991): Micromotion of cemented and uncemented femoral components. *J Bone Joint Surg [Br]* 73(1): 33-7.

Callaghan JJ (1992): Total hip arthroplasty. Clinical perspective. *Clin Orthop*(276): 33-40.

Callaghan JJ, Fulghum CS, Glisson RR and Stranne SK (1992): The effect of femoral stem geometry on interface motion in uncemented porous-coated total hip prostheses. Comparison of straight-stem and curved-stem designs. *J Bone Joint Surg [Am]* 74(6): 839-48.

Cameron HU, Pilliar RM and MacNab I (1973): The effect of movement on the bonding of porous metal to bone. *J Biomed Mater Res* 7(4): 301-11.

Capello WN (1990): Technical aspects of cementless total hip arthroplasty. *Clin Orthop*(261): 102-6.

Chao EY and Rim K (1973): Application of optimization principles in determining the applied moments in human leg joints during gait. *J Biomech* 6(5): 497-510.

Chareancholvanich K, Bourgeault CA, Schmidt AH, Gustilo RB and Lew WD (2002): *In vitro* stability of cemented and cementless femoral stems with compaction. Clin Orthop(394): 290-302.

Charnley J, Follacci FM and Hammond BT (1968): The long-term reaction of bone to self-curing acrylic cement. J Bone Joint Surg Br 50(4): 822-9.

Cheal EJ, Spector M and Hayes WC (1992): Role of loads and prosthesis material properties on the mechanics of the proximal femur after total hip arthroplasty. J Orthop Res 10(3): 405-22.

Claes L, Fiedler S, Ohnmacht M and Duda GN (2000): Initial stability of fully and partially cemented femoral stems. Clin Biomech (Bristol, Avon) 15(10): 750-5.

Cristofolini L, Viceconti M, Cappello A and Toni A (1996): Mechanical validation of whole bone composite femur models [see comments]. J Biomech 29(4): 525-35.

Cristofolini L, Viceconti M, Toni A and Giunti A (1995): Influence of thigh muscles on the axial strains in a proximal femur during early stance in gait. J Biomech 28(5): 617-24.

Dall DM, Learmonth ID, Solomon M and Davenport JM (1993): 811 Charnley hips followed for 3-17 years. Acta Orthop Scand 64(3): 252-6.

Davidson JA, Mishra AK, Kovacs P and Poggie RA (1994): New surface-hardened, low-modulus, corrosion-resistant Ti-13Nb-13Zr alloy for total hip arthroplasty. Biomed Mater Eng 4(3): 231-43.

Davies MS, Parker BC, Ward DA, Hua J and Walker PS (1999): Migration of the uncemented CLS femoral component. Orthopedics 22(2): 225-8.

Davy DT, Kotzar GM, Brown RH, Heiple KG, Goldberg VM, Heiple KG, Jr., Berilla J and Burstein AH (1988): Telemetric force measurements across the hip after total arthroplasty. J Bone Joint Surg Am 70(1): 45-50.

De Visser E, Mulder T, Schreuder HW, Veth RP and Duysens J (2000): Gait and electromyographic analysis of patients recovering after limb-saving surgery. *Clin Biomech* (Bristol, Avon) 15(8): 592-9.

Delaunay C, Cazeau C and Kapandji AI (1998): Cementless primary total hip replacement. Four to eight year results with the Zweymuller-Alloclassic prosthesis. *Int Orthop* 22(1): 1-5.

Delaunay C and Kapandji AI (1998): [10-year survival of Zweymuller total prostheses in primary uncemented arthroplasty of the hip]. *Rev Chir Orthop Reparatrice Appar Mot* 84(5): 421-32.

Doehring TC, Rubash HE and Dore DE (1999): Micromotion measurements with hip center and modular neck length alterations. *Clin Orthop*(362): 230-9.

Doehring TC, Rubash HE, Shelley FJ, Schwendeman LJ, Donaldson TK and Navalgund YA (1996): Effect of superior and superolateral relocations of the hip center on hip joint forces. An experimental and analytical analysis. *J Arthroplasty* 11(6): 693-703.

Donnelly WJ, Kobayashi A, Freeman MA, Chin TW, Yeo H, West M and Scott G (1997): Radiological and survival comparison of four methods of fixation of a proximal femoral stem. *J Bone Joint Surg Br* 79(3): 351-60.

Dorr LD, Lewonowski K, Lucero M, Harris M and Wan Z (1997): Failure mechanisms of anatomic porous replacement I cementless total hip replacement. *Clin Orthop*(334): 157-67.

Dorr LD, Wan Z, Song M and Ranawat A (1998): Bilateral total hip arthroplasty comparing hydroxyapatite coating to porous-coated fixation. *J Arthroplasty* 13(7): 729-36.

Ducheyne P, De Meester P and Aernoudt E (1977): Influence of a functional dynamic loading on bone ingrowth into surface pores of orthopedic implants. *J Biomed Mater Res* 11(6): 811-38.

Duda GN, Heller M, Albinger J, Schulz O, Schneider E and Claes L (1998a): Influence of muscle forces on femoral strain distribution. *J Biomech* 31(9): 841-6.

Duda GN, Heller M, Albinger J, Schulz O, Schneider E and Claes L (1998b): Influence of muscle forces on femoral strain distribution. *J Biomech* 31(9): 841-6.

Duda GN, Schneider E and Chao EY (1997): Internal forces and moments in the femur during walking. *J Biomech* 30(9): 933-41.

Effenberger H, Heiland A, Ramsauer T, Plitz W and Dorn U (2001): A model for assessing the rotational stability of uncemented femoral implants. *Arch Orthop Trauma Surg* 121(1-2): 60-4.

Eingartner C, Volkmann R, Putz M and Weller S (1997): Uncemented revision stem for biological osteosynthesis in periprosthetic femoral fractures. *Int Orthop* 21(1): 25-9.

Engh CA, O'Connor D, Jasty M, McGovern TF, Bobyn JD and Harris WH (1992): Quantification of implant micromotion, strain shielding, and bone resorption with porous-coated anatomic medullary locking femoral prostheses. *Clin Orthop*(285): 13-29.

Engh CA, Sr. and Culpepper WJ, 2nd (1997): Femoral fixation in primary total hip arthroplasty. *Orthopedics* 20(9): 771-3.

English TA and Kilvington M (1979): *In vivo* records of hip loads using a femoral implant with telemetric output (a preliminary report). *J Biomed Eng* 1(2): 111-5.

Eyb R, Kutschera HP, Schartelmueller T, Toma C and Zweymueller K (1993): Midterm experience with the cementless Zweymueller system. Results of a minimum five-year follow-up study. *Acta Orthop Belg* 59 Suppl 1: 138-43.

Fetto J, Leali A and Moroz A (2002): Evolution of the Koch model of the biomechanics of the hip: clinical perspective. *J Orthop Sci* 7(6): 724-30.

Fischer KJ, Carter DR and Maloney WJ (1992): *In vitro* study of initial stability of a conical collared femoral component. *J Arthroplasty* 7(Suppl): 389-95.

Flahiff CM, Gober GA and Nicholas RW (1995): Pullout strength of fixation screws from polymethylmethacrylate bone cement. *Biomaterials* 16(7): 533-6.

Freeman MA and Plante-Bordeneuve P (1994): Early migration and late aseptic failure of proximal femoral prostheses [published erratum appears in *J Bone Joint Surg Br* 1994 Nov;76(6):999]. *J Bone Joint Surg Br* 76(3): 432-8.

Galante J, Sumner DR and Gachter A (1987): [Surface structures and bone ingrowth in cement-free fixed prostheses]. *Orthopade* 16(3): 197-205.

Garcia-Cimbrelo E, Cruz-Pardos A, Madero R and Ortega-Andreu M (2003): Total Hip Arthroplasty with Use of the Cementless Zweymuller Alloclassic System: A Ten to Thirteen-Year Follow-up Study. *J Bone Joint Surg Am* 85-A(2): 296-303.

Gebauer D, Refior HJ and Haake M (1989): Micromotions in the primary fixation of cementless femoral stem prostheses. *Arch Orthop Trauma Surg* 108(5): 300-7.

Gebauer D, Refior HJ and Haake M (1990): [Experimental studies of the effect of surgical technical errors on primary stability of cementless hip endoprosthesis shafts]. *Z Orthop Ihre Grenzgeb* 128(1): 100-7.

Geesink RG (1989): Experimental and clinical experience with hydroxyapatite-coated hip implants [published erratum appears in *Orthopedics* 1990 Feb;13(2):following 200]. *Orthopedics* 12(9): 1239-42.

Geesink RG and Hoefnagels NH (1995): Six-year results of hydroxyapatite-coated total hip replacement. *J Bone Joint Surg Br* 77(4): 534-47.

Ghista D, Toridis T and Srinivasan TM (1976): Human gait analysis: determination of instantaneous joint reactive forces, muscle forces and the stress distribution in bone segments. Part 11. *Biomed Tech (Berl)* 21(3): 66-74.

Gibbons CE, Davies AJ, Amis AA, Olearnik H, Parker BC and Scott JE (2001): Periprosthetic bone mineral density changes with femoral components of differing design philosophy. *Int Orthop* 25(2): 89-92.

Gillies RM, Morberg PH, Bruce WJ, Turnbull A and Walsh WR (2002): The influence of design parameters on cortical strain distribution of a cementless titanium femoral stem. *Med Eng Phys* 24(2): 109-14.

Glitsch U and Baumann W (1997): The three-dimensional determination of internal loads in the lower extremity. *J Biomech* 30(11-12): 1123-31.

Gotze C, Steens W, Vieth V, Poremba C, Claes L and Steinbeck J (2002): Primary stability in cementless femoral stems: custom-made versus conventional femoral prosthesis. *Clin Biomech (Bristol, Avon)* 17(4): 267-273.

Graves EJ and Kozak LJ (1998): Detailed diagnoses and procedures, National Hospital Discharge Survey, 1996. *Vital Health Stat* 13(138): i-iii, 1-151.

Gustilo RB, Bechtold JE, Giacchetto J and Kyle RF (1989): Rationale, experience, and results of long-stem femoral prosthesis. *Clin Orthop*(249): 159-68.

Haddad RJ, Jr., Cook SD and Thomas KA (1987): Biological fixation of porous-coated implants. *J Bone Joint Surg Am* 69(9): 1459-66.

Hardinge K, Porter ML, Jones PR, Hukins DW and Taylor CJ (1991): Measurement of hip prostheses using image analysis. The maxima hip technique. *J Bone Joint Surg Br* 73(5): 724-8.

Harman MK, Toni A, Cristofolini L and Viceconti M (1995): Initial stability of uncemented hip stems: an in-vitro protocol to measure torsional interface motion. *Med Eng Phys* 17(3): 163-71.

Harrington MA, Jr., O'Connor DO, Lozynsky AJ, Kovach I and Harris WH (2002): Effects of femoral neck length, stem size, and body weight on strains in the proximal cement mantle. *J Bone Joint Surg Am* 84-A(4): 573-9.

Harris WH, Mulroy RD, Jr., Maloney WJ, Burke DW, Chandler HP and Zalenski EB (1991): Intraoperative measurement of rotational stability of femoral components of total hip arthroplasty. *Clin Orthop*(266): 119-26.

Havelin LI, Espehaug B, Vollset SE and Engesaeter LB (1995): Early aseptic loosening of uncemented femoral components in primary total hip replacement. A review based on the Norwegian Arthroplasty Register [published erratum appears in J Bone Joint Surg Br 1995 Nov;77(6):985]. J Bone Joint Surg Br 77(1): 11-7.

Havelin LI, Espehaug B, Vollset SE, Engesaeter LB and Langeland N (1993): The Norwegian arthroplasty register. A survey of 17,444 hip replacements 1987-1990. Acta Orthop Scand 64(3): 245-51.

Hayashi K, Mashima T and Uenoyama K (1999): The effect of hydroxyapatite coating on bony ingrowth into grooved titanium implants. Biomaterials 20(2): 111-9.

Heiner AD and Brown TD (2001): Structural properties of a new design of composite replicate femurs and tibias. J Biomech 34(6): 773-81.

Heller MO, Bergmann G, Deuretzbacher G, Durselen L, Pohl M, Claes L, Haas NP and Duda GN (2001): Musculoskeletal loading conditions at the hip during walking and stair climbing. J Biomech 34(7): 883-93.

Herren T, Remagen W and Schenk R (1987): [Histology of the implant-bone interface in cemented and uncemented endoprostheses]. Orthopade 16(3): 239-51.

Hua J and Walker PS (1994): Relative motion of hip stems under load. An *in vitro* study of symmetrical, asymmetrical, and custom asymmetrical designs. J Bone Joint Surg Am 76(1): 95-103.

Huiskes R (1997): Total joint replacement: on innovation, ambition, courage, irony and morsellized bone, of course. Iowa Orthop J 17: 130-3.

Jaffe WL and Scott DF (1996): Total hip arthroplasty with hydroxyapatite-coated prostheses. J Bone Joint Surg Am 78(12): 1918-34.

Karrholm J (1989): Roentgen stereophotogrammetry. Review of orthopedic applications. Acta Orthop Scand 60(4): 491-503.

Karrholm J, Nivbrant B, Thanner J, Anderberg C, Borlin N, Herberts P and Malchau H (2000): Radiostereometric evaluation of hip implant design and surface finish.

Kendrick JB, 2nd, Noble PC and Tullos HS (1995): Distal stem design and the torsional stability of cementless femoral stems. *J Arthroplasty* 10(4): 463-9.

Khalily C and Lester DK (2002): Results of a tapered cementless femoral stem implanted in varus. *J Arthroplasty* 17(4): 463-6.

Kim YH and Kim VE (1993): Early migration of uncemented porous coated anatomic femoral component related to aseptic loosening. *Clin Orthop*(295): 146-55.

Kishida Y, Sugano N, Sakai T, Nishii T, Haraguchi K, Ohzono K and Yoshikawa H (2001): Full weight-bearing after cementless total hip arthroplasty. *Int Orthop* 25(1): 25-8.

Kitamura S, Hasegawa Y, Iwasada S, Yamauchi K, Kawamoto K, Kanamono T and Iwata H (1999): Catastrophic failure of cementless total hip arthroplasty using a femoral component without surface coating. *J Arthroplasty* 14(8): 918-24.

Kobayashi A, Donnelly WJ, Scott G and Freeman MA (1997): Early radiological observations may predict the long-term survival of femoral hip prostheses. *J Bone Joint Surg Br* 79(4): 583-9.

Kobayashi S, Eftekhari NS, Terayama K and Joshi RP (1997): Comparative study of total hip arthroplasty between younger and older patients. *Clin Orthop*(339): 140-51.

Kobayashi S, Saito N, Horiuchi H, Iorio R and Takaoka K (2000): Poor bone quality or hip structure as risk factors affecting survival of total-hip arthroplasty. *Lancet* 355(9214): 1499-504.

Korovessis P, Piperos G, Michael A, Baikousis A and Stamatakis M (1997): Changes in bone mineral density around a stable uncemented total hip arthroplasty. *Int Orthop* 21(1): 30-4.

Kotzar GM, Davy DT, Goldberg VM, Heiple KG, Berilla J, Heiple KG, Jr., Brown RH and Burstein AH (1991): Telemeterized *in vivo* hip joint force data: a report on two patients after total hip surgery. *J Orthop Res* 9(5): 621-33.

Krebs DE, Robbins CE, Lavine L and Mann RW (1998): Hip biomechanics during gait. *J Orthop Sports Phys Ther* 28(1): 51-9.

Krismer M, Biedermann R, Stockl B, Fischer M, Bauer R and Haid C (1999): The prediction of failure of the stem in THR by measurement of early migration using EBRA-FCA. Einzel-Bild-Roentgen-Analyse-femoral component analysis. *J Bone Joint Surg Br* 81(2): 273-80.

Kronick JL, Barba ML and Paprosky WG (1997): Extensively coated femoral components in young patients. *Clin Orthop*(344): 263-74.

Kummer FJ, Pearlman CA, Koval KJ and Ceder L (1997): Use of the Medoff sliding plate for subtrochanteric hip fractures. *J Orthop Trauma* 11(3): 180-2.

Laine HJ, Puolakka TJ, Moilanen T, Pajamaki KJ, Wirta J and Lehto MU (2000): The effects of cementless femoral stem shape and proximal surface texture on 'fit-and-fill' characteristics and on bone remodeling. *Int Orthop* 24(4): 184-90.

Latour RA, Jr. and Brattain MA (2000): Femoral strain profiles under simulated 3-D muscle and joint loads for heel strike, midstance, and toe off. *Crit Rev Biomed Eng* 28(1-2): 109-13.

Laupacis A, Bourne R, Rorabeck C, Feeny D, Wong C, Tugwell P, Leslie K and Bullas R (1993): The effect of elective total hip replacement on health-related quality of life. *J Bone Joint Surg Am* 75(11): 1619-26.

Lee TQ, Danto MI and Kim WC (1998): Initial stability comparison of modular hip implants in synthetic femurs. *Orthopedics* 21(8): 885-8.

Letournel E (1987): Non cemented hip implants. Failures of biologically fixed devices: causes and treatment. *Hip*: 318-50.

Liu C, Green SM, Watkins ND, Gregg PJ and McCaskie AW (2003): A preliminary hip joint simulator study of the migration of a cemented femoral stem. *Proc Inst Mech Eng [H]* 217(2): 127-35.

Lu TW, JJ OC, Taylor SJ and Walker PS (1998): Validation of a lower limb model with *in vivo* femoral forces telemetered from two subjects. J Biomech 31(1): 63-9.

Lu TW, Taylor SJ, JJ OC and Walker PS (1997): Influence of muscle activity on the forces in the femur: an *in vivo* study. J Biomech 30(11-12): 1101-6.

Maher SA and Prendergast PJ (2002): Discriminating the loosening behaviour of cemented hip prostheses using measurements of migration and inducible displacement. J Biomech 35(2): 257-65.

Malchau H, Herberts P and Ahnfelt L (1993): Prognosis of total hip replacement in Sweden. Follow-up of 92,675 operations performed 1978-1990. Acta Orthop Scand 64(5): 497-506.

Malchau H, Herberts P, Garellick G, Söderman P and Eisler T (2002). Prognosis of Total Hip Replacement: Update of Results and Risk-Ratio Analysis for Revision and Re-revision from the Swedish National Hip Arthroplasty Register 1979-2000. 69th Annual Meeting of the American Academy of Orthopaedic Surgeons, Dallas, USA, AAOS.

Malchau H, Karrholm J, Wang YX and Herberts P (1995): Accuracy of migration analysis in hip arthroplasty. Digitized and conventional radiography, compared to radiostereometry in 51 patients. Acta Orthop Scand 66(5): 418-24.

Maloney WJ, Jasty M, Burke DW, O'Connor DO, Zalenski EB, Bragdon C and Harris WH (1989): Biomechanical and histologic investigation of cemented total hip arthroplasties. A study of autopsy-retrieved femurs after *in vivo* cycling. Clin Orthop(249): 129-40.

McKellop H, Ebrahimzadeh E, Niederer PG and Sarmiento A (1991): Comparison of the stability of press-fit hip prosthesis femoral stems using a synthetic model femur [published erratum appears in J Orthop Res 1991 Nov;9(6):933]. J Orthop Res 9(2): 297-305.

McNamara BP, Cristofolini L, Toni A and Taylor D (1994): Evaluation of experimental and finite element models of synthetic and cadaveric femora for pre-clinical design-analysis. *Clin Mater* 17(3): 131-40.

McNamara BP, Cristofolini L, Toni A and Taylor D (1997): Relationship between bone-prosthesis bonding and load transfer in total hip reconstruction. *J Biomech* 30(6): 621-30.

Mitoma H, Hayashi R, Yanagisawa N and Tsukagoshi H (2000): Characteristics of parkinsonian and ataxic gaits: a study using surface electromyograms, angular displacements and floor reaction forces. *J Neurol Sci* 174(1): 22-39.

Mjoberg B (1991): Fixation and loosening of hip prostheses. A review [see comments]. *Acta Orthop Scand* 62(5): 500-8.

Mjoberg B, Selvik G, Hansson LI, Rosenqvist R and Onnerfalt R (1986): Mechanical loosening of total hip prostheses. A radiographic and roentgen stereophotogrammetric study. *J Bone Joint Surg Br* 68(5): 770-4.

Monti L, Cristofolini L and Viceconti M (1999): Methods for quantitative analysis of the primary stability in uncemented hip prostheses [In Process Citation]. *Artif Organs* 23(9): 851-9.

Morlock M, Schneider E, Bluhm A, Vollmer M, Bergmann G, Muller V and Honl M (2001): Duration and frequency of every day activities in total hip patients. *J Biomech* 34(7): 873-81.

Morscher E (1987): [Experiences, requirements and development of cement-free hip endoprostheses]. *Orthopade* 16(3): 185-96.

Morscher EW (2003): Failures and successes in total hip replacement--why good ideas may not work. *Scand J Surg* 92(2): 113-20.

Mulroy RD, Jr., Sedlacek RC, DO OC, Estok DMd and Harris WH (1991): Technique to detect migration of femoral components of total hip arthroplasties on conventional radiographs. *J Arthroplasty* 6 Suppl: S1-4.

Munting E and Verhelpen M (1993): Mechanical simulator for the upper femur. *Acta Orthop Belg* 59(2): 123-9.

Murray CJ and Lopez AD (1997): Regional patterns of disability-free life expectancy and disability-adjusted life expectancy: global Burden of Disease Study. *Lancet* 349(9062): 1347-52.

Naidu SH, Cuckler JM, Burkholder T and Ducheyne P (1996): Initial stability of a modular uncemented, porous-coated femoral stem: a mechanical study. *Am J Orthop* 25(12): 829-34.

Neumann DA and Cook TM (1985): Effect of load and carrying position on the electromyographic activity of the gluteus medius muscle during walking. *Phys Ther* 65(3): 305-11.

Neumann DA and Hase AD (1994): An electromyographic analysis of the hip abductors during load carriage: implications for hip joint protection. *J Orthop Sports Phys Ther* 19(5): 296-304.

Nistor L, Blaha JD, Kjellstrom U and Selvik G (1991): *In vivo* measurements of relative motion between an uncemented femoral total hip component and the femur by roentgen stereophotogrammetric analysis. *Clin Orthop*(269): 220-7.

Noble PC, Alexander JW, Lindahl LJ, Yew DT, Granberry WM and Tullos HS (1988): The anatomic basis of femoral component design [see comments]. *Clin Orthop*(235): 148-65.

Nourbash PS and Paprosky WG (1998): Cementless femoral design concerns. Rationale for extensive porous coating. *Clin Orthop*(355): 189-99.

Nunn D, Freeman MA, Tanner KE and Bonfield W (1989): Torsional stability of the femoral component of hip arthroplasty. Response to an anteriorly applied load. *J Bone Joint Surg [Br]* 71(3): 452-5.

O'Connor DO, Burke DW, Jasty M, Sedlacek RC and Harris WH (1996): *In vitro* measurement of strain in the bone cement surrounding the femoral component of

total hip replacements during simulated gait and stair-climbing. *J Orthop Res* 14(5): 769-77.

Ornstein E, Franzen H, Johnsson R and Sundberg M (2000): Radiostereometric analysis in hip revision surgery--optimal time for index examination: 6 patients revised with impacted allografts and cement followed weekly for 6 weeks. *Acta Orthop Scand* 71(4): 360-4.

Otani T and Whiteside LA (1992): Failure of cementless fixation of the femoral component in total hip arthroplasty. *Orthop Clin North Am* 23(2): 335-46.

Otani T, Whiteside LA, White SE and McCarthy DS (1995): Reaming technique of the femoral diaphysis in cementless total hip arthroplasty. *Clin Orthop*(311): 210-21.

Pahl G and Beitz W (1993). *Konstruktionslehre. Methoden und Anwendung*. Berlin, Springer-Verlag.

Pancanti A, Bernakiewicz M and Viceconti M (2003): The primary stability of a cementless stem varies between subjects as much as between activities. *J Biomech* 36(6): 777-85.

Pauwels F (1951): Über die Bedeutung der Bauprinzipien des Stütz- und Bewegungsapparates für die Beanspruchung des Röhrenknochens. *Acta Anat*(12): 207-227.

Pauwels F (1973). *Atlas zur Biomechanik der gesunden und kranken Hüfte*. Berlin, Springer Verlag.

Pedersen DR, Brand RA and Davy DT (1997): Pelvic muscle and acetabular contact forces during gait. *J Biomech* 30(9): 959-65.

Phillips NJ, Stockley I and Wilkinson JM (2002): Direct plain radiographic methods versus EBRA-Digital for measuring implant migration after total hip arthroplasty. *J Arthroplasty* 17(7): 917-25.

Phillips TW, Messieh SS and McDonald PD (1990): Femoral stem fixation in hip replacement. A biomechanical comparison of cementless and cemented prostheses. *J Bone Joint Surg [Br]* 72(3): 431-4.

Phillips TW, Nguyen LT and Munro SD (1991): Loosening of cementless femoral stems: a biomechanical analysis of immediate fixation with loading vertical, femur horizontal. *J Biomech* 24(1): 37-48.

Pieringer H, Auersperg V, Griessler W and Bohler N (2003): Long-term results with the cementless Alloclassic brand hip arthroplasty system. *J Arthroplasty* 18(3): 321-8.

Pilliar RM, Lee JM and Maniopoulos C (1986): Observations on the effect of movement on bone ingrowth into porous-surfaced implants. *Clin Orthop*(208): 108-13.

Plitz W (1993): [Biomechanics of cement-free endoprostheses]. *Z Orthop Ihre Grenzgeb* 131(6): 483-7.

Polgar K, Gill HS, Viceconti M, Murray DW and O'Connor JJ (2003): Strain distribution within the human femur due to physiological and simplified loading: finite element analysis using the muscle standardized femur model. *Proc Inst Mech Eng [H]* 217(3): 173-89.

Pugh KJ, Morgan RA, Gorczyca JT and Pienkowski D (1998): A mechanical comparison of subtrochanteric femur fracture fixation. *J Orthop Trauma* 12(5): 324-9.

Rao RR, Sharkey PF, Hozack WJ, Eng K and Rothman RH (1998): Immediate weightbearing after uncemented total hip arthroplasty. *Clin Orthop*(349): 156-62.

Reading AD, McCaskie AW and Gregg PJ (1999): The inadequacy of standard radiographs in detecting flaws in the cement mantle. *J Bone Joint Surg Br* 81(1): 167-70.

Rhalmi S, Odin M, Assad M, Tabrizian M, Rivard CH and Yahia LH (1999): Hard, soft tissue and *in vitro* cell response to porous nickel-titanium: a biocompatibility evaluation. *Biomed Mater Eng* 9(3): 151-62.

Rice DP (2000): Cost of illness studies: what is good about them? *Inj Prev* 6(3): 177-9.

Rohlmann A, Bergmann G and Kolbel R (1980): [The stresses in femur. I. Intact femur without consideration of the iliotibial tract (author's transl)]. *Z Orthop Ihre Grenzgeb* 118(6): 897-904.

Rohlmann A, Mossner U, Bergmann G, Hees G and Kolbel R (1983a): [Stresses on the femur following hip joint replacement]. *Z Orthop* 121(1): 47-57.

Rohlmann A, Mossner U, Bergmann G and Kolbel R (1982): Finite-element-analysis and experimental investigation of stresses in a femur. *J Biomed Eng* 4(3): 241-6.

Rohlmann A, Mossner U, Bergmann G and Kolbel R (1983b): Finite-element-analysis and experimental investigation in a femur with hip endoprosthesis. *J Biomech* 16(9): 727-42.

Rosenberg A (1989): Cementless total hip arthroplasty: femoral remodeling and clinical experience. *Orthopedics* 12(9): 1223-33.

Rosenberg A (2002): Fixation for the millennium: the hip. *J Arthroplasty* 17(4 Suppl 1): 3-5.

Rubin PJ, Rakotomanana RL, Leyvraz PF, Zysset PK, Curnier A and Heegaard JH (1993): Frictional interface micromotions and anisotropic stress distribution in a femoral total hip component. *J Biomech* 26(6): 725-39.

Rybicki EF, Simonen FA and Weis EB, Jr. (1972): On the mathematical analysis of stress in the human femur. *J Biomech* 5(2): 203-15.

Ryd L (1992): Roentgen stereophotogrammetric analysis of prosthetic fixation in the hip and knee joint. *Clin Orthop*(276): 56-65.

Rydell NW (1966): Forces acting on the femoral head-prosthesis. A study on strain gauge supplied prostheses in living persons. *Acta Orthop Scand* 37(Suppl): 1-132.

Sabo D, Reiter A, Simank HG, Thomsen M, Lukoschek M and Ewerbeck V (1998): Periprosthetic mineralization around cementless total hip endoprosthesis: longitudinal study and cross-sectional study on titanium threaded acetabular cup and cementless Spotorno stem with DEXA. *Calcif Tissue Int* 62(2): 177-82.

Sakai T, Sugano N, Nishii T, Haraguchi K, Ochi T and Ohzono K (2000): Optimizing femoral anteversion and offset after total hip arthroplasty, using a modular femoral neck system: an experimental study. *J Orthop Sci* 5(5): 489-94.

Schmidt C, Ignatius AA and Claes LE (2001): Proliferation and differentiation parameters of human osteoblasts on titanium and steel surfaces. *J Biomed Mater Res* 54(2): 209-15.

Schmotzer H, Tchejyan G and Song J (1992): A comparison of various loading configurations of the proximal femur for the evaluation of reconstructive surgical procedures. *Proc Inst Mech Eng [H]* 206(1): 29-36.

Schneider E, Eulenberger J, Steiner W, Wyder D, Friedman RJ and Perren SM (1989a): Experimental method for the *in vitro* testing of the initial stability of cementless hip prostheses. *J Biomech* 22(6-7): 735-44.

Schneider E, Kinast C, Eulenberger J, Wyder D, Eskilsson G and Perren SM (1989b): A comparative study of the initial stability of cementless hip prostheses. *Clin Orthop*(248): 200-9.

Schneider U, Breusch SJ, Thomsen M, Wirtz DC and Lukoschek M (2002): [Influence of implant position of a hip prosthesis on alignment exemplified by the CLS shaft]. *Unfallchirurg* 105(1): 31-5.

Schramm M, Keck F, Hohmann D and Pitto RP (2000): Total hip arthroplasty using an uncemented femoral component with taper design: outcome at 10-year follow-up [In Process Citation]. *Arch Orthop Trauma Surg* 120(7-8): 407-12.

Seireg A and Arvikar (1975): The prediction of muscular load sharing and joint forces in the lower extremities during walking. *J Biomech* 8(2): 89-102.

Seireg A and Arvikar RJ (1973): A mathematical model for evaluation of forces in lower extremities of the musculoskeletal system. *J Biomech* 6(3): 313-26.

Selvik G (1990): Roentgen stereophotogrammetric analysis. *Acta Radiol* 31(2): 113-26.

Sharkey PF, Albert TJ, Hume EL and Rothman RH (1990): Initial stability of a collarless wedge-shaped prosthesis in the femoral canal. *Semin Arthroplasty* 1(1): 87-90.

Shelley FJ, Anderson DD, Kolar MJ, Miller MC and Rubash HE (1996): Physical modelling of hip joint forces in stair climbing. *Proc Inst Mech Eng [H]* 210(1): 65-8.

Siebold R, Scheller G, Schreiner U and Jani L (2001): [Long-term results with the cement-free Spotorno CLS shaft]. *Orthopade* 30(5): 317-22.

Simoës JA, Vaz MA, Blatcher S and Taylor M (2000): Influence of head constraint and muscle forces on the strain distribution within the intact femur. *Med Eng Phys* 22(7): 453-9.

Soballe K (1993): Hydroxyapatite ceramic coating for bone implant fixation. Mechanical and histological studies in dogs. *Acta Orthop Scand Suppl* 255: 1-58.

Soballe K, Hansen ES, H BR, Jorgensen PH and Bunger C (1992): Tissue ingrowth into titanium and hydroxyapatite-coated implants during stable and unstable mechanical conditions. *J Orthop Res* 10(2): 285-99.

Sommer HJd, Miller NR and Pijanowski GJ (1982): Three-dimensional osteometric scaling and normative modelling of skeletal segments. *J Biomech* 15(3): 171-80.

Speirs AD, Slomczykowski MA, Orr TE, Siebenrock K and Nolte LP (2000): Three-dimensional measurement of cemented femoral stem stability: an *in vitro* cadaver study. *Clin Biomech (Bristol, Avon)* 15(4): 248-55.

Spotorno L, Schenk RK, Dietschi C, Romagnoli S and Mumenthaler A (1987): Personal experiences with uncemented prostheses. *Orthopade* 16(3): 225-38.

Stansfield BW and Nicol AC (2002): Hip joint contact forces in normal subjects and subjects with total hip prostheses: walking and stair and ramp negotiation. *Clin Biomech* (Bristol, Avon) 17(2): 130-9.

Stansfield BW, Nicol AC, Paul JP, Kelly IG, Graichen F and Bergmann G (2003): Direct comparison of calculated hip joint contact forces with those measured using instrumented implants. An evaluation of a three-dimensional mathematical model of the lower limb. *J Biomech* 36(7): 929-36.

Stolk J, Verdonschot N and Huiskes R (2001): Hip-joint and abductor-muscle forces adequately represent *in vivo* loading of a cemented total hip reconstruction. *J Biomech* 34(7): 917-26.

Sugiyama H, Whiteside LA and Kaiser AD (1989): Examination of rotational fixation of the femoral component in total hip arthroplasty. A mechanical study of micromovement and acoustic emission. *Clin Orthop*(249): 122-8.

Sutherland CJ, Wilde AH, Borden LS and Marks KE (1982): A ten-year follow-up of one hundred consecutive Muller curved-stem total hip-replacement arthroplasties. *J Bone Joint Surg Am* 64(7): 970-82.

Sutherland DH (2001): The evolution of clinical gait analysis part I: kinesiological EMG. *Gait Posture* 14(1): 61-70.

Szivek JA, Benjamin JB and Anderson PL (2000): An experimental method for the application of lateral muscle loading and its effect on femoral strain distributions. *Med Eng Phys* 22(2): 109-16.

Szivek JA and Gealer RL (1991): Comparison of the deformation response of synthetic and cadaveric femora during simulated one-legged stance. *J Appl Biomater* 2(4): 277-80.

Szivek JA, Thomas M and Benjamin JB (1993): Characterization of a synthetic foam as a model for human cancellous bone. *J Appl Biomater* 4(3): 269-72.

Taylor ME, Tanner KE, Freeman MA and Yettram AL (1996): Stress and strain distribution within the intact femur: compression or bending? *Med Eng Phys* 18(2): 122-31.

Torchia ME, Klassen RA and Bianco AJ (1996): Total hip arthroplasty with cement in patients less than twenty years old. Long-term results. *J Bone Joint Surg Am* 78(7): 995-1003.

Traulsen FC, Hassenpflug J and Hahne HJ (2001): [Long-term results with cement-free total hip prostheses (Zweymuller)]. *Z Orthop Ihre Grenzgeb* 139(3): 206-11.

Valstar ER, Vrooman HA, Toksvig-Larsen S, Ryd L and Nelissen RG (2000): Digital automated RSA compared to manually operated RSA. *J Biomech* 33(12): 1593-9.

van den Bogert AJ, Read L and Nigg BM (1999): An analysis of hip joint loading during walking, running, and skiing. *Med Sci Sports Exerc* 31(1): 131-42.

Van Rietbergen B, Huiskes R, Weinans H, Sumner DR, Turner TM and Galante JO (1993): ESB Research Award 1992. The mechanism of bone remodeling and resorption around press-fitted THA stems. *J Biomech* 26(4-5): 369-82.

Vander Sloten J, Labey L, Van Audekercke R and Van der Perre G (1993): The development of a physiological hip prosthesis: evaluation of the strains after implantation of a prototype of hip implant: experiment in a dry femur. *Biomed Mater Eng* 3(1): 1-13.

VDI-Richtlinie 2221 (1986). Methodik zum Entwickeln und Konstruieren technischer Systeme und Produkte. Düsseldorf, VDI-Verlag.

Viceconti M, Toni A and Giunti A (1995): Effects of some technological aspects on the fatigue strength of a cementless hip stem. *J Biomed Mater Res* 29(7): 875-81.

Waide V, Cristofolini L, Stolk J, Verdonschot N and Toni A (2003): Experimental investigation of bone remodelling using composite femurs. *Clin Biomech (Bristol, Avon)* 18(6): 523-36.

Walker PS, Mai SF, Cobb AG, Bentley G and Hua J (1995): Prediction of clinical outcome of THR from migration measurements on standard radiographs. A study of cemented Charnley and Stanmore femoral stems. *J Bone Joint Surg Br* 77(5): 705-14.

Weissinger M and Helmreich C (2001): [Long-term results with Zweymuller cement-free Alloclassic stem]. *Z Orthop Ihre Grenzgeb* 139(3): 200-5.

Whiteside LA, McCarthy DS and White SE (1996): Rotational stability of noncemented total hip femoral components. *Am J Orthop* 25(4): 276-80.

Wilkinson JM, Hamer AJ, Elson RA, Stockley I and Eastell R (2002): Precision of EBRA-Digital software for monitoring implant migration after total hip arthroplasty. *J Arthroplasty* 17(7): 910-6.

Willert HG (1993): [Fixation of endoprotheses with or without cement?]. *Z Orthop Ihre Grenzgeb* 131(6): 601-9.

Willert HG and Buchhorn GH (1999): Osseointegration of cemented and noncemented implants in artificial hip replacement: long-term findings in man. *J Long Term Eff Med Implants* 9(1-2): 113-30.

Wolff J (1892). *Das Gesetz der Transformation der Knochen*. Berlin, A. Hirschwald.

Woolson ST and Adler NS (2002): The effect of partial or full weight bearing ambulation after cementless total hip arthroplasty. *J Arthroplasty* 17(7): 820-5.

Wroblewski BM (1979): The mechanism of fracture of the femoral prosthesis in total hip replacement. *Int Orthop* 3(2): 137-9.

Wroblewski BM and Siney PD (1993): Charnley low-friction arthroplasty of the hip. Long-term results. *Clin Orthop*(292): 191-201.

Wykman A, Selvik G and Goldie I (1988): Subsidence of the femoral component in the noncemented total hip. A roentgen stereophotogrammetric analysis. *Acta Orthop Scand* 59(6): 635-7.

Zerah B, Storgaard M, Johansen T, Olsen C, Lausten G and Kanstrup IL (1998): Changes in bone mineral density adjacent to two biomechanically different types of cementless femoral stems in total hip arthroplasty. *Int Orthop* 22(4): 225-9.

Appendix

A-I Hip and thigh muscles of the complex model

Muscle	Origin	Insertion
M. adductor brevis part 1	Pelvis	Femur
M. adductor brevis part 2	Pelvis	Femur
M. adductor longus	Pelvis	Femur
M. adductor magnus part 1	Pelvis	Femur
M. adductor magnus part 2	Pelvis	Femur
M. adductor magnus part 3	Pelvis	Femur
M. gluteus maximus part 1 segment 1	Pelvis	Pelvis
M. gluteus maximus part 1 segment 2	Pelvis	Femur
M. gluteus maximus part 2 segment 1	Pelvis	Pelvis
M. gluteus maximus part 2 segment 2	Pelvis	Femur
M. gluteus maximus part 3 segment 1	Pelvis	Pelvis
M. gluteus maximus part 3 segment 2	Pelvis	Femur
M. gluteus maximus part 3 segment 3	Femur	Femur
Tractus iliotibialis segment 1	Pelvis	Pelvis
Tractus iliotibialis segment 2	Pelvis	Femur
Tractus iliotibialis segment 3	Femur	Femur
M. gluteus medius part 1	Pelvis	Femur
M. gluteus medius part 2	Pelvis	Femur
M. gluteus medius part 3	Pelvis	Femur
M. gluteus minimus part 1	Pelvis	Femur
M. gluteus minimus part 2	Pelvis	Femur
M. gluteus minimus part 3	Pelvis	Femur
M. iliacus part 1	Pelvis	Pelvis
M. iliacus part 2	Pelvis	Femur
M. iliacus part 3	Pelvis	Femur
M. psoas major part 1	Pelvis	Pelvis
M. psoas major part 2	Pelvis	Pelvis
M. psoas major part 3	Pelvis	Femur
M. psoas major part 4	Femur	Femur
M. inferior gmellus	Pelvis	Femur
M. obturator externus	Pelvis	Femur
M. obturator internus	Pelvis	Femur
M. pectineus	Pelvis	Femur
M. piriformis	Pelvis	Femur
M. quadratus femoris	Pelvis	Femur
M. gmellus superior	Pelvis	Femur
M. bicep femoris caput longum segment 1	Pelvis	Femur
M. bicep femoris caput longum segment 2	Femur	Tibia
M. gracilis segment 1	Pelvis	Femur
M. gracilis segment 2	Femur	Tibia
M. gracilis segment 3	Tibia	Tibia
M. rectus femoris segment 1	Pelvis	Femur
M. rectus femoris segment Patella	Patella	Patella
M. rectus femoris segment 2	Patella	Tibia
M. satorius segment 1	Pelvis	Femur
M. satorius segment 2	Femur	Tibia
M. satorius segment 3	Tibia	Tibia
M. semitendinosus segment 1	Pelvis	Femur
M. semitendinosus segment 2	Femur	Tibia

A-I Hip and thigh muscles of the complex model (suite)

Muscle	Origin	Insertion
M. semimembranosus segment 1	Pelvis	Femur
M. semimembranosus segment 2	Femur	Tibia
M. tensor fascia latae segment 1	Pelvis	Femur
M. tensor fascia latae segment 2	Femur	Tibia
M. gastrocnemius medialis segment 1	Femur	Femur
M. gastrocnemius medialis segment 2	Femur	Tibia
M. gastrocnemius medialis segment 3	Tibia	Foot
M. gastrocnemius lateralis segment 1	Femur	Femur
M. gastrocnemius lateralis segment 2	Femur	Tibia
M. gastrocnemius lateralis segment 3	Tibia	Foot
M. biceps femoris caput brevis segment 1	Femur	Femur
M. biceps femoris caput brevis segment 2	Femur	Tibia
M. vastus intermedius segment 1	Femur	Femur
M. vastus intermedius segment Patella	Patella	Patella
M. vastus intermedius segment 2	Patella	Tibia
M. vastus lateralis segment 1	Femur	Femur
M. vastus lateralis segment Patella	Patella	Patella
M. vastus lateralis segment 2	Patella	Tibia
M. vastus medius segment 1	Femur	Femur
M. vastus medius segment Patella	Patella	Patella
M. vastus medius segment 2	Patella	Tibia
M. popliteus	Femur	Tibia
M. tibialis anterior segment 1	Tibia	Tibia
M. tibialis anterior segment 2	Tibia	Foot
M. tibialis anterior segment 3	Foot	Foot
M. extensor digitorum longus segment 1	Tibia	Tibia
M. extensor digitorum longus segment 2	Tibia	Foot
M. extensor digitorum longus segment 3	Foot	Foot
M. extensor hallucis segment 1	Tibia	Tibia
M. extensor hallucis segment 2	Tibia	Foot
M. extensor hallucis segment 3	Foot	Foot
M. flexor digitorum segment 1	Tibia	Tibia
M. flexor digitorum segment 2	Tibia	Foot
M. flexor digitorum segment 3	Foot	Foot
M. flexor hallucis segment 1	Tibia	Tibia
M. flexor hallucis segment 2	Tibia	Foot
M. flexor hallucis segment 3	Foot	Foot
M. peroneus brevis segment 1	Tibia	Tibia
M. peroneus brevis segment 2	Tibia	Foot
M. peroneus longus segment 1	Tibia	Tibia
M. peroneus longus segment 2	Tibia	Foot
M. peroneus longus segment 3	Foot	Foot
M. peroneus tertius segment 1	Tibia	Tibia
M. peroneus tertius segment 2	Tibia	Foot
M. peroneus tertius segment 3	Foot	Foot
M. tibialis posterior segment 1	Tibia	Tibia
M. tibialis posterior segment 2	Tibia	Foot
M. tibialis posterior segment 3	Foot	Foot
M. soleus part 1	Tibia	Tibia
M. soleus part 2	Tibia	Foot
Lig. cruratum anterius	Femur	Tibia
Lig. cruratum posterius	Femur	Tibia
Lig. cruratum medius	Femur	Tibia
Lig. cruratum laterius	Femur	Tibia
Lig. patellar	Patella	Tibia

A-II Hip and thigh muscles of the simplified model

Muscle	Origin	Insertion
M. gluteus	Pelvis	Femur
M. adductor	Pelvis	Femur
Tractus iliotibialis segment 1	Pelvis	Pelvis
Tractus iliotibialis segment 2	Pelvis	Femur
M. gracilis segment 1	Pelvis	Femur
M. gracilis segment 2	Femur	Tibia
M. gracilis segment 3	Tibia	Tibia
M. rectus femoris segment 1	Pelvis	Femur
M. rectus femoris segment Patella	Patella	Patella
M. rectus femoris segment 2	Patella	Tibia
M. satorius segment 1	Pelvis	Femur
M. satorius segment 2	Femur	Tibia
M. satorius segment 3	Tibia	Tibia
M. semitendinosus segment 1	Pelvis	Femur
M. semitendinosus segment 2	Femur	Tibia
M. semimembranosus segment 1	Pelvis	Femur
M. semimembranosus segment 2	Femur	Tibia
M. tensor fascia latae segment 1	Pelvis	Femur
M. tensor fascia latae segment 2	Femur	Tibia
M. gastrocnemius medialis segment 1	Femur	Femur
M. gastrocnemius medialis segment 2	Femur	Tibia
M. gastrocnemius medialis segment 3	Tibia	Foot
M. gastrocnemius lateralis segment 1	Femur	Femur
M. gastrocnemius lateralis segment 2	Femur	Tibia
M. gastrocnemius lateralis segment 3	Tibia	Foot
M. biceps femoris caput brevis segment 1	Femur	Femur
M. biceps femoris caput brevis segment 2	Femur	Tibia
M. vastus lateralis segment 1	Femur	Femur
M. vastus lateralis segment Patella	Patella	Patella
M. vastus lateralis segment 2	Patella	Tibia
M. vastus medius segment 1	Femur	Femur
M. vastus medius segment Patella	Patella	Patella
M. vastus medius segment 2	Patella	Tibia
M. popliteus	Femur	Tibia
M. tibialis anterior segment 1	Tibia	Tibia
M. tibialis anterior segment 2	Tibia	Foot
M. tibialis anterior segment 3	Foot	Foot
M. extensor digitorum longus segment 1	Tibia	Tibia
M. extensor digitorum longus segment 2	Tibia	Foot
M. extensor digitorum longus segment 3	Foot	Foot
M. extensor hallucis segment 1	Tibia	Tibia
M. extensor hallucis segment 2	Tibia	Foot
M. extensor hallucis segment 3	Foot	Foot
M. flexor digitorum segment 1	Tibia	Tibia
M. flexor digitorum segment 2	Tibia	Foot
M. flexor digitorum segment 3	Foot	Foot
M. flexor hallucis segment 1	Tibia	Tibia
M. flexor hallucis segment 2	Tibia	Foot
M. flexor hallucis segment 3	Foot	Foot
M. peroneus brevis segment 1	Tibia	Tibia
M. peroneus brevis segment 2	Tibia	Foot

A-I Hip and thigh muscles of the simplified model (suite)

Muscle	Origin	Insertion
M. peroneus longus segment 1	Tibia	Tibia
M. peroneus longus segment 2	Tibia	Foot
M. peroneus longus segment 3	Foot	Foot
M. peroneus tertius segment 1	Tibia	Tibia
M. peroneus tertius segment 2	Tibia	Foot
M. peroneus tertius segment 3	Foot	Foot
M. tibialis posterior segment 1	Tibia	Tibia
M. tibialis posterior segment 2	Tibia	Foot
M. tibialis posterior segment 3	Foot	Foot
M. soleus part 1	Tibia	Tibia
M. soleus part 2	Tibia	Foot
Lig. cruratum anterius	Femur	Tibia
Lig. cruratum posterius	Femur	Tibia
Lig. cruratum medius	Femur	Tibia
Lig. cruratum laterius	Femur	Tibia

Curriculum Vitae

Jean-Pierre Kassi

Born in Yaoundé - Cameroon

October 19, 1971

Education

Elementary and High School

Ecole Départementale, Yaoundé – Cameroon

C.E.S. Ngoa-Ekele & Lycée Général Leclerc, Yaoundé

Degree: Baccalauréat

1977 - 1990

Language School Scholarship

Carl Duisberg Gesellschaft (CDG), Radolfzell – Germany

Degree: German Proficiency Certificate

1990 - 1991

Mechanical Engineering

Technical University of Berlin, Germany

Degree: Diplom Ingenieur (Dipl.-Ing.)

1991 - 1999

Professional Experience

Research Assistantship

Biomechanics Laboratory - Centre of Musculoskeletal Surgery

Charité, University Medicine

Humboldt-University and Free University, Berlin – Germany

Since 1999

Awards

S.M. Perren Research Award

European Society of Biomechanics (ESB)

2002